AD-A032 131 SYRACUSE UNIV N Y DEPT OF ELECTRICAL AND COMPUTER E--ETC F/G 9/5
SOLID STATE ARRAY STUDIES RELEVANT TO OTP REGULATIONS. PART 2. --ETC(U)
AUG 76 A T ADAMS, P HSI, A FARRAR F30602-75-C-0121
UNCLASSIFIED RADC-TR-76-241-PT-2 NL

1 OF 2
AD
A032131

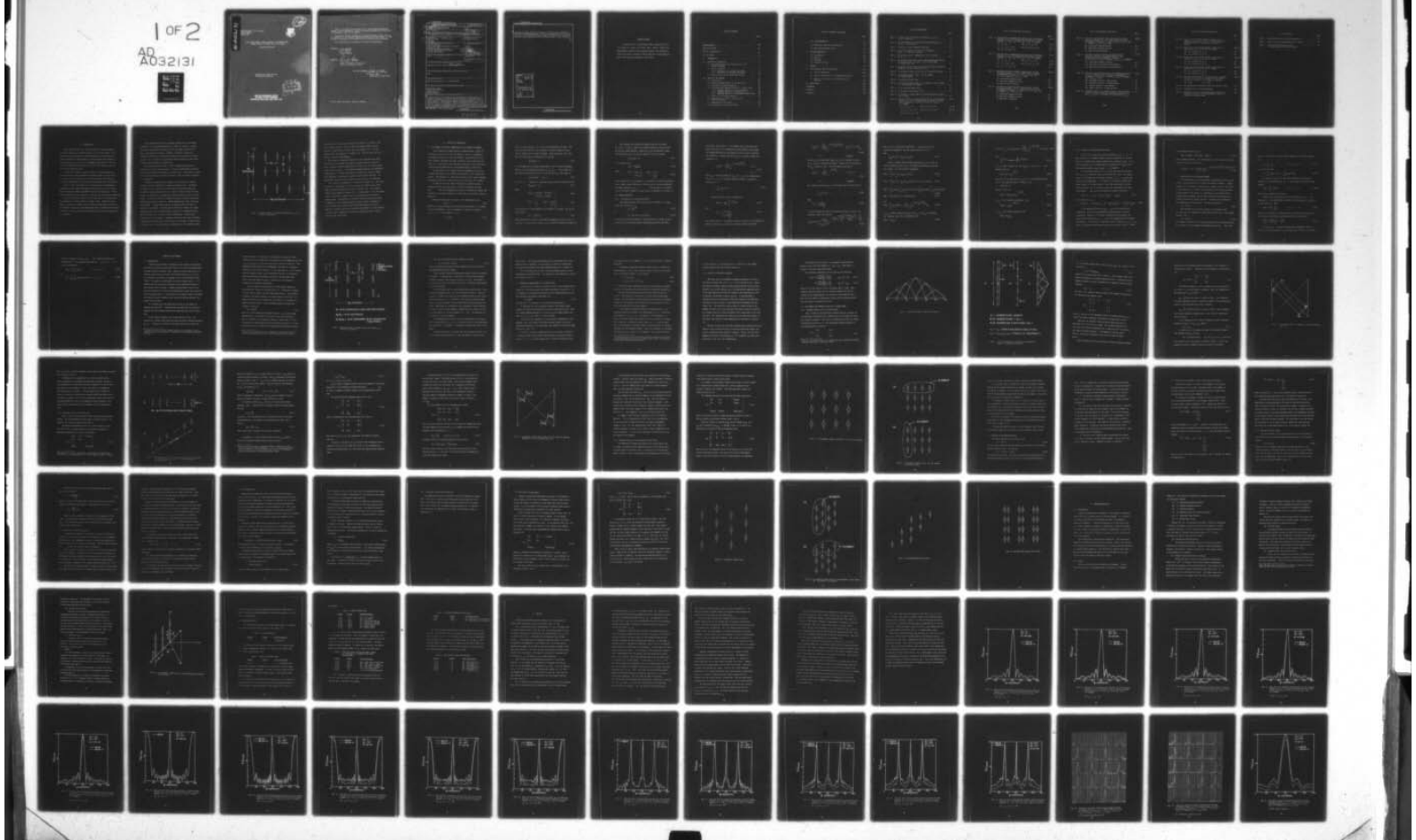

12

RADC-TR-76-241, Pt 2 (of two)
Interim Report
August 1976

SOLID STATE ARRAY STUDIES RELEVANT TO OTP REGULATIONS
Random Effects in Planar Arrays of Dipoles

Syracuse University

ROME AIR DEVELOPMENT CENTER
AIR FORCE SYSTEMS COMMAND
GRIFFISS AIR FORCE BASE, NEW YORK 13441

Some of the charts in this report are of poor quality reproduction. However, this is unimportant because the relevant information on the charts is sufficiently clear to the reader.

This report has been reviewed by the RADC Information Office (OI) and is releasable to the National Technical Information Service (NTIS). At NTIS it will be releasable to the general public, including foreign nations.

This report has been reviewed and approved for publication.

APPROVED: R. H. Chilton

R. H. CHILTON
Project Engineer

APPROVED: Rudolf C. Paltauf

RUDOLF C. PALTAUF, Lt Col, USAF
Chief, Surveillance Division

FOR THE COMMANDER: John P. Huss

JOHN P. HUSS
Acting Chief, Plans Office

Do not return this copy. Retain or destroy.

UNCLASSIFIED

SECURITY CLASSIFICATION OF THIS PAGE *(When Data Entered)*

REPORT DOCUMENTATION PAGE

READ INSTRUCTIONS BEFORE COMPLETING FORM

1. REPORT NUMBER: RADC-TR-76-241 Pt-2 ~~(of two)~~	2. GOVT ACCESSION NO.
3. RECIPIENT'S CATALOG NUMBER	
4. TITLE *(and Subtitle)*: SOLID STATE ARRAY STUDIES RELEVANT TO OTP REGULATIONS. Random Effects in Planar Arrays of Dipoles. Part. 2.	5. TYPE OF REPORT & PERIOD COVERED: Interim Report. Sep 74 - Feb 76
	6. PERFORMING ORG. REPORT NUMBER: N/A
7. AUTHOR(s): Arlan T. Adams, Peter Hsi, A. Farrar	8. CONTRACT OR GRANT NUMBER(s): F30602-75-C-0121
9. PERFORMING ORGANIZATION NAME AND ADDRESS: Syracuse University, Dept of Electrical and Computer Engineering, Syracuse NY 13210	10. PROGRAM ELEMENT, PROJECT, TASK AREA & WORK UNIT NUMBERS: 62702F, 95670003
11. CONTROLLING OFFICE NAME AND ADDRESS: Rome Air Development Center (OCTE), Griffiss AFB NY 13441	12. REPORT DATE: Aug 1976
	13. NUMBER OF PAGES: 168 (12) 165 p.
14. MONITORING AGENCY NAME & ADDRESS *(if different from Controlling Office)*: Same (16) 9567	15. SECURITY CLASS. *(of this report)*: UNCLASSIFIED
	15a. DECLASSIFICATION/DOWNGRADING SCHEDULE: N/A

16. DISTRIBUTION STATEMENT *(of this Report)* (17) 00

Approved for public release; ~~distribution~~ unlimited.

17. DISTRIBUTION STATEMENT *(of the abstract entered in Block 20, if different from Report)*

Same

18. SUPPLEMENTARY NOTES

RADC Project Engineer: R. H. Chilton (OCTE)

19. KEY WORDS *(Continue on reverse side if necessary and identify by block number)*

Phased Array Radar
Solid State Amplifiers
Dipole Arrays
Method of Moments

20. ABSTRACT *(Continue on reverse side if necessary and identify by block number)*

A computer program for the analysis of random effects in planar arrays is described. The method of moments is applied iteratively in conjunction with a random sampling process, to obtain mean far field beam patterns and their expected variation. Block-Toeplitz impedance redundancies and the zeros of the excitation matrix are utilized in a special efficient solution routine. Separate array analysis at fundamental and harmonic frequencies yields the expected ratio of harmonic to fundamental levels. The theory of the computer program is →

DD FORM 1 JAN 73 1473 EDITION OF 1 NOV 65 IS OBSOLETE

UNCLASSIFIED

SECURITY CLASSIFICATION OF THIS PAGE *(When Data Entered)*

406 737

outlined and typical results are presented. Significant gain degradation is predicted at harmonic frequencies. The results are applied to the OTP regulations and it is concluded that certain types of microwave solid state devices tested are viable candidates for array elements in view of these regulations.

ACKNOWLEDGEMENT

The authors wish to acknowledge useful suggestions by Drs. D.K. Cheng, B.J. Strait, D. Sinnott, and T. Sarkar. Special acknowlegement is given to the computer programs [13] and [19] of Sarkar and Sinnott, portions of which were used in developing the planar array program presented in this report.

TABLE OF CONTENTS

		Page
ACKNOWLEDGEMENT		iii
TABLE OF CONTENTS		iv
LIST OF ILLUSTRATIONS		vi
LIST OF TABLES		x
I.	INTRODUCTION	1
II.	STATISTICAL FORMULATION	5
2.1	The General Statistical Formulation for the Method of Moments	5
2.2	Source Statistics	7
2.2.1	Statistics for a Single Excitation	7
2.2.2	Statistics for Multiple Excitations	12
2.3	Statistics of the Far Field Beam Pattern	13
III.	THEORY OF THE PROGRAM	16
3.1	Introduction	16
3.2	Generating Random Errors in the Excitation	20
3.3	Setting Up the Matrix Equations	22
3.4	The Generalized Impedance Matrix of a Planar Array	23
3.4.1	Impedance Matrix of an Isolated Dipole	23
3.4.2	Impedance Matrix of a Linear Array	29
3.4.3	Impedance Matrix of a Rectangular Planar Array	35
3.5	Solution of the Matrix Equation	39
3.6	Computation of Currents - Zeros of the Excitation Matrix	41
3.7	Computation of Far Fields	42
3.8	Processing of the Far Field Data	43

TABLE OF CONTENTS (Continued)

		Page
	3.9 Gain Degradation	45
	3.10 Additional Beam Pattern Quantities	47
	3.11 Some Special Planar Arrays	48
IV.	PROGRAM DESCRIPTION	54
	4.1 Introduction	54
	4.2 Options	54
	4.3 Modeling	57
	4.4 Input Data Set-Up	59
V.	RESULTS	62
VI.	APPLICATION OF THE OTP REGULATIONS	108
	6.1 The OTP Regulations	108
	6.2 Summary and Discussion of Experimental Results	116
	6.3 Effects of the Array on Far Field Levels of Harmonics	120
VII.	CONCLUSIONS	123
	REFERENCES	124
	APPENDIX A	126
	APPENDIX B	130

LIST OF ILLUSTRATIONS

Page

Fig. 1. A planar array of dipoles with spacing S_x, S_z in the X, Z directions. 3

Fig. 2. Thin wire model of a planar array with spacing S_x, S_z in the X, Z directions. 18

Fig. 3. Sinusoidal current expansion functions. 24

Fig. 4. An isolated dipole (a) dipole (b) filamentary model (c) expansion functions. 25

Fig. 5. An isolated dipole - symmetries of the [Y] matrix ($M_1 = 5$). 28

Fig. 6. An equally spaced linear array with N+1 identical dipoles (a) perpendicular line case (b) thin-wire model (c) skewed line case. 30

Fig. 7. An equally spaced linear array with N+1 identical dipoles - symmetries of the [Y] matrix ($M_3 = 5$). 34

Fig. 8. A rectangular planar array with 3 x 4 identical dipoles. . . 37

Fig. 9. A rectangular planar array (a) row element (b) column element. 38

Fig.10. A triangular planar array. 50

Fig. 11. A triangular planar array (a) two adjacent column element (b) two adjacent row element. 51

Fig. 12. A parallelogram planar array. 52

Fig. 13. An unequally spaced planar array. 53

Fig. 14. A rectangular planar array of z-directed dipoles lying in the X-Z plane. 58

Fig. 15. Mean and (M-σ) broadside beam patterns (in the principal H-plane) of a 10 x 10 planar array of dipoles at fundamental frequency ($L = 0.5\lambda$, $S_x = 0.5\lambda$, $S_z = 1.0\lambda$, $a = 0.0005\lambda$) . . 67-71

(a) $\sigma_a = \sigma_p = 0$ (b) $\sigma_a = 0$, $\sigma_p = 20°$ 67, 68

(c) $\sigma_a = 0$, $\sigma_p = 40°$ (d) $\sigma_a = 0.2$, $\sigma_p = 40°$ 69, 70

(e) $\sigma_a = 0.5$, $\sigma_p = 40°$. 71

LIST OF ILLUSTRATIONS (Continued)

Page

Fig. 16. Mean and (M-σ) broadside beam patterns (in the principal H-plane) of a 10 x 10 planar array of dipoles at second harmonic ($L = 1.0\lambda$, $S_x = 1.0\lambda$, $S_z = 2.0\lambda$, $a = 0.001\lambda$) . . . 72-76

(a) $\sigma_a = \sigma_p = 0$ (b) $\sigma_a = 0$, $\sigma_p = 20°$ 72,73

(c) $\sigma_a = 0$, $\sigma_p = 40°$ (d) $\sigma_a = 0.2$, $\sigma_p = 40°$ 74,75

(e) $\sigma_a = 0.5$, $\sigma_p = 40°$ 76

Fig. 17. Mean and (M-σ) broadside beam patterns (in the principal H-plane) of a 10 x 10 planar array of dipoles at third harmonic ($L = 1.5\lambda$, $S_x = 1.5\lambda$, $S_z = 3.0\lambda$, $a = 0.0015\lambda$). . . . 77-81

(a) $\sigma_a = \sigma_p = 0$ (b) $\sigma_a = 0$, $\sigma_p = 20°$ 77,78

(c) $\sigma_a = 0$, $\sigma_p = 40°$ (d) $\sigma_a = 0.2$, $\sigma_p = 40°$ 79,80

(e) $\sigma_a = 0.5$, $\sigma_p = 40°$. 81

Fig. 18. Individual and mean broadside beam patterns (in the principal H-plane) of a 5 x 5 planar array of dipoles at fundamental frequency ($L = 0.5\lambda$, $S_x = 0.5\lambda$, $S_z = 1.0\lambda$, $a = 0.0005\lambda$, $\sigma_a = 0.5$, $\sigma_p = 40°$) . . . 82-84

(a) Individual (sample) patterns. . . . 82

(b) Individual (sample) patterns. . . . 83

(c) Mean and (M-σ) patterns. . . . 84

Fig. 19. Individual and mean broadside bean patterns (in the principal H-plane) of a 5 x 5 planar array of dipoles at fundamental frequency ($L = 0.5\lambda$, $S_x = 0.5\lambda$, $S_z = 1.0\lambda$ $a = 0.0005\lambda$, $\sigma_a = 3.0$, $\sigma_p = 40°$) . . . 85-87

(a) Individual (sample) patterns . . . 85

(b) Individual (sample) patterns . . . 86

(c) Mean and M-σ patterns. . . . 87

LIST OF ILLUSTRATIONS (Continued)

Page

Fig. 20. Individual and broadside mean beam patterns (in the principal H-plane) of a 5 x 5 planar array of dipoles at fundamental frequency ($L = 0.5\lambda$, $S_x = 0.5\lambda$, $S_z = 1.0\lambda$, $a = 0.0005\lambda$, $\sigma_a = 0.5$, $\sigma_p = 180°$) . . . 88-90

(a) Individual (sample) patterns . . . 88

(b) Individual (sample) patterns . . . 89

(c) Mean and (M-σ) patterns. . . . 90

Fig. 21. Individual and mean broadside patterns (in the principal H-plane) of an eleven element linear array of dipoles at fundamental frequency ($L = 0.5\lambda$, $S_x = 0.5\lambda$, $a = 0.005\lambda$, $\sigma_a = 0$, $\sigma_p = \infty$(random)) . . . 91-93

(a) Individual (sample) patterns . . . 91

(b) Mean and (n-σ) patterns with mutuals . . . 92

(c) Mean and (n-σ) patterns without mutuals. . . . 93

Fig. 22. Mean and (M-σ) beam patterns (in the principal H-plane) of a 5 x 5 planar array of dipoles at fundamental frequency ($L = 0.5\lambda$, $S_x = 0.5\lambda$, $S_z = 1.0\lambda$, $a = 0.0005\lambda$, $\sigma_a = 0.02$, $\sigma_p = 20°$) . . . 94-97

(a) Broadside patterns - with mutuals . . . 94

(b) Broadside patterns - without mutuals . . . 95

(c) Endfire patterns - with mutuals . . . 96

(d) Endfire patterns - without mutuals. . . . 97

Fig. 23. Sidelobe levels of a 9-element linear array of dipoles in the principal H-plane at fundamental frequency ($L = 0.5\lambda$, $S_x = 0.5\lambda$, $a = 0.0005\lambda$) as a function of σ_a. σ_p. . . . 98

LIST OF ILLUSTRATIONS (Continued)

Page

Fig. 24. Gain G_o for a uniformly-excited linear array of dipoles ($L = 0.5\lambda$, $S_x = 0.5\lambda$, $a = 0.005\lambda$) with and without mutuals as a function of the number of dipoles. 99

Fig. 25. Ratio G_1/G_0 for an eleven element linear array of dipoles ($L = 0.5\lambda$, $S_x = 0.5\lambda$, $a = 0.005\lambda$) 100,101

(a) as a function of σ_a, σ_p 100

(b) as a function of σ_p, σ_a. 101

Fig. 26. Ratio G_1/G_0 for an eleven element linear array of dipoles ($L = 0.5\lambda$, $S_z = 0.6\lambda$, $a = 0.005\lambda$) 102,103

(a) as a function of σ_a, σ_p 102

(b) as a function of σ_p, σ_a. 103

Fig. 27. Ratio G_2/G_0 for an eleven element linear array of dipoles ($L = 0.5\lambda$, $S_x = 0.5\lambda$, $a = 0.005\lambda$) 104,105

(a) as a function of σ_a, σ_p 104

(b) as a function of σ_p, σ_a. 105

Fig. 28. Ratios G_1/G_0 and G_2/G_0 for a linear array of dipoles ($L = 0.5\lambda$, $S_x = 0.5\lambda$, $a = 0.005\lambda$) with and without mutuals as a function of the number of dipoles 106,107

(a) G_1/G_0 (b) G_2/G_0

Fig. 29. OTP Regulations on Emission Levels and Sidelobe Levels. . . . 109

Fig. 30. Weighting Factor k (OTP Regulations). 110

Fig. 31. Reflection Loss for a centerfed dipole of length L, diameter D, fed by a 50 ohm transmission line, as a function of antenna length. 122

LIST OF TABLES

		Page
TABLE 1	Bandwidth Definitions for OTP Regulations	111
TABLE 2	Values of F_0, P_t Corresponding to S = 60 dB	112
TABLE 3	Second and Third Harmonic Levels of Some Microwave Solid State Devices	117

I. INTRODUCTION

This volume is part II of the final report, "Solid State Array Evaluation Relevant to OTP Regulations," [1]. The final report is concerned with the evaluation of current microwave solid state devices and an assessment of their potential as array elements with regard to the regulations of the Office of Telecommunications Policy. The regulations are being revised and are not yet in final form; we refer to the current regulations [24].

In brief, the questions posed are "Which of the microwave solid state devices are viable candidates for array elements in view of the OTP regulations on in-band and out-of-band emissions" and, "What are the device requirements which result from OTP regulations on emissions?"

Part I of the final report [1] is concerned with an experimental evaluation of some current microwave solid state devices (L and S-band bipolar transistor modules and TRAPATT devices were evaluated). Out-of-band characteristics and the effect of varying load were studied extensively.

Part II (the present volume) of the final report is concerned with the computation of random effects in planar arrays. Random effects in arrays, in particular random errors in phase and amplitude excitation of the elements of an array, can significantly affect the beam pattern characteristics of an array and thus affect whether or not the OTP regulations are satisfied.

These random effects are not extremely significant at fundamental frequency, for well-designed modules at L band, for instance. Typical variations from module to module are $\pm$ 1 db in amplitude and $\pm 10°$ in phase under matched conditions. However, at harmonic frequencies, significant variations in amplitude and phase are encountered, as noted in part I [1]. In addition, one obtains larger variations at the fundamental under conditions of variable load.

The variations noted in part I [1] are significant and must be taken into account in array analysis. Effects of random phase and amplitude variations have been studied in the past [2-7]. These earlier studies do not take mutuals into account (It turns out that the effect of mutuals is significant.).

A computer program has been prepared for the analysis of planar arrays of thin-wire dipoles with random excitation errors. The method of moments [8,9] is used in conjunction with an iterative method and mutuals are taken fully into account. Figure 1 shows the physical model studied, a planar array of dipoles with uniform spacing in the x,z directions. The array is driven by voltage sources with a nominal (specified) amplitude and phase distribution. Random amplitude and phase errors may be specified. Average beam patterns are computed and their range of variation is indicated. The array may be treated at harmonic (or other) frequencies and thus an average ratio of harmonic to fundamental levels may be obtained (as a function of space coordinates). Expected gain levels may also be computed. A number of steps have been taken to improve computational efficiency and thereby permit the treatment of planar arrays of moderate size. The block-Toeplitz redundancies of the impedance matrix

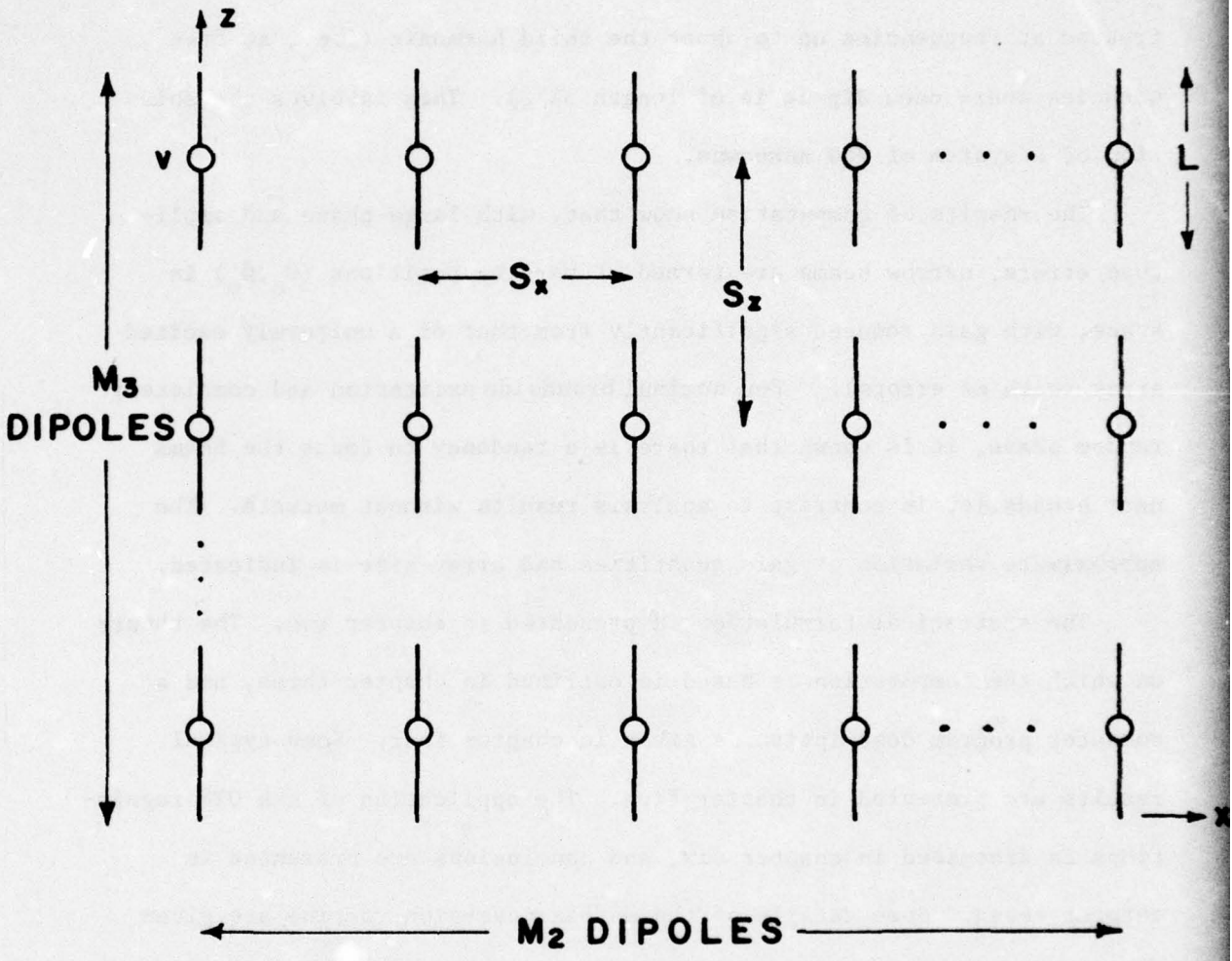

Fig. 1. A planar array of dipoles with spacing S_x, S_z in the X, Z directions.

and the zeros of the excitation matrix are utilized in a special, efficient solution routine. Arrays of about 100 dipole elements may be treated at frequencies up to about the third harmonic (i.e., at frequencies where each dipole is of length $3\lambda/2$). This involves the solution of a system of 700 unknowns.

The results of computation show that, with large phase and amplitude errors, narrow beams are formed at varying positions (θ_o, ϕ_o) in space, with gain reduced significantly from that of a uniformly excited array (with no errors). For nominal broadside excitation and completely random phase, it is shown that there is a tendency to focus the beams near broadside, in contrast to analysis results without mutuals. The approximate variation of gain quantities and array size is indicated.

The statistical formulation is presented in chapter two. The theory on which the computation is based is outlined in chapter three, and a computer program description is given in chapter four. Some typical results are presented in chapter five. The application of the OTP regulations is discussed in chapter six, and conclusions are presented in chapter seven. Some details of the matrix inversion routine are given in Appendix A and a computer program listing is given in Appendix B. Our conclusions are in brief that well-designed bipolar transistor modules and TRAPATT devices are reasonable candidates for array elements (assuming that reasonable array design procedures are used to ensure required side lobe levels).

2. STATISTICAL FORMULATION

2.1 THE GENERAL STATISTICAL FORMULATION FOR THE METHOD OF MOMENTS

In the analysis of random effects in antenna arrays, there are essentially many factors to be considered as sources of randomness, for example, positions of the array elements, characteristics of the array elements, amplitude and phase variations of the excitation voltages, etc. Many efforts have been made previously to find the effects of these random errors upon far field beam patterns or gain [2-7].

In this report, it is assumed that the randomness of the array is restricted solely to the random errors present in the voltage excitations. The question is: given the statistics of the inputs (voltage excitations) what will be the statistics of the outputs (far fields)?

In order to solve the linear equations of an antenna array, a procedure called the matrix method, or method of moments, has been used. The basic mathematical concept is the method of moments [8] by which the functional equations of field theory are reduced to matrix equations.

Consider deterministic equations of the inhomogeneous type

$$F(e) = v \tag{2-1}$$

where F is a linear operator over linear functional space V, v is known, e is to be determined. Let e be expanded in a series of functions e_1, e_2, e_e .... in the domain of F, as

$$e = \sum_n \alpha_n e_n \tag{2-2}$$

where α_n are constants. The e_n are called expansion functions. For the exact solution, Eq. (2-1) is usually an infinite summation and e_n forms a complete set of basis functions. Substituting Eq. (2-2) into Eq. (2-1) and using the linearity of F, one has

$$\sum_n \alpha_n F(e_n) = v \tag{2-3}$$

It is assumed that a suitable inner product <e,v> has been determined. Define a set of weighting functions, w_1, w_2, w_3, ... in the range of F, and take the inner product of Eq. (2-3) with each w_m. The result is

$$\sum_n \alpha_n \langle w_m, Fe_n \rangle = \langle w_m, v \rangle \tag{2-4}$$

m = 1, 2, 3, ... This set of equations can be written in matrix form as

$$[f_{mn}][\alpha_n] = [v_n] \tag{2-5}$$

where

$$[f_{mn}] = \begin{bmatrix} \langle w_1, Fe_1 \rangle & \langle w_1, Fe_2 \rangle \cdots \\ \langle w_2, Fe_1 \rangle & \langle w_2, Fe_2 \rangle \end{bmatrix} \tag{2-6}$$

$$[\alpha_n] = \begin{bmatrix} \alpha_1 \\ \alpha_2 \end{bmatrix} \qquad [v_n] = \begin{bmatrix} \langle w_1, v \rangle \\ \langle w_2, v \rangle \end{bmatrix} \tag{2-7}$$

If the matrix [f] is non-singular, its inverse $[f^{-1}]$ exists. The α_n are then given by

$$[\alpha_n] = [f_{mn}^{-1}][v_m] \tag{2-8}$$

This solution may be exact or approximate, depending upon the choice of e_n and w_m. The particular choice $w_n = e_n$ is known as Galerkin's method [9].

Now consider the statistical problems involved in solving Eq. (2-1). Let $\underline{g}$ be a function of random variables, where the under-bar denotes random quantity. Since the e_n are deterministic expansion functions, and F is a linear operator, Eq. (2-3) becomes

$$\sum_n \underline{\alpha}_n F(e_n) = \underline{g} \tag{2-9}$$

or, in matrix form,

$$[\underline{\alpha}_n] = [\ell_{nm}^{-1}][\underline{v}_m] \tag{2-10}$$

where

$$[\underline{v}_m] = \begin{bmatrix} \langle w_1, \underline{v} \rangle \\ \langle w_2, \underline{v} \rangle \\ \end{bmatrix} \qquad [\underline{\alpha}_n] = \begin{bmatrix} \underline{\alpha}_1 \\ \underline{\alpha}_2 \end{bmatrix} \tag{2-11}$$

If the statistics of $\underline{v}_m$ are known, it is possible to find the statistics for $\underline{\alpha}_n$ under certain conditions, since $\underline{\alpha}_i$ now is a linear combination of random variables $\underline{v}_1, \underline{v}_2, \ldots$. The details of the formulation of the matrix method for planar arrays is explained in Section 3.1.

2.2 SOURCE STATISTICS

2.2.1. Statistics for a single excitation.

The complex voltage excitation of the i-th element of a planar array can be written as

$$\underline{V}_i = \underline{A}_i e^{j\underline{\theta}_i} \tag{2-12}$$

or

$$\underline{V}_i = \underline{A}_i \cos \underline{\theta}_i + j\underline{A}_i \sin \underline{\theta}_i \tag{2-13}$$

As before, the under-bar denotes a random quantity or random variable. $\underline{A}_i$ and $\underline{\theta}_i$ are real random numbers representing amplitude and phase

variations, respectively. It is assumed that the amplitude and phase variations of the excitation are each normally distributed. Since magnitude does not have negative values, strictly apeaking, the probability density function of $\underline{A}_i$ is a truncated normal distribution, i.e.

$$f_{\underline{A}_i}(a_i) = \frac{K_{a_i}}{\sqrt{2\pi}\,\sigma_{a_i}} e^{-(a_i - a_{m_i})^2/2\sigma^2_{a_i}} \qquad a_i \geq 0$$
$$= 0 \qquad a_i < 0 \tag{2-14}$$

where a_{m_i} is the mean amplitude ($a_{m_i} \geq 0$), σ_{a_i} is the standard deviation of a_i. K_{a_i} is a constant multiplier which is obtained by normalization :

$$\int_{-\infty}^{\infty} f_{\underline{A}_i}(a_i)\, da_i = 1 \tag{2-15}$$

The error function erf(x) is defined as:

$$\text{erf}(x) = \frac{1}{\sqrt{2\pi}} \int_0^x e^{-y^2/2} dy \tag{2-16}$$

Thus

$$K_{a_i} = \frac{1}{\frac{1}{2} + \text{erf}\left(\frac{a_{m_i}}{\sigma_{a_i}}\right)} \tag{2-17}$$

Since phase angle θ is a periodic function of period 2π, the probability density function of $\underline{\theta}_i$ is again a truncated normal distribution.

$$f_{\underline{\theta}_i}(\theta_i) = \frac{K_{\theta_i}}{\sqrt{2\pi}\,\sigma_{\theta_i}} e^{-(\theta_i-\theta_{m_i})^2/(2\sigma^2_{\theta_i})} \qquad \theta_{m_i} - \pi < \theta_i \leq \pi + \theta_{m_i}$$

(2-18)

$$= 0 \qquad \text{elsewhere}$$

where θ_{m_i} is the mean phase angle, σ_{θ_i} is the standard deviation of θ_i. K_{θ_i} is a constant multiplier. Without loss of generality, let θ_{m_i} be equal to zero. Thus the density function is

$$f_{\underline{\theta}_i}(\theta_i) = \frac{K_{\theta_i}}{\sqrt{2\pi}\,\sigma_{\theta_i}} e^{-\theta_i^2/2\sigma^2_{\theta_i}} \qquad -\pi \leq \theta_i \leq \pi$$

(2-19)

$$= 0 \qquad \text{elsewhere}$$

The constant multiplier K_{θ_i} can be obtained also by normalization:

$$\int_{-\infty}^{\infty} f_{\theta_i}(\theta_i)\, d\theta_i = 1 \tag{2-20}$$

Thus

$$K_{\theta_i} = \frac{1}{2\ \mathrm{erf}(\frac{\pi}{\sigma_{\theta_i}})} \tag{2-21}$$

It may be assumed that the joint density function of (a_i, θ_i) is a bivariate normal distribution.

$$f_{\underline{A}_i\underline{\theta}_i}(a_i,\theta_i) = \frac{K_{a_i} K_{\theta_i}}{2\pi\sigma_{a_i}\sigma_{\theta_i}\sqrt{1-\rho^2}} e^{-\frac{1}{2(1-\rho^2)}\left(\frac{(a_i-a_{m_i})^2}{\sigma^2_{a_i}} - \frac{2\rho(a_i-a_{m_i})\theta_i}{\sigma_{a_i}\sigma_{\theta_i}} + \frac{\theta_i^2}{\sigma^2_{\theta_i}}\right)} \tag{2-22}$$

where ρ is the correlation coefficient. If $\underline{A}_i$ and $\underline{\theta}_i$ are statistically independent, they are uncorrelated, i.e. $\rho = 0$.

Thus

$$f_{\underline{A}_i\underline{\theta}_i}(a_i,\theta_i) = f_{\underline{A}_i}(a_i)\cdot f_{\underline{\theta}_i}(\theta_i) \tag{2-23}$$

Given a complex random voltage excitation, $\underline{V}_i$, it is easy to find the expected value of $\underline{V}_i$ if the amplitude and phase variations are assumed to be statistically independent.

$$E[\underline{V}_i] = \int_0^{\infty} da_i \int_{-\pi}^{\pi} d\theta_i \, f_{\underline{A}_i\underline{\theta}_i}(a_i,\theta_i)\, \underline{V}_i \tag{2-24}$$

$$E[\underline{V}_i] = \int_0^{\infty} da_i \int_{-\pi}^{\pi} d\theta_i \, f_{\underline{A}_i}(a_i) f_{\underline{\theta}_i}(\theta_i)[a_i \cos\theta_i + j a_i \sin\theta_i] \tag{2-25}$$

$$E[\underline{V}_i] = \int_0^{\infty} f_{\underline{A}_i}(a_i)da_i \int_{-\pi}^{\pi} f_{\underline{\theta}_i}(\theta_i)\cos\theta_i d\theta_i + j\int_0^{\infty} f_{\underline{A}_i}(a_i)a_i da_i \int_{-\pi}^{\pi} f_{\underline{\theta}_i}(\theta_i)\sin\theta_i \, d\theta_i \tag{2-26}$$

$$E[\underline{V}_i] = E[\underline{A}_i]E[\cos\underline{\theta}_i] + jE[\underline{A}_i]E[\sin\underline{\theta}_i] \tag{2-27}$$

Then

$$E[\underline{A}_i] = \int_0^{\infty} a_i f_{\underline{A}_i}(a_i)da_i = \frac{K_{a_i}}{\sqrt{2\pi}\,\sigma_{a_i}} \int_0^{\infty} a_i e^{-(a_i-a_{m_i})^2/2\sigma_{a_i}^2} da_i \tag{2-28}$$

If σ_{a_i} is small compared with a_{m_i}, say $\sigma_{a_i} < 0.5\, a_{m_i}$ for instance, the expected value can be approximated by

$$E[\underline{A}_i] \doteq K_{a_i} a_{m_i} \tag{2-29}$$

$$E[\cos \underline{\theta}_i] = \int_{-\pi}^{\pi} \cos \theta_i f_{\underline{\theta}_i}(\theta_i) d\theta_i = \frac{2K_{\theta_i}}{2\pi\sigma_{\theta_i}} \int_0^{\pi} e^{-(\theta_i^2/\, 2\sigma_{\theta_i}^2)} \cos \theta_i d\theta_i \quad (2\text{-}30)$$

From

$$\int_0^{\infty} e^{-a^2x^2} \cos mx dx = \frac{\sqrt{\pi}}{2a} e^{-m^2/(4a^2)} \quad (2\text{-}31)$$

If σ_{θ_i} is small enough, such that $f_{\underline{\theta}_i}(\theta_i) \simeq 0$ for $\theta_i \doteq \pm\pi$, the expected value is

$$E[\cos \underline{\theta}_i] \doteq K_{\theta_i} e^{-\sigma_{\theta_i}^2/2} \quad (2\text{-}32)$$

Since sin θ is an odd function, $f_{\underline{\theta}_i}(\theta_i)$ is an even function over $[-\pi,\pi]$. The expected value of sin $\underline{\theta}_i$ is zero.

$$E[\sin \underline{\theta}_i] = 0 \quad (2\text{-}33)$$

Thus Eq. (2-27) is

$$E[\underline{V}_i] \doteq (K_{a_i} a_{m_i})(K_{\theta_i} e^{-(\sigma_{\theta_i}^2/2)}) \quad (2\text{-}34)$$

If $\sigma_{a_i} = 0$ (no amplitude variation), then

$$E[\underline{V}_i] = a_{m_i} K_{\theta_i} e^{-(\sigma_{\theta_i}^2/2)} \quad (2\text{-}35)$$

If $\sigma_{\theta_i} = 0$ (no phase variation), then

$$E[\underline{V}_i] = K_{a_i} a_{m_i}. \quad (2\text{-}36)$$

2.2.2 Statistics for Multiple Excitations

Let $[V_n]$ be a column matrix with n-elements v_1, v_2, ... v_n. If each element v_i is a complex random voltage as defined in Eq. (2-12), $[V_n]$ is an n-dimensional complex random vector, denoted as $[\underline{V}_n]$. Or it can be redefined as a 2-n dimensional real random vector $[\underline{V}_{2n}]$, with real random variables, $\underline{a}_1, \underline{\theta}_1, \underline{a}_2, \underline{\theta}_2$, ... as elements.

It is assumed in Section 2.2.1 that the joint-density function of (a_i, θ_i) is a bivariate normal distribution (Eq. 2-22). For simplicity, it is assumed that the random variables $\underline{v}_1$, v_2, ..., $\underline{v}_n$ are also statistically independent. It is possible to partially isolate each input channel of the array system. Thus, the random errors in each input excitation can be assumed statistically independent with some justification. Thus, the joint-probability density function is

$$f_n(\underline{v}_1, \underline{v}_2, \ldots, \underline{v}_n) = f_{\underline{V}_1}(v_1)\, f_{\underline{V}_2}(v_2) \ldots f_{\underline{V}_n}(v_n) \qquad (2\text{-}37)$$

Or in terms of a_i, θ_i:

$$f_{2n}(\underline{a}_1, \underline{a}_2 \ldots, \underline{a}_n, \underline{\theta}_1, \underline{\theta}_2 \ldots \underline{\theta}_n) = f_{\underline{A}_1}(a_1) f_{\underline{A}_2}(a_2) \ldots f_{\underline{\theta}_1}(\theta_1) f_{\underline{\theta}_2}(\theta_2) \qquad (2\text{-}38)$$

If the random excitations $\underline{v}_1, \underline{v}_2$, ... $\underline{v}_n$ are not statistically independent, then the joint probability density function is quite complicated. However, if the phase variations are not present, the joint density function $\underline{v}_1$, $\underline{v}_2$, ..., $\underline{v}_n$ is an n-dimensional joint-normal distribution. Let $[B_n]$ be a column matrix with n elements b_1, b_2, ..., b_n. Each b_i is defined as the expected value of $\underline{v}_i$ (see Eq. (2-36)). Define

the covariance matrix $[M_n]$ as:

$$[M_n] = E[([\underline{V}_n] - [B_n])([\underline{V}_n] - [B_n])^T] \tag{2-39}$$

where T means transpose. The n-dimensional jointly-normal distribution function can then be written as

$$f_n(\underline{v}_1,\underline{v}_2,\ldots,\underline{v}_n) = \frac{1}{(2\pi)^{n/2}\,|[M_n]|}\, e^{-\frac{1}{2}([\underline{V}_n]-[B_n])^T[M_n]^{-1}([\underline{V}_n]-[B_n])} \tag{2-40}$$

2.3 STATISTICS OF FAR FIELD BEAM PATTERN

The calculation of an electromagnetic field problem can be simplified to a matrix equation(Eq. (2-8)) by the method of moments. Suppose a matrix [F] of order mxn is obtained for a planar array, so that given a column matrix [v] of order n which represents the voltage excitation on each element of the array, a column matrix [e] of order m can be obtained which represents the far field electric field intensity at m different positions in space, provided suitable sets of expansion and weighting functions are used. The matrix equation is

$$[e] = [F][v]. \tag{2-41}$$

Now consider the statistical problem of the planar array. Eq. (2-41) is still applicable, except that both [v] and [e] are random vectors. Thus,

$$[\underline{e}] = [F][\underline{v}] \tag{2-42}$$

The elements of matrix [F] are uniquely determined by the given geometry of the array, and the expansion and weighting functions. Thus, each

far field quantity $\underline{e}_i$ is only a linear combination of random variables $\underline{v}_i$'s.

$$\underline{e}_i = \sum_{j=1}^{n} f_{ij}\, \underline{v}_j \qquad i = 1, 2, \ldots, m \tag{2-43}$$

or, in another form,

$$\underline{e}_i = \sum_{j=1}^{n} f_{ij}\underline{a}_j \cos \underline{\theta}_j + j \sum_{j=1}^{n} f_{ij}\underline{a}_j \sin \underline{\theta}_j \tag{2-44}$$

The expected value of the far field quantities can easily be obtained if the excitations $\underline{v}_1$, $\underline{v}_2$, ... are assumed statistically independent.

$$E[\underline{e}_i] = \sum_{j=1}^{n} f_{ij} E[\underline{v}_j] \qquad i = 1, 2, \ldots, m \tag{2-45}$$

where $E[\underline{v}_j]$ is shown in Eq. (2-34).

Suppose that the statistics of the excitations $\underline{v}_1$, $\underline{v}_2$, ... are identical, i.e. the probability distribution functions $f_{\underline{v}_1}(v_1), f_{\underline{v}_2}(v_2), \ldots$ are all identical. Then

$$E[\underline{e}_i] = E[\underline{v}] \sum_{j=1}^{n} f_{ij} \qquad i = 1, 2, \ldots, m \tag{2-46}$$

The ratio of average far field patterns with random error excitations to the error-free patterns (uniformly excited) is obtained by

$$\frac{E[\underline{e}_i]}{e_i} = \frac{E[\underline{v}] \sum f_{ij}}{v \sum f_{ij}} = \frac{E[\underline{v}]}{v} \tag{2-47}$$

If the $\underline{v}_1$, $\underline{v}_2$, ... are not statistically independent, the statistics of far field quantity $\underline{e}_i$ are complicated. However, if no phase

variation is present, then $\underline{v}_1$, $\underline{v}_2$, ... are normally distributed in n-dimensions[23]. The expected value and the variance of $\underline{e}_i$ are, respectively,

$$E[\underline{e}_i] = \sum_{j=1}^{n} f_{ij} E[v_j] \qquad i = 1, \ldots, m \tag{2-48}$$

and

$$\sigma^2_{e_i} = \sum_{j=1}^{n} \sum_{k=1}^{n} f_{ij} f_{ik} E[v_j] E[v_k] \qquad i = 1, \ldots, m \tag{2-49}$$

3. THEORY OF THE PROGRAM

3.1 INTRODUCTION

Computer program PLAN is developed for the purpose of analyzing the effects of phase and amplitude errors on the far field beam pattern of planar arrays of dipoles. Fig. 1 shows a typical planar array of dipoles, lying in the x-z plane, with uniform spacing S_x, S_z in the x,z direction, and with M_2, M_3 dipoles in the x,z directions, respectively. The dipoles are centerfed with ideal voltage sources. It is assumed that the statistical variation of the amplitude and phase of the voltage sources is known. Computer program PLAN is used to compute the statistics of the far field beam pattern, given the statistics of the voltage sources. In other words, the program is used to generate the transfer function between source statistics and beam pattern statistics for the array.

It is assumed that the amplitude and phase of the signal are individually Gaussian*. A nominal phase and amplitude are specified, together with the standard deviation for amplitude (σ_A) and for phase (σ_P).

In the computer program, the voltage sources of Fig. 1 are selected by a random number generator using the given standard deviations σ_A, σ_P. The array is filled in this manner and the far field beam

*It should be noted that the complex voltage is not Gaussian. For a complex signal to be Gaussian, the phase must be uniformly distributed $(0 - 2\pi)$.

pattern computed. The process is then repeated a number of times (typically 40 or 60 times*) and the statistics of the magnitude and phase of the resulting far field beam patterns and gains are computed. This analysis can be carried out at fundamental frequency for a halfwave dipole ($L = 0.5\lambda$) and at second ($L = 1.0\lambda$) and third ($L = 1.5\lambda$) harmonic and thus harmonic levels can be established relative to fundamental. Mean beam patterns are computed, as well as the individual beam patterns and the expected range of variation of the patterns at fundamental and harmonic frequencies.

Once the array is filled up by the random number generator, the problem is treated as a deterministic one. The method of moments [3,9] is used to compute the far field beam patterns. In the method of moments, the dipole antennas are subsectioned as shown in Fig. 2. Antenna currents are not assumed but are computed. All mutuals are taken fully into account. The relationship between currents and voltages is given by

$$[v] = [z]]i] \tag{3-1}$$

where [z] is the generalized impedance matrix. z_{ij} is the voltage (proportional to the tangential electric field) at subsection i, due to a current of unit magnitude flowing on subsection j. [v] is a column vector representing the known voltage excitation of the subsections and [i] is a column vector representing the unknown currents.

*This repetitive procedure can be implemented efficiently since the second and subsequent iterations are much faster than the first.

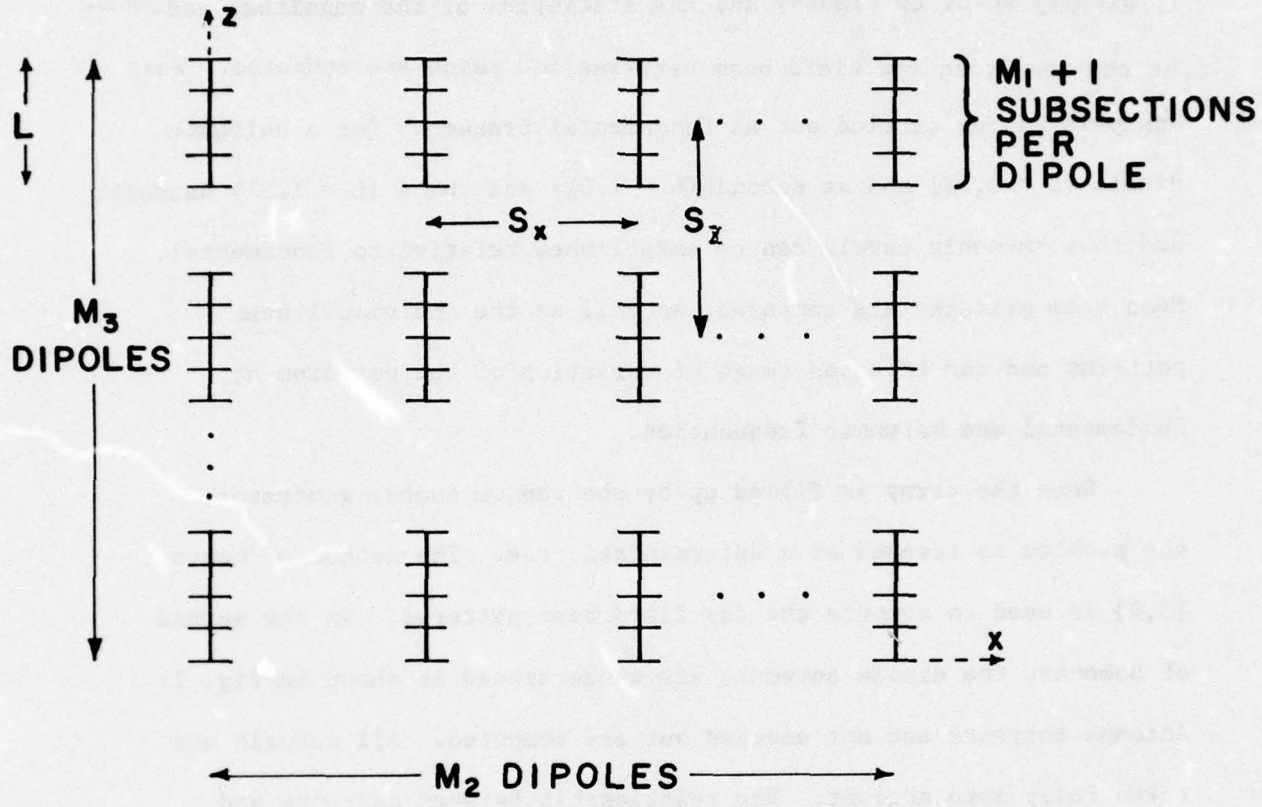

M_1 = # OF EXPANSION FUNCTIONS PER DIPOLE

$M_2 M_3$ = # OF ANTENNAS

$M_1 M_2 M_3$ = # OF UNKNOWNS (# OF EXPANSION FUNCTIONS)

Fig. 2. Thin wire model of a planar array with spacing S_x, S_z in the X, Z directions.

Eq. (3-1) is solved by matrix inversion to obtain

$$[i] = [z]^{-1}[v] = [y][v] \tag{3-2}$$

Thus, the currents are found by matrix inversion; the far fields are then determined from the currents.

There are many current representations possible within the method of moments. In program PLAN, a Galerkin [9] solution with piecewise sinusoidal expansion and weighting functions is used. This yields a very accurate solution and permits one to use a relatively small number of current unknowns.

For the planar array of subsectioned dipoles shown in Fig. 2, the generalized impedance matrix has certain special features. There are a number of symmetries present and the impedance matrix has the form of a block-Toeplitz matrix. In addition, the voltage excitation column matrix [v] consists mostly of zeros since most subsections are not excited. Subroutines are developed to take advantage of these features. The result is an efficient computer program which may be used to treat up to 100 dipoles at the third harmonic ($L = 1.5\lambda$). The analysis can be carried out at any frequency.

The program PLAN can also be used for deterministic array analysis, one need merely set $\sigma_A = \sigma_P = 0$ and just carry out one computation (no iterations). The program is reasonably efficient when used in this manner.

Statistical effects in antennas have been treated previously [4-7] but the previous analyses have not taken the effect of mutuals fully

into account. The program PLAN permits one to include mutuals or not. Results show, as expected, that the effect of mutuals is significant. If mutuals are excluded, the array problem becomes quite a simple one.

In this introductory section, the basic methods employed in program PLAN are outlined briefly. The details of these methods are covered in sections 3.2 to 3.7.

3.2 GENERATING RANDOM ERRORS IN THE EXCITATIONS

The process of filling up the array of Fig. 1 with voltage sources chosen on a statistical basis was briefly described in section 3.1. It is assumed that the magnitude and phase of the voltage excitation $\underline{v}$ are both normally distributed (truncated), e.g.

$$\underline{V} = \underline{A}e^{i\underline{B}} \tag{3-3}$$

See Section 2.2 for details of the statistical formulation.

A subroutine is used to generate normally distributed random numbers for amplitude and phase by the power residue method [10]. Negative random numbers generated for $\underline{A}$ as well as the random numbers outside the $[\theta_m-\pi, \theta_m+\pi]$ range for $\underline{\theta}_i$ are discarded.

$\underline{A}$ and $\underline{\theta}$ are also assumed to be statistically independent in this program. Thus, two normally distributed random numbers $\underline{a}$ and $\underline{\theta}$ are generated separately by the subroutine, and combined to form the voltage excitation $\underline{v}$ (Eq. 3-3).

In fact, a bivariate sampling process can be chosen to generate two jointly normal random numbers with specified correlation coefficient ρ, $(-1 \leq \rho \leq 1)$, which enables one to relate the amplitude error

to the phase error in any degree, i.e. from no correlation to linearly dependent .

The bivariate sampling procedure consists simply of taking two random numbers y_1 and y_2, say, from the normal distribution with mean zero and standard deviation 1, and forming

$$a = a_m + \sigma_a y_1 \tag{3-4a}$$

$$\theta = \theta_m + \rho a + \sqrt{1-\rho^2}\, \sigma_\theta y_2 \tag{3-4b}$$

The random number generator routine in this program is a modification of one appearing in the IBM Scientific Subroutine Package* [11].

The array is thus filled up with sources chosen by the subroutine. The analysis is carried out to obtain the far-field beam pattern. Then the array is filled up again and the analysis repeated. A number of such analysis are carried out and the statistics of the resulting beam pattern are then computed.

In the computer program, the phase and amplitude error of an individual source are assumed to be independent ($\rho = 0$). In addition, the voltages $\underline{v}_1, \underline{v}_2, \ldots, \underline{v}_n$ are assumed to be independent. As noted, a bivariate normal distribution ($\rho \neq 0$) can readily be treated, and in addition, correlation between sources $\underline{v}_1 \ldots \underline{v}_n$ can be taken into account using the covariance matrix (some subroutines are already available for this purpose in IMSL). Also, the assumption of a Gaussian distribution is not critical to the analysis. Any other distribution

*The newest version of the Scientific Subroutine Package is the International Mathematical Statistical Library (IMSL) which includes more random number generating subroutines.

can be simulated; it is necessary only to substitute a new random number generator with the desired statistics.

3.3 SETTING UP THE MATRIX EQUATION

The first step in the method of moments technique is to set up the matrix equation (Eq. (3-1)), i.e. to fill the matrix [z]. Within the method of moments, there are many possible methods for the computation of the typical element z_{ij} of the generalized impedance matrix. If the same functions are used for expansion and weighting [9], then a Galerkin (variational) solution results. In program PLAN, a Galerkin solution with piecewise sinusoidal expansion and weighting functions is used, similar to those developed by Richmond [12] and Sarkar [13]. The subroutine used in PLAN is a modification of the program of Sarkar [13], the principal modification being the addition of a simple method of filling the matrix from a knowledge of the first row only. This simplification results from the symmetries present in the array; the details of these symmetries are discussed in section 3-4.

The use of piecewise sinusoidal expansion and weighting functions yields a very accurate solution of the array problem and permits one to use a relatively small number of unknowns. Three, five and seven expansion functions (corresponding to 3,5,7 unknowns) per dipole are used for $L = 0.5, 1.0, 1.5\lambda$, respectively.

A Galerkin solution results in an impedance matrix which is symmetric about the main diagonal i.e. $z_{ij} = z_{ji}$. This leads to a savings in inversion time and storage.

The piecewise sinusoidal function used can be written as

$$I_n(Z) = \hat{\mu}_Z \frac{\sin k(Z - Z_{n-1})}{\sin k(Z_n - Z_{n-1})} \qquad Z_{n-1} \leq Z < Z_n \qquad (3\text{-}5a)$$

$$= \hat{\mu}_Z \frac{\sin k(Z_{n+1} - Z)}{\sin k(Z_{n+1} - Z_n)} \qquad Z_n \leq Z < Z_{n+1} \qquad (3\text{-}5b)$$

where $\hat{\mu}_Z$ is a unit vector in the z direction, and $k = 2\pi/\lambda$. Each expansion function exists over two adjacent subsections; the resulting current approximation for a dipole is illustrated in Fig. 3. Note that the number of subsections in this case is always one more than the number of expansion functions.

3.4 THE GENERALIZED IMPEDANCE MATRIX OF A PLANAR ARRAY

3.4.1 Impedance Matrix of an Isolated Dipole

Fig. 4a shows an isolated dipole antenna and Fig. 4b shows the corresponding filamentary model commonly used in the method of moments for thin-wire antennas*. The number of subsections is n+1; the number of expansion functions is n. The generalized impedance matrix for this antenna may be written as

$$[z] = \begin{bmatrix} z_{11} & \cdots & z_{1n} \\ \vdots & & \vdots \\ z_{n1} & \cdots & z_{nn} \end{bmatrix} \qquad (3\text{-}6)$$

*Note that the dipole radius a is taken fully into account by applying boundary conditions at the wire surface.

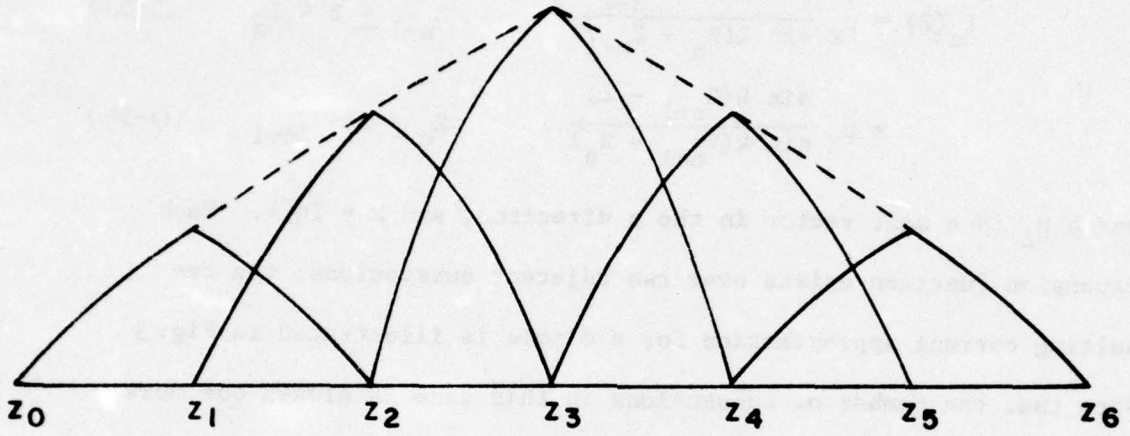

Fig. 3. Sinusoidal current expansion functions.

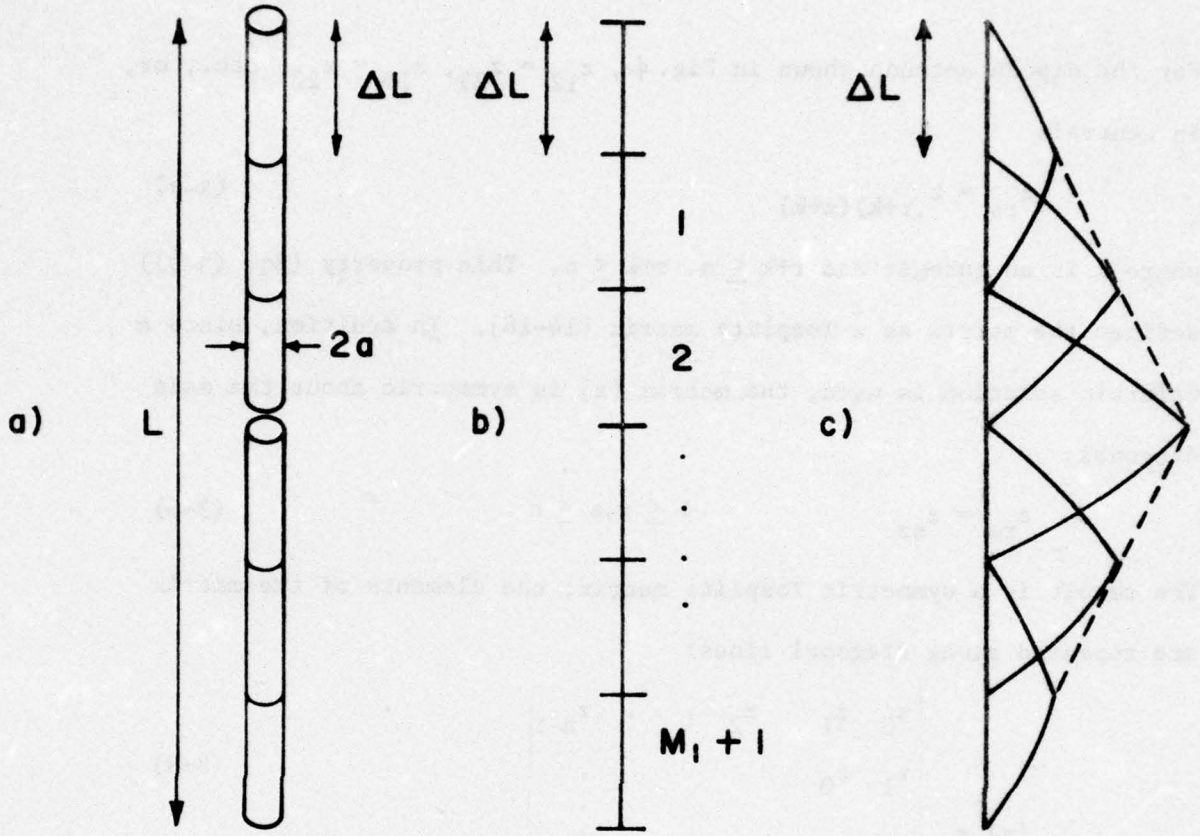

ΔL = SUBSECTION LENGTH

OF SUBSECTIONS = $M_1 + 1$

OF EXPANSION FUNCTIONS = $M_1 = n$

$z_{ij} = z_{ji}$ (FOR A GALERKIN SOLUTION)

$z_{ij} = z_{(i+k)(j+k)}$ (TOEPLITZ PROPERTY)

Fig. 4. An isolated dipole (a) dipole (b) filamentary model (c) expansion functions.

For the dipole antenna shown in Fig. 4, $z_{12} = z_{23}$, $z_{11} = z_{22}$, etc., or, in general

$$z_{rs} = z_{(r+k)(s+k)} \tag{3-7}$$

where k is an integer and $r+k \leq n$, $s+k \leq n$. This property (Eq. (3-7)) defines the matrix as a Toeplitz matrix [14-18]. In addition, since a Galerkin solution is used, the matrix [z] is symmetric about the main diagonal:

$$z_{rs} = z_{sr} \qquad 1 \leq r,s \leq n \tag{3-8}$$

The result is a symmetric Toeplitz matrix; the elements of the matrix are repeated along diagonal lines:

$$[z] = \begin{bmatrix} z_0 & z_1 & z_2 & \cdots & z_{n-1} \\ z_1 & z_0 & & & \cdot \\ \cdot & \cdot & & & \cdot \\ \cdot & \cdot & & & z_1 \\ z_{n-1} & z_{n-2} & \cdot & \cdots & z_0 \end{bmatrix} \tag{3-9}$$

where z_o defines the self-impedance term of one subsection and $z_{|r-s|}$ defines the mutual impedance term between two subsections r and s.

Note that the symmetric Toeplitz matrix shown above can be generated by the first row or column. This greatly simplifies the fill time (fill time is proportional to n rather than n^2) and reduces the computer storage required. A non-symmetric Toeplitz matrix would be generated by knowledge of the first row and the first column.

Toeplitz matrices occur in the theory of discrete random processes.

Several special algorithms have been developed for the inversion of such matrices [15-16]. The matrix [y] is defined as the inverse of [z]:

$$[y] = [z]^{-1} = \begin{bmatrix} y_{11} & \cdots & y_{1n} \\ \cdot & & \cdot \\ \cdot & & \cdot \\ y_{n1} & & y_{nn} \end{bmatrix} \tag{3-10}$$

The Toeplitz symmetry of the [z] matrix is lost upon inversion, but there is a fourfold symmetry remaining. This can be explained by the definition of y_{ij} and Fig. 5.

$y_{ii} = \frac{i_i}{v_i}$ (with all other v's equal to zero). This represents the input admittance at port i (defined in terms of the ith expansion function) *with all other ports short circuited.*

$y_{ij} = \frac{i_i}{v_j}$ (with all other v's equal to zero). This represents the transfer admittance between ports i and j with all other ports short circuited.

[y] is symmetrical about the main diagonal because a Galerkin solution is used, i.e. $z_{ij} = z_{ji}$ implies

$$y_{ij} = y_{ji} \tag{3-11}$$

In addition, [y] is symmetrical about the secondary diagonal (the diagonal from y_{1n} to y_{n1}):

$$y_{ij} = y_{(n-j+1)(n-i+1)} \qquad \text{for } (1 \leq i \leq n,\ 1 \leq j \leq n). \tag{3-12}$$

This property can be explained by reference to Fig. 5; it is a consequence of physical symmetry about the center of the dipole.

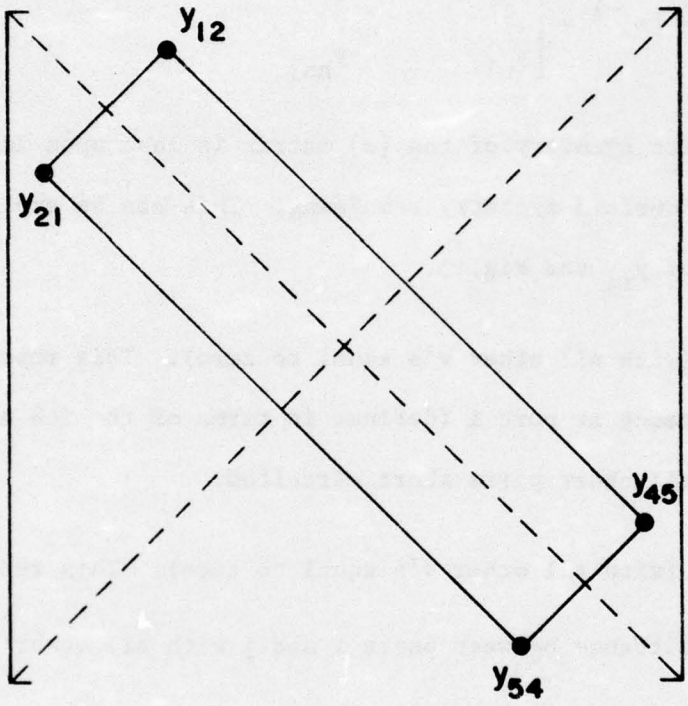

Fig. 5. An isolated dipole - symmetries of the [Y] matrix ($M_1 = 5$).

Thus the [y] has a fourfold symmetry (about main and secondary diagonals) as illustrated in Fig. 5.

In addition to the symmetries in [z] and [y], which may be called redundancies in impedance and admittance elements, and which are independent of excitation, there may be symmetries in the currents. For instance, if the dipole is center fed, there is an additional two-fold symmetry in currents. Current symmetries can readily be taken into account by using special symmetry subroutines which reduce the number of unknowns if the current symmetries present are specified. In program PLAN there are no such symmetries present because of the mutual effects and because of the randomness of the voltage excitations.

3.4.2 Impedance Matrix of a Linear Array

Fig. 6a shows an equally spaced linear array with N+1 identical dipoles. The corresponding thin-wire model is shown in Fig. 6b . M1 expansion functions are used for each dipole.

The generalized impedance matrix is a square matrix of order M1 x (N+1). For a suitable ordering of expansion functions*, the generalized impedance matrix can be partioned as

$$[z] = \begin{bmatrix} \underset{\sim}{z}_{11} & \underset{\sim}{z}_{12} & \cdots & \underset{\sim}{z}_{1(N+1)} \\ \underset{\sim}{z}_{21} & \underset{\sim}{z}_{22} & & \\ \vdots & & & \vdots \\ \underset{\sim}{z}_{(N+1)1} & & & \underset{\sim}{z}_{N+1 \times N+1} \end{bmatrix} \qquad (3\text{-}13)$$

*The expansion functions are ordered continuously over each dipole, beginning at a corresponding point on each dipole as shown in Fig. 6b.

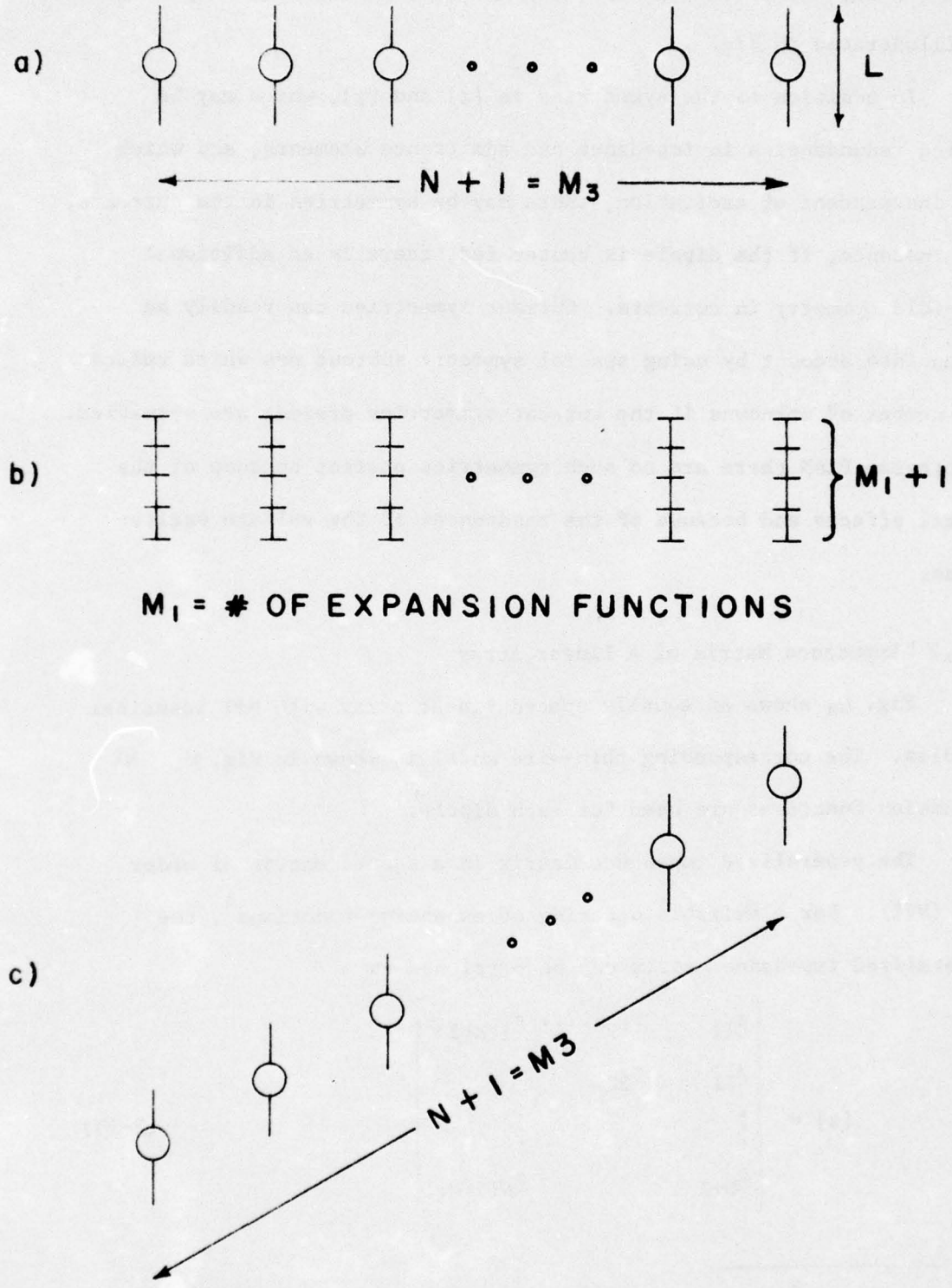

Fig. 6. An equally spaced linear array with N+1 identical dipoles (a) perpendicular line case (b) thin-wire model (c) skewed line case.

where each submatrix $\underset{\sim}{z}_{ij}$ is a square matrix of order M1. $\underset{\sim}{z}_{ii}$ represents interaction among portions of antenna i and $\underset{\sim}{z}_{ij}$ represents interactions between antennas i and j*. $\underset{\sim}{z}_{ii}$ is thus a matrix identical to that of Eq. (3-6) for the isolated dipole. Since all antennas are identical, all $\underset{\sim}{z}_{ii}$ are identical, i.e.

$$\underset{\sim}{z}_{ii} \triangleq \underset{\sim}{z}_0 \qquad \text{for } i = 1,2,\ldots,N+1 \tag{3-14}$$

where $\triangleq$ designates a definition. All $\underset{\sim}{z}_{ii}$ are thus symmetric Toeplitz matrices (symmetric because a Galerkin solution is used).

The typical submatrix $\underset{\sim}{z}_{ij}$ involves the interactions between antennas i and j. The matrix [z] is symmetric about the main diagonal and thus

$$\underset{\sim}{z}_{ij} = \underset{\sim}{z}_{ji}^{T} \tag{3-15}$$

in general. For the particular case in which the line of the array is perpendicular to the dipoles (the "perpendicular line" case of Fig. 6a)

$$\underset{\sim}{z}_{ij} = \underset{\sim}{z}_{ji}^{T} = \underset{\sim}{z}_{ji} \tag{3-16}$$

where superscript T indicates the transpose operation.

For members i,j of the linear arrays of Fig.6a, $\underset{\sim}{z}_{ij}$ depends only on the distance between antenna centers and thus

---

*Note that each generalized impedance element represents the interaction between two current expansions. For $\underset{\sim}{z}_{ii}$, both expansion functions are located on the same antenna and, for $\underset{\sim}{z}_{ij}$, the expansion functions are located on different antennas ($i \neq j$).

$$\underset{\sim}{z}_{ij} \triangleq \underset{\sim}{z}_{|i-j|} \tag{3-17}$$

for $(1 \leq i \leq N+1,\ 1 \leq j \leq N+1)$.

$\underset{\sim}{z}_{ij}$ is itself a Toeplitz matrix, since the elements of the matrix depend only on the difference between subscripts. $\underset{\sim}{z}_{ij}$ is itself a symmetric Toeplitz matrix for the "perpendicular line" case.

The resulting entire impedance matrix [z] is then

$$[z] = \begin{bmatrix} \underset{\sim}{z}_0 & \underset{\sim}{z}_1 & \cdot & \cdot & \cdot & \underset{\sim}{z}_N \\ \underset{\sim}{z}_1^T & \underset{\sim}{z}_0 & \cdot & \cdot & \cdot & \underset{\sim}{z}_{N-1} \\ \cdot & & & & & \cdot \\ \cdot & & & & & \cdot \\ \underset{\sim}{z}_N^T & \underset{\sim}{z}_{N-1}^T & \cdot & \cdot & & \underset{\sim}{z}_0 \end{bmatrix} \tag{3-18}$$

which is simplified in the "perpendicular line" case to

$$z = \begin{bmatrix} \underset{\sim}{z}_0 & \underset{\sim}{z}_1 & \cdot & \cdot & \underset{\sim}{z}_N \\ \underset{\sim}{z}_1 & \underset{\sim}{z}_0 & & & \underset{\sim}{z}_{N-1} \\ \vdots & & & & \\ \underset{\sim}{z}_N & \underset{\sim}{z}_{N-1} & & & \underset{\sim}{z}_0 \end{bmatrix} \tag{3-19}$$

Note that for Eq. (3-19), all submatrices are symmetric Toeplitz matrices.

A matrix of the form (3-19) is called a "block-Toeplitz" matrix since Eq. (3-19) is of the same form as Eq. (3-9) if elements are replaced with submatrices, i.e. the blocks are repeated along diagonal lines.

The entire matrix of (3-18) can be generated by the first row and the first column. The entire matrix of (3-19) can be generated by the first row or the first column. This latter statement can be verified by noting that the matrix can be generated by the first row of (N+1) submatrices ($\underset{\sim}{z}_0$, $\underset{\sim}{z}_1$, ... $\underset{\sim}{z}_N$). Each submatrix can be generated from its first row since it is individually Toeplitz. Thus the number of independent impedance elements is equal to the number of elements in the first row, which is equal to $M1(N+1)$ or or M_1M_3.

[y], the inverse of [z], is designated as follows:

$$[y] = \begin{bmatrix} \underset{\sim}{y}_{00} & \underset{\sim}{y}_{01} & \underset{\sim}{y}_{02} \cdots & \underset{\sim}{y}_{0N} \\ \underset{\sim}{y}_{10} & \underset{\sim}{y}_{11} & \underset{\sim}{y}_{12} & \underset{\sim}{y}_{1N} \\ \vdots & & & \\ \underset{\sim}{y}_{N0} & \underset{\sim}{y}_{N1} & \underset{\sim}{y}_{N2} \cdots & \underset{\sim}{y}_{NN} \end{bmatrix} \qquad (3\text{-}20)$$

Since a Galerkin solution is used, the full matrix is symmetrical about the main diagonal, and the blocks $\underset{\sim}{y}_{ij}$ are symmetrical about the main diagonal after transposition, i.e.

$$\underset{\sim}{y}_{ij} = \underset{\sim}{y}^{T}_{ji} \qquad \text{for } (0 \leq i, j \leq N) \qquad (3\text{-}21)$$

In addition there is a fourfold symmetry of the blocks:

$$\underset{\sim}{y}_{ij} = \underset{\sim}{y}_{(N-i)(N-j)} = \underset{\sim}{y}^{T}_{(N-j)(N-i)} \qquad (3\text{-}22)$$

Thus the entire y matrix can be generated from one-quarter of the blocks (see Fig. 7). The above is valid for both the "perpendicular line" and "skewed line" cases.

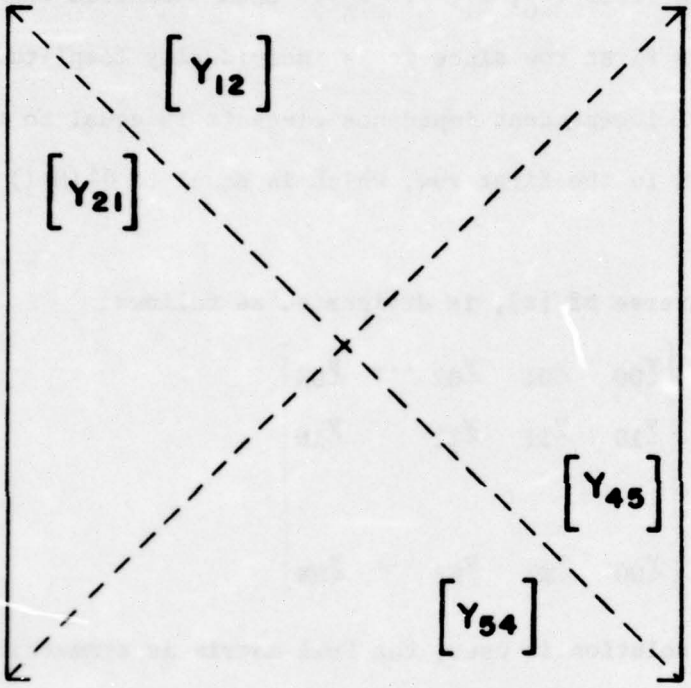

Fig. 7. An equally spaced linear array with N+1 identical dipoles - symmetries of the [Y] matrix ($M_3 = 5$).

The individual blocks also have some redundancies of admittance elements. Consider first the blocks y_{ii}. These blocks have a fourfold symmetry about the main diagonal for the "perpendicular line" (see Fig. 6a). For the "skewed line" case, there is a twofold symmetry about the main diagonal (see Fig. 6c).

Next consider the blocks y_{ij}. First of all the blocks along the secondary diagonal have a fourfold symmetry in the "perpendicular line" case which is lost in the "skewed line" case. The only blocks remaining are those both off the main and secondary diagonals. These blocks have a different type of symmetry; namely a twofold reflection symmetry about the center element in the "perpendicular line" case (see Fig. 7). This symmetry is lost in the "skewed line" case.

In summary, there are many redundancies in the [z] and [y] matrices. For the "perpendicular line" case [z] can be generated by the first row; in other words there are $M_1(N+1)$ independent elements of [z]. For the "perpendicular line" case, there is a fourfold symmetry of blocks, and at least a twofold symmetry in the blocks themselves. [y] can thus be generated by somewhat less than one eighth of the elements.

3.4.3 Impedance Matrix of a Rectangular Planar Array.

The impedance and admittance matrices of a planar array are, of course, considerably more complex than those of the linear array. It would require considerable space to present all of the relationships in detail. Some of the essential relationships can be outlined

briefly by considering the planar array as a linear array of elements, each element being a linear array itself.

For example the rectangular planar array of Fig. 8 can be treated as a linear array by taking either (a) a row of dipoles or (b) a column of dipoles as an element. The resulting linear arrays are shown in Figs. 9a, 9b.

The impedance matrix of the array may be written as follows:

$$[z] = \begin{bmatrix} \underset{\sim}{Z}_{11} & \underset{\sim}{Z}_{12} & \cdot & \cdot & \underset{\sim}{Z}_{1(N+1)} \\ \underset{\sim}{Z}_{21} & \underset{\sim}{Z}_{22} & & & \underset{\sim}{Z}_{2(N+1)} \\ \cdot & & & & \cdot \\ \cdot & & & & \cdot \\ \underset{\sim}{Z}_{(N+1)1} & \underset{\sim}{Z}_{(N+1)2} & \cdot & \cdot & \underset{\sim}{Z}_{(N+1)(N+1)} \end{bmatrix} \tag{3-23}$$

where $\underset{\sim}{Z}_{ii}$ denotes interaction among expansion functions of array i and $\underset{\sim}{Z}_{ij}$ denotes interactions between arrays i and j.

Since all arrays are identical $\underset{\sim}{Z}_{ii}$ may be defined as $\underset{\sim}{Z}_0$ and $\underset{\sim}{Z}_{ij}$ may be defined as $\underset{\sim}{Z}_{|i-j|}$, in analogy to Eqs. (3-14) and (3-17). The result is a matrix of the block-Toeplitz form:

$$[z] = \begin{bmatrix} \underset{\sim}{Z}_0 & \underset{\sim}{Z}_1 & \underset{\sim}{Z}_2 & \cdot\cdot & \underset{\sim}{Z}_N \\ \underset{\sim}{Z}_1 & \underset{\sim}{Z}_0 & \underset{\sim}{Z}_1 & & \underset{\sim}{Z}_{N-1} \\ \vdots & & & & \vdots \\ \underset{\sim}{Z}_N & \underset{\sim}{Z}_{N-1} & \underset{\sim}{Z}_{N-2} & \cdot\cdot & \underset{\sim}{Z}_0 \end{bmatrix} \tag{3-24}$$

Note that $\underset{\sim}{Z}_0$ is the impedance matrix of an array and it is thus also of the block-Toeplitz form. The same is true of the off-diagonal blocks. Since each block of (3-24) is block-Toeplitz, the impedance

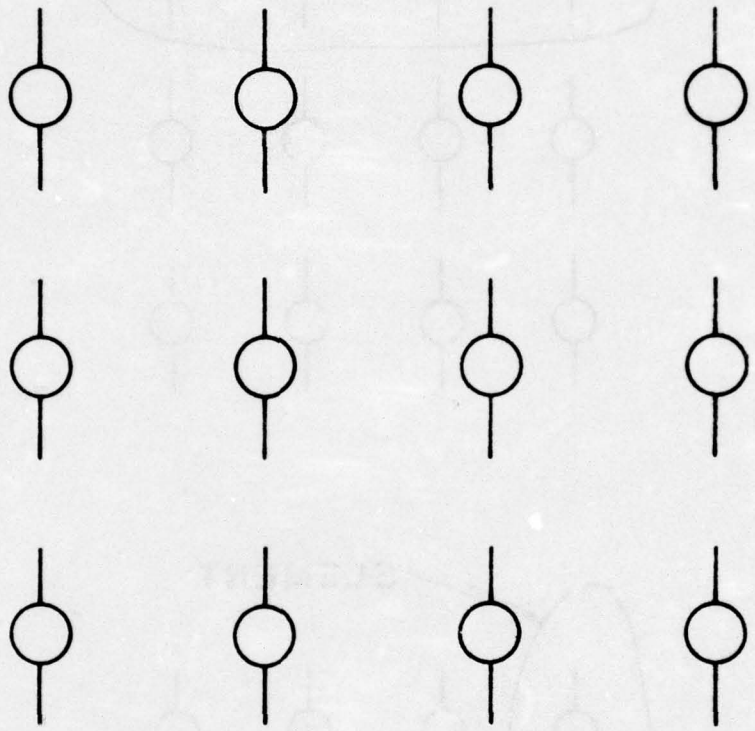

Fig. 8. A rectangular planar array with 3 x 4 identical dipoles.

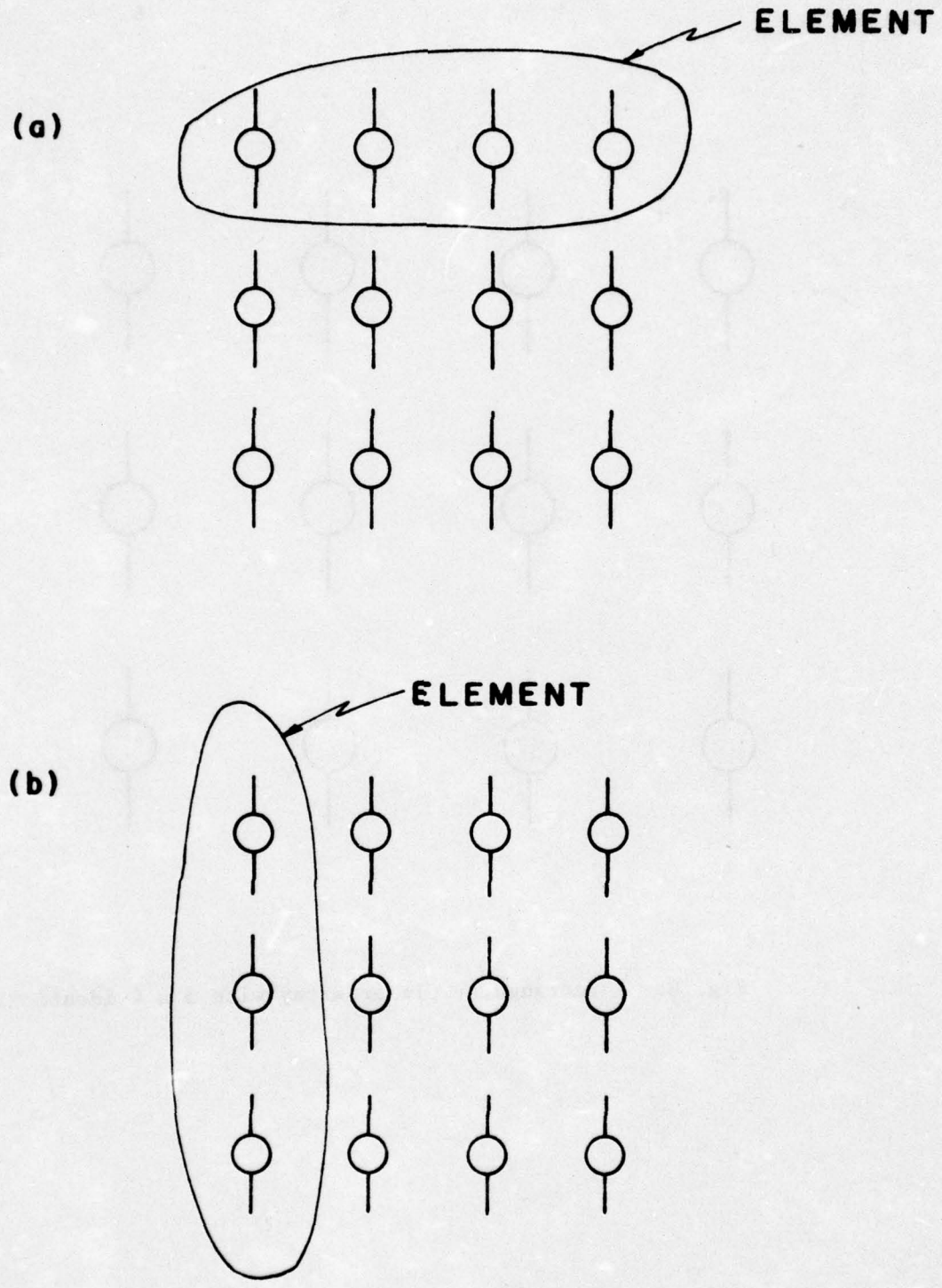

Fig. 9. A rectangular planar array (a) row element (b) column element.

matrix of a planar array may be termed a block-block Toeplitz matrix.

If the planar array is square (M2 = M3) then the matrix inversion problem can be treated equally well by taking (a) rows or (b) columns of dipoles as elements. If the planar array is not a square, the shorter side of the rectangular array should be taken as an element. This gives the best results as explained in Appendix A.

For example, a planar array of 3 by 4 dipoles is shown in Fig. 9. It is preferable to choose the 3-dipole column as an element rather than the 4-dipole row. The resulting impedance matrix will contain 16 submatrices in comparison with the 9 submatrices resulting from the choice of the 4-dipole row as an element.

Note that by analogy to the previous section the generalized impedance matrix of the rectangular planar array can be generated from the first row or column of [z].

The admittance matrix [y] has a fourfold symmetry about the main and secondary diagonals, as before, for the rectangular planar array.

3.5 SOLUTION OF THE MATRIX EQUATION

The matrix equation for the planar array,

$$[v] = [z][i] \tag{3-25}$$

is first set up using the methods described in section 3.3 and the symmetries outlined in 3.4. The solution

$$[i] = [z]^{-1}[v] = [y][v] \tag{3-26}$$

is obtained in two steps. The first step involves the inversion of the generalized impedance matrix [z] which is of the block-block-Toeplitz

form. This is accomplished by a special routine which is described in detail in Appendix A. Essentially the routine is derived from the method used by Sinnott for linear arrays. In the routine described in Appendix A, there are three additions to the method of Sinnott:

(1) The method is applied to planar arrays by considering either a column or row of elements as an element. Details are given in Appendix A.

(2) The zeros of the excitation matrix are utilized to simplify the inversion and reduce the core storage. Most of the elements of the voltage excitation matrix [v] are zeros. In the final solution (3-26) then, only the columns of the matrix [y] corresponding to the non-zero elements of [v] are required. In other words, the entire [y] matrix is not required. The inversion routine can be correspondingly simplified. In addition, the matrix multiplication (3-26) can be simplified by omitting the corresponding multiplications. This is explained further in Appendix A.

(3) The main (core) computer memory requirements are reduced by the use of peripheral devices (disk storage). Two disc files are used as temporary storage. Details are given in Appendix A.

3.6 COMPUTATION OF CURRENTS - ZEROS OF THE EXCITATION MATRIX

As noted in section 3.5, most of the elements of the voltage excitation matrix [v] are zeros. Therefore, only a few columns of [y] are required in the matrix multiplication [y][v], namely those corresponding to the non-zero elements of [v].

To illustrate the method, consider [y] and [v] matrices where [y] is an nxn matrix and [v] is an n-element column vector. There are only certain non-zero elements in [v]. Suppose that there are k such non-zero elements. The matrix equation (3-26) may then be written

$$[i] = [Y_1 Y_2 \ \ldots \ Y_k] \begin{bmatrix} v_1 \\ v_2 \\ \vdots \\ v_k \end{bmatrix} \tag{3-27}$$

where the elements $v_1 \ \ldots \ v_k$ are non-zero. For simplicity, use a numbering system for expansion functions, unknown currents and voltages which starts with the driven sections 1 ... k. Then the matrix equation becomes

$$[i] = [Y_1 Y_2 \ \ldots \ Y_k \ \ldots \ Y_n] \begin{bmatrix} v_1 \\ v_2 \\ \vdots \\ v_k \\ \vdots \\ 0 \end{bmatrix} \tag{3-28}$$

where Y_i is the ith column of the [y] matrix. Eq. (3-26) may, of course, be simplified to

$$[i] = [Y_1\ Y_2\ \ldots\ Y_k] \begin{bmatrix} v_1 \\ v_2 \\ \vdots \\ v_k \end{bmatrix} \qquad (3\text{-}29)$$

Only the columns $Y_1 \ldots Y_k$ of the [y] matrix need be computed and only the multiplications indicated in Eq. (3-29) need be carried out.

Thus the inversion routine and the computation of currents can be simplified by taking advantage of the zeros of the excitation matrix. This is especially useful for cases where the number of expansion functions per dipole is large, for instance, for the third harmonic analysis of a dipole which is one-half wavelength long at the fundamental frequency. In the computed results, seven subsections per dipole have typically been used for the third harmonic analysis. For this choice, only one seventh of the columns of the [y] matrix need be computed or stored and only one seventh of the multiplications of Eq. (3-26) need be carried out.

3.7 COMPUTATION OF FAR FIELDS

Once the currents [i] have been obtained, the far fields may be found directly by an additional matrix multiplication. For z-directed dipoles

$$[E] = [F][i] \qquad (3\text{-}30)$$

where [E] is an n-element column vector representing values of the electric field at n different points in the far field. F_{ij} is the electric field at point i (in the far field) due to current expansion function j of unit magnitude. Thus, [F] is proportioned to the far field form of the generalized impedance matrix [z].

Once the far field [E] has been calculated, the array gain, G, may also be found by

$$G \triangleq \frac{4\pi R^2 |E|^2}{P_{in}} \tag{3-31}$$

where P_{in} is the total input power to the array, which can be obtained simply by adding the input powers to each element of the array.

$$P_{in} = \mathrm{Re} \sum_{i=1}^{N+1} V_i I_i^* \tag{3-32}$$

There are many subroutines available for the computation of far fields. The subroutine developed by Sarkar [13] has been utilized here. This subroutine computes the far fields due to a piecewise sinusoidal current distribution.

3.8 PROCESSING OF THE FAR FIELD DATA

The sampling procedure for filling up the array is described in section 3.2. Given the statistics of the sources, i.e., the standard deviations σ_A, σ_P in amplitude and phase, a random number generator is used to select a set of sources for the array. Then the matrix equation is solved and the far fields are computed.

Next a new set of sources is selected for the array and the whole process is repeated. Of course, on the second round, [y] need not be recomputed, but only the matrix multiplications [y][v] and [F][i] need be carried out. This is fortunate, since the matrix multiplications are very rapid as compared to the original matrix inversion $[y] = [z]^{-1}$.

The process is repeated further. Finally, K sets of array sources have been selected and K sets of currents and far field data have been

obtained. Only one matrix inversion $[y] = [z]^{-1}$ has been performed; K matrix multiplications [y][i] and [F][i] have been carried out. Typical values for K are 40, 60 in the data shown in section 4. K is specified by the user as part of the input data.

Now the far field data must be processed. First the complex far field data is converted to magnitude form. At each point in the far field, the average magnitude of the far field and gain is obtained, yielding the average beam pattern and gain magnitude. Next the magnitude data at each far field point is examined and the standard deviation σ is obtained. Mean (M) and Mean minus sigma (M-σ) beam patterns are then plotted for the array and the given source statistics. The beam pattern M-σ reveals the expected range of variation for the given problem. One can, of course, examine further the data at each far field point and readily obtain any statistics desired.

For example, the covariance matrix of the far field points tells the correlation between each far field point. The Tchebycheff inequality equation, i.e.

$$P(|x - x_m| > \varepsilon) \leq \frac{\sigma^2}{\varepsilon^2} \quad , (\varepsilon > 0) \tag{3-33}$$

gives a range of variation with specified probability of occurrence within that range.

All beam patterns are normalized, but in addition, the absolute level of the maximum is indicated by a normalization number which is printed on each beam pattern plot.

The procedure outlined above can be carried out at harmonic ($2F_0$,$3F_0$) as well as fundamental (F_0) frequencies and thus the levels of harmonics relative to fundamental may be obtained.

3.9 GAIN DEGRADATION

Random phase and amplitude errors in an array have the effect of reducing directive gain. For large phase and amplitude errors, this gain reduction is quite significant. This effect is important in the analysis of 2nd and 3rd harmonic emissions in arrays since phase and amplitude errors are in general significant at these frequencies [1]. Thus, there will be in general at 2nd and 3rd harmonics a significant reduction in gain over that obtained from an optimally-excited array (such as a uniformly excited array). The gain of a uniformly excited (non-random) array is denoted G_o.

There are several definitions of gain which are of interest here. Suppose, for instance, that an array is excited for broadside radiation. Consider a set of typical sample beam patterns such as those shown in Fig. 18-20. One important quantity would be the expected directive gain for a given location (θ_o,ϕ_o).

$$E[\underline{G}(\theta_o,\phi_o)] = \text{Expected directive gain at } \theta_o\phi_o \tag{3-34}$$

The expected gain will, of course, vary with location. It represents the "expected" interference for an observer at (θ_o,ϕ_o).

The maximum expected gain is also of interest, where the maximum expected gain is defined as the maximum value of the expected gain over all angles θ_o,ϕ_o. This quantity is denoted G_1:

$$\begin{aligned} G_1 &= \text{Maximum Expected Gain} \\ &= \text{MAX}[E[\underline{G}(\theta_o,\phi_o)]] \end{aligned} \tag{3-35}$$

(where the above quantity is the maximum over all angles θ_o,ϕ_o).

For the samples of Figs. 18-20, these values of maximum directive gain occur at different angles. Maximum gain is thus defined as the maximum directive gain of an individual sample pattern.

To compute maximum expected gain, one computes an expected gain (by averaging over the sample patterns) for each angle θ_o, ϕ_o and then chooses the largest of these expected gains. For nominal broadside excitation, for instance, maximum expected gain will occur at broadside. G_1 thus represents the expected gain at a particular position at which the expected gain is largest.

Another important quantity is the "expected maximum gain" which is defined as follows. Consider the sample patterns such as those of Figs. 18-20. For a particular sample pattern, there is a value of maximum directive gain. The expected maximum gain is then an average over all samples:

$$G_2 = \text{Expected maximum gain}$$
$$= E[\underline{G}_{max}] \qquad (3\text{-}36)$$

where G_{max} is the maximum directive gain of a particular sample pattern and $\underline{G}_{max}$ is the associated random variable. The expected maximum gain thus represents an important measure of worst-case interference capability.

The quantities G_o, $E[\underline{G}(\theta_o,\phi_o)]$, G_1, G_2 differ significantly in many cases. To adequately analyze an array with random errors, it may be necessary to take all these quantities into account.

3.10 ADDITIONAL BEAM PATTERN QUANTITIES

The quantities discussed in sections 3.1-3.9 are computed in program PLAN. There are, of course, other beam pattern quantities which could readily be computed from the sample patterns by modification of program PLAN. Some of these are (1) expected beam pointing error, (2) expected beam broadening, (3) expected ratio of power in main beam to power in sidelobes, etc.

3.11 SOME SPECIAL PLANAR ARRAYS

Computer program PLAN (described in section 3) is designed to solve problems for the class of rectangular or square planar arrays. It can also readily be modified to treat some other special planar arrays. It is the purpose of this section to describe these special arrays and the modifications necessary for their analysis.

First, consider the class of triangular planar arrays (Fig. 10) which is often encountered in practical design. If two adjacent columns (Fig. 11a) of antennas are taken as an element, the result is a linear array (perpendicular case). If two adjacent rows (Fig. 11b) are taken as an element, the result is also a linear array (skewed line case). In either case, the generalized impedance matrix can be partioned as:

$$[z] = \begin{bmatrix} \underset{\sim}{Z}_{11} & \underset{\sim}{Z}_{1\,2} & \cdots & \underset{\sim}{Z}_{1\,(N+1)} \\ \underset{\sim}{Z}_{2\,1} & \underset{\sim}{Z}_{2\,2} & & \\ \vdots & & & \\ \underset{\sim}{Z}_{(N+1)\,1} & \ldots\ldots & & \underset{\sim}{Z}_{(N+1)(N+1)} \end{bmatrix} \qquad (3\text{-}37)$$

where $\underset{\sim}{Z}_{ii}$ represents the generalized impedance of element i which consists of a double row or column linear array. $\underset{\sim}{Z}_{ij}$ represents the interactions between elements i and j, each of which is a double row (or column) linear array.

Note that submatrices $\underset{\sim}{Z}_{ij}$ depend only on the magnitude of the difference between i and j:

$$\underset{\sim}{Z}_{ij} = \underset{\sim}{Z}_{ji} = \underset{\sim}{Z}_{|i-j|} \tag{3-38}$$

for ($1 \leq i, j \leq N+1$) and [z] may be expressed in the following form which coincides with (3-24)

$$[z] = \begin{bmatrix} \underset{\sim}{Z}_0 & \underset{\sim}{Z}_1 & \cdots & \underset{\sim}{Z}_N \\ \underset{\sim}{Z}_1 & \underset{\sim}{Z}_0 & & \underset{\sim}{Z}_{N-1} \\ \vdots & & & \vdots \\ \underset{\sim}{Z}_N & \underset{\sim}{Z}_{N-1} & \cdots & \underset{\sim}{Z}_0 \end{bmatrix} \tag{3-39}$$

The impedance matrix [z] is a block-Toeplitz matrix. The sub-matrices $\underset{\sim}{Z}_i$, $0 \leq i \leq N$ are not necessarily block-Toeplitz matrices, because a double row (or column) element has been used. The computer program PLAN is already designed to treat matrices of the form of (3-38) and thus the only change required is to generate the elements $\underset{\sim}{Z}_0$ to $\underset{\sim}{Z}_N$ for the particular geometries of Figs. 11 a, b. There are, of course, several different ways of generating the elements $\underset{\sim}{Z}_0$ to $\underset{\sim}{Z}_N$. One could, for instance, use one of the general subroutines [13,20,21] available for arbitrary arrangements of elements.

Figs. 12 and 13 show a parallelogram and an unequally spaced planar array. These arrays can also be treated by considering single or double rows or columns as elements. The generalized impedance matrix is of the form (3-38) and one need only add a subroutine for the generation of the elements $\underset{\sim}{Z}_0$ to $\underset{\sim}{Z}_N$ of the matrix.

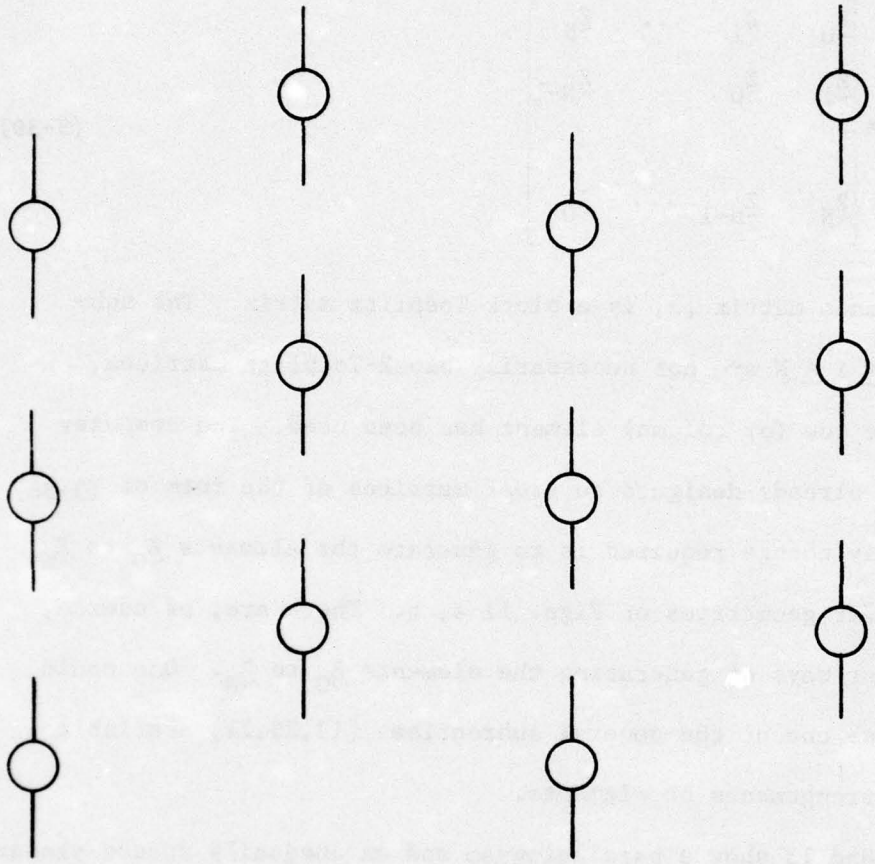

Fig.10. A triangular planar array.

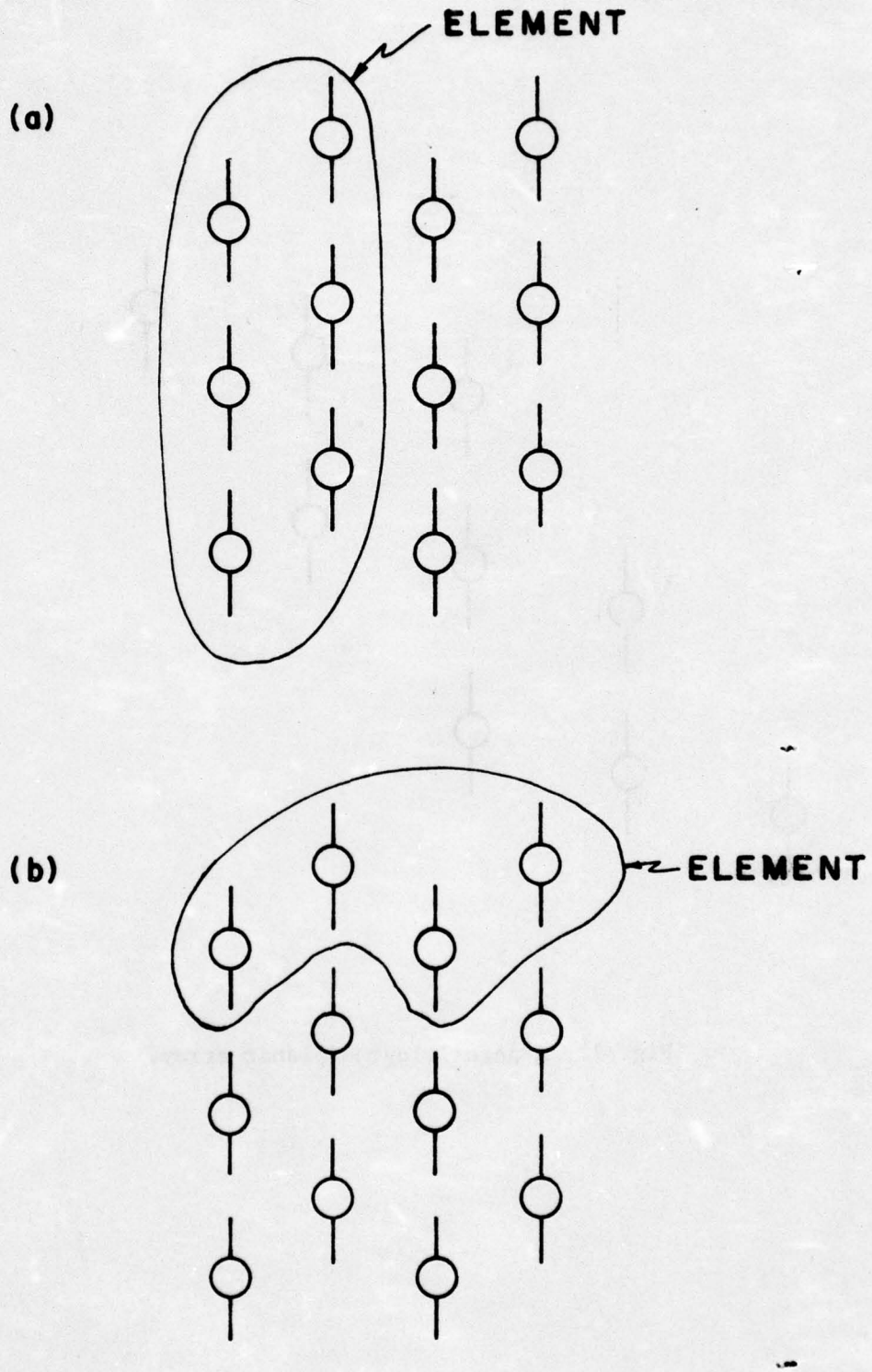

Fig. 11. A triangular planar array (a) two adjacent column element (b) two adjacent row element.

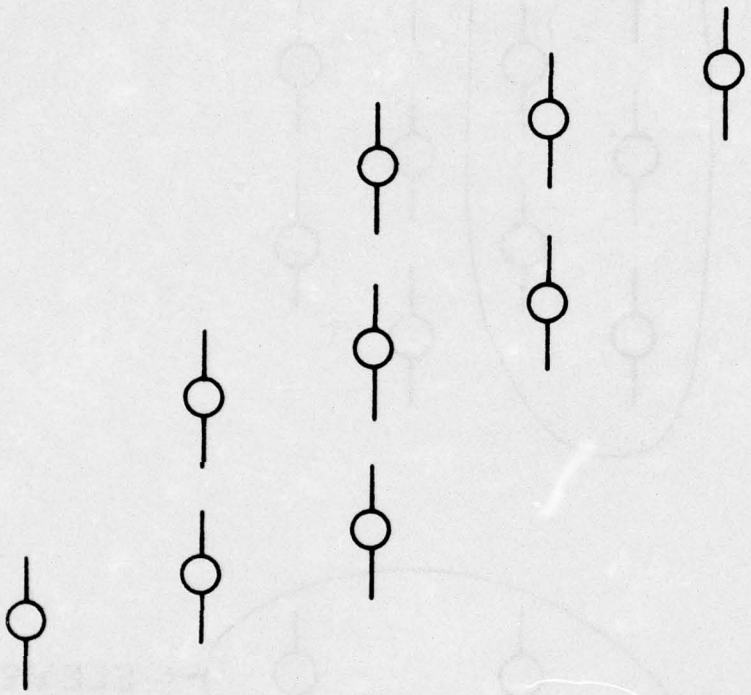

Fig. 12. A parallelogram planar array.

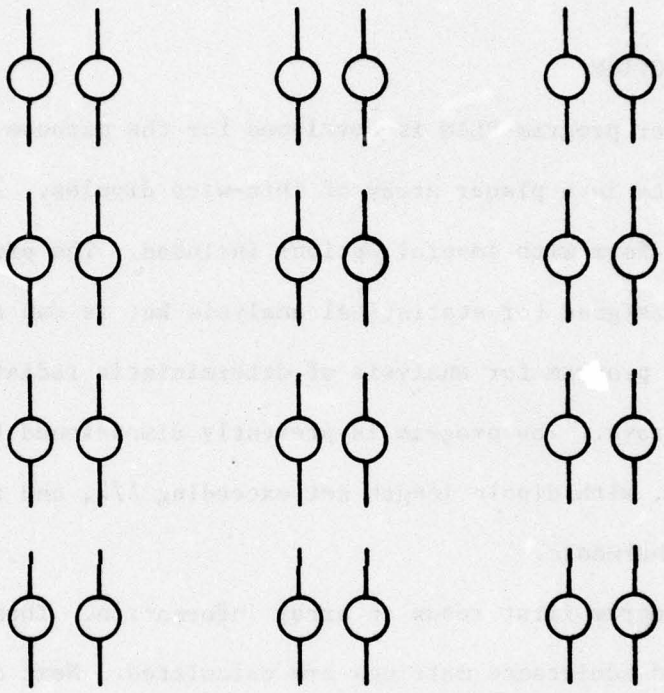

Fig. 13. An unequally spaced planar array.

4. PROGRAM DESCRIPTION

4.1 INTRODUCTION

Computer program PLAN is developed for the purpose of analyzing random effects in a planar array of thin-wire dipoles. It is written in a general form with several options included. The program is especially designed for statistical analysis but it can also be used as a general program for analysis of deterministic radiation problems of planar arrays. The program is presently dimensioned for a 10 by 10 planar array, with dipole length not exceeding $\lambda/2$, and frequency mode up to third harmonic.

The program first reads in array information. Then generalized impedance and admittance matrices are calculated. Next is the procedure to calculate the far field beam patterns for a given excitation generated by a random number generator. This procedure is repeated many times to obtain mean and standard deviations of far field magnitude and gain. Two disc files are needed as auxiliary storage.

4.2 OPTIONS

There are several options provided in the program. Each of these options has a corresponding option code which is an integral

power of 2. The options are specified by adding up all the code numbers of the options desired.

(1) 1 - Generalized Impedance Matrix.

(2) 2 - Compact Admittance Matrix.

(3) 4 - No Mutual Effects.

(4) 8 - Amplitude Taper and Progressive Phase.

(5) 16 - Individual Beam Patterns.

(6) 32 - Random Phase Errors

Options (1), (2), (5) are printout options. Option (3) represents a choice in the method of solution and option (4) represents a choice or nominal excitation. (6) is a special case of random excitation for which the phase is uniformly distributed between $-\pi$, π. A brief description of each of these options follows:

(1) Generalized Impedance Matrix.

The generalized impedance matrix [z] for the array may be printed out by selecting this option. Because of the block-Toeplitz property, only the first column is printed out. This printout option is used primarily for checking.

(2) Compact Generalized Admittance Matrix.

Recall that only a portion of the generalized admittance matrix $[y] = [z]^{-1}$ is computed, namely those columns corresponding to the non-zero elements of the excitation matrix. This portion of the matrix [y] is called the compact generalized admittance matrix. It may be printed out by selecting this option. The compact generalized admittance matrix is k by $(M_1M_2M_3)$ where the latter term represents

the number of unknown expansion functions and k represents the number of dipoles contained in this rectangular array since k columns, each of lengths M_1 M_2M_3, are required for the matrix multiplication [y][i]. Because of symmetry, only k/2 or half of the columns are printed out.

Note that this compact matrix contains within it the N-port short circuit admittance parameters of the antenna system. This matrix is a kxk square matrix within the compact matrix [22].

(3) No Mutual Effects

In program PLAN mutual effects between portions of each dipole and between different dipoles are taken fully into account. If this option is selected, then, in addition, the program is run neglecting mutuals between different dipoles but taking into account mutuals within each antenna. This additional computation is extremely rapid as compared to the full analysis. When compared with the complete analysis, it may provide some insight into the role of mutual effects.

(4) Amplitude Taper and Progressive Phase

If this option is selected, then the user may specify nominal exponential* amplitude taper and separate prograssive phase shifts in the x and z directions. Thus, the beam can be steered to an arbitrary

*Note that amplitude taper function can readily be changed by replacing FUNX and FUNZ with any desired taper function.

direction in $(\theta,\emptyset)$ space. If this option is not selected, then the excitation is automatically made uniform, i.e. all non-zero elements of the voltage excitation matrix are unity.

(5) Individual Beam Patterns

Note that the mean beam pattern magnitude is determined by averaging the magnitudes of a number of separate beam patterns. In some cases the individual beam patterns are of interest, as well as the mean and mean minus sigma patterns. If this option is selected, then all of the individual beam patterns are printed out. Some examples are shown in section 4. This option is of interest if the typical beam pattern differs significantly from the mean beam pattern. This is the case, for instance, if the random phase errors are very large.

(6) Random Phase Errors

This option selects uniformly distributed random numbers instead of normally distributed ones for the phase errors of the excitation. This option is of interest if the phase error of the excitation is completely random.

4.3 MODELING

(1) Array Orientation - The planar (or linear) array of dipoles treated in this program lie in a plane parallel to the Z-axis. For simplicity, it is best to choose an xz plane. Each dipole is identical and z-directed. Separate uniform spacing is required in each dimension of the planar array (Fig. 8).

For simplicity in far field specification, a planar array lying in the x-z plane with dipoles pointing in the $\hat{z}$-direction is recommended as shown in Fig. 14

(2) Dipole modeling - All dipoles are assumed to be straight, thin-wire ($L \gg a$, $a \ll \lambda$) elements, where L is antenna length and a is antenna radius. All dipoles are center-fed. The number of expansion

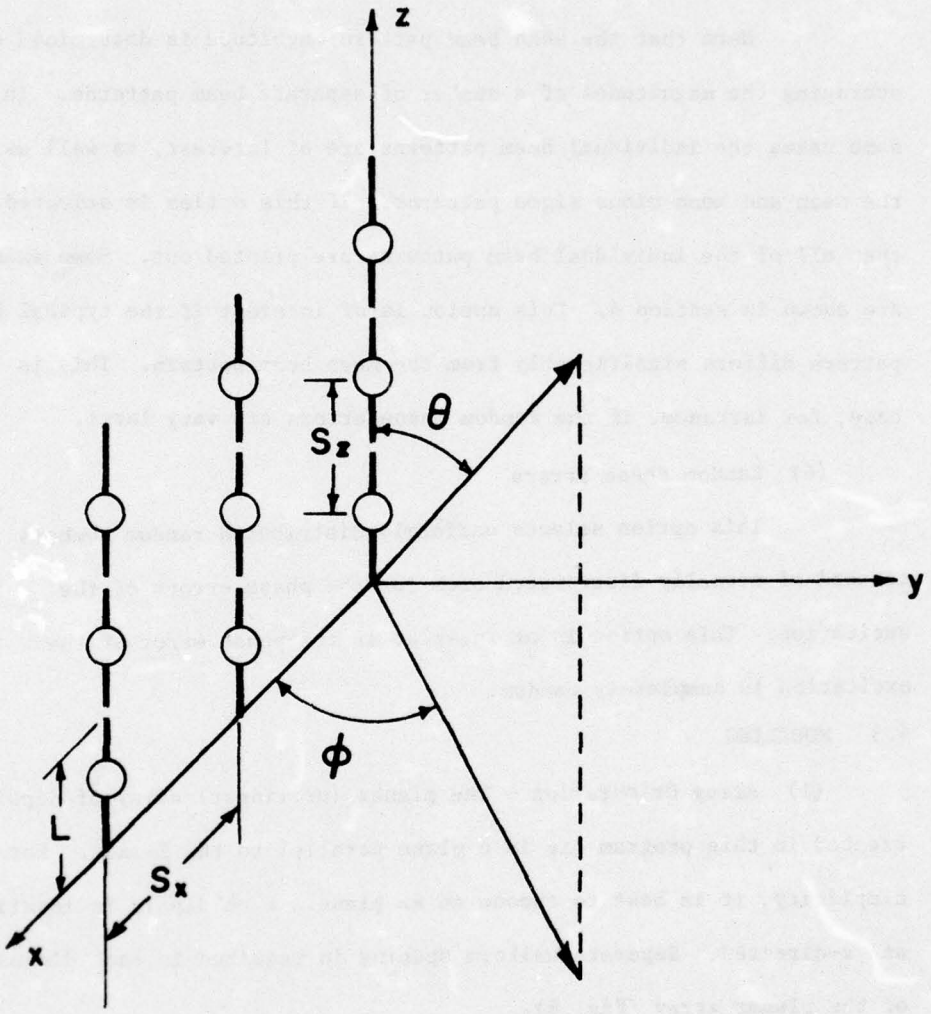

Fig. 14. A rectangular planar array of z-directed dipoles lying in the X-Z plane.

functions used per dipole is determined automatically within the program. Three, five, and seven expansion functions are used for L = $\lambda/2$, λ, $3\lambda/2$, respectively.

4.4 INPUT DATA SET-UP

(1) The first card ontains an integer number which is the summation of all the option codes selected. See section 4.2.

Table 1. CARD FOR OPTIONS

Column	Format	Data Description
1 - 5	I5	Option Code

(2) The second card contains information on the frequency mode. JF = 1 means fundamental frequency; JF = 2 means 2nd harmonic; and JF = 3 means 3rd harmonic, etc.

Table 2. CARD FOR FREQUENCY MODE

Column	Format	Data Description
1 - 5	I5	JF - Frequency mode

The JF code is chosen for simplicity in treating the array at fundamental and harmonic frequencies. One can, of course, choose any frequency by separately choosing antenna length L and selecting fundamental frequency.

(3) The third card specifies the array data, i.e. the number of rows and columns in the planar array, form spacing between dipoles in X Y Z-direction, length and radius of each dipole (all in units of

wavelength).

Table 3. CARD FOR ARRAY DATA

Column	Format	Data Description
1-5	I5	M2 = # of columns
6-10	I5	M3 = # of rows
11-20	F10.5	SX - X-direction spacing
21-30	F10.5	SY - Y-direction spacing
31-40	F10.5	SZ - Z-direction spacing
41-50	F10.5	HL - Dipole length
51-60	F10.5	AK - Dipole radius

(4) The fourth card contains mean and standard deviation values for both amplitude and phase. Also, the number of repetitions K is specified. If more than one far field pattern is needed for one excitation, set the pattern code JT to the desired number. All phase angles are given in degrees. If option (6) is selected, then SD2 is ignored by the program, whether or not a number is placed there.

Table 4. CARD FOR VOLTAGE EXCITATION ERROR, NUMBER OF ITERATIONS (K), NUMBER OF FAR FIELD BEAM PATTERNS.

Column	Format	Data Description
1-10	F10.5	AM1 - Mean value of amplitude
11-20	F10.5	AM2 - Mean value of phase
21-30	F10.5	SD1 - STD value of amplitude
31-40	F10.5	SD2 - STD value of phase
41-45	I5	IT - # of repetition
46-50	I5	JT - # of far field pattern

(5) If option of amplitude taper and progressive phase is selected, then the desired shift angle of the main beam in both directions must be specified (in degrees).

Table 5. CARD FOR PROGRESSIVE PHASE SHIFT

Column	Format	Data Description
1-10	F10.5	RX - Beam shift in X-direction
11-20	F10.5	RZ - Beam shift in Z direction

(6) This card specifies how the far field beam pattern is to be selected. All far field points are assumed to be equally spaced either along a circular arc in θ or ϕ direction, or over an area by specifying the starting angle of θ_i and ϕ_i, and ending angle of θ_f and ϕ_f. The increment angle in both directions is specified by $\Delta\theta$ and $\Delta\phi$ (Fig. 14). All angles are in degrees. If more than one pattern is required, then more cards specifying far field points are needed.

Table 6. CARD FOR FAR FIELD BEAM PATTERNS

Column	Format	Data Description
1-5	I5	NR - Start angle of θ
6-10	I5	NT - End angle of θ
11-15	I5	NY - Increment of θ
16-20	I5	NW - Start angle of ϕ
21-25	I5	NH - End angle of ϕ
26-30	I5	NJ - Increment of ϕ

5. RESULTS

Computer program PLAN has been exercised on the Honeywell 635 computer and some typical results are shown in Figs. 15 -28.

Fig. 15 shows mean and m-σ beam patterns of a 10 x 10 planar array of dipoles (Refer to Fig. 1; $M_2 = M_3 = 10$) for various values of σ_a, σ_p. The nominal excitation is uniform and the nominal pattern ($\sigma_a = \sigma_p = 0$) is shown in Fig. 15a. σ represents the rms departure from the mean pattern. It is assumed that the nominal voltage excitation is 1.0 volts. All patterns are normalized to the maximum value of the mean pattern. Normalization numbers (N) printed on each plot provide a measure of the mean field intensity. Note that the mean pattern does not differ significantly from the nominal. The range of variation (σ) increases with increasing σ_a, σ_p. The effect of σ_p is more pronounced.

Fig. 16 shows the corresponding beam patterns for the second harmonic. It is assumed that the geometry is unchanged from that of Fig. 15, but the frequency is changed from f_0 to $2f_0$. Since the spacing is $S_x = 1.0\ \lambda$ at second harmonic, grating lobes appear at $\phi = 0, 180°$. The nominal pattern ($\sigma_a = \sigma_p = 0$) is shown in Fig. 16a. Note that the mean patterns do differ more significantly from the nominal than was the case in Fig. 15.

Fig. 17 shows the corresponding beam patterns for the third harmonic. Note that the grating lobes are considerably closer to the main beam.

The nominal pattern ($\sigma_a = \sigma_p = 0$) is shown in Fig. 17a. Note that the deviations of the mean from the nominal pattern are significant and that the range of variation increases with σ_a, σ_p. In comparing the beam patterns for f_0, $2f_0$, $3f_0$, note that deviation of mean from the nominal pattern and the range of variation (σ) both increase as frequency increases (for given σ_a, σ_p).

In addition to mean and (M-σ) patterns, the individual patterns due to the various sample excitations are also of interest. The computer program includes an option to print out the individual beam patterns from which the mean and (M-σ) patterns were computed. If the shape of the mean and (M-σ) patterns are relatively close to that of the nominal pattern, then this option may not be necessary. In some cases, the individual patterns are useful. If the shapes of the mean and M-σ patterns differ significantly from the nominal, then the option may be useful. Figs. 18 a, b show the individual beam patterns of the 40 samples used in treating a 5 x 5 planar array. In this case ($\sigma_a = 0.5$, $\sigma_p = 40°$) the sample patterns are reasonably close to the mean pattern (Fig. 18c). Figs. 19 a, b show the individual beam patterns for a greater amplitude variation ($\sigma_a = 3.0$, $\sigma_p = 40°$). Note that the sidelobe levels differ greatly from the mean pattern, but that the main beam in most cases is located near broadside. Fig. 19c shows the mean beam pattern. Fig. 20 a,b show the individual beam patterns for a large phase variation ($\sigma_a = 0.5$, $\sigma_p = 180°$). In this case, the position of the main beam pattern varies considerably. Fig. 20c shows the mean beam pattern.

Note that the individual pattern data is really necessary here. The mean beam pattern is broad, whereas the individual beam patterns are narrow but with positions of main beam varying.

Fig. 21a shows the individual (sample) patterns of an eleven element linear array for the extreme case of completely random phase errors. Note that the beams are relatively narrow but that the positions of the maxima vary considerably. Fig. 21b shows the mean and $(m - \sigma)$ patterns. Note that the maximum of the mean beam pattern occurs near broadside. In other words, there is a tendency, despite the random phase errors, to point the beam near broadside. This is due to mutuals, as shown by Fig. 20c, which indicates the mean and $(m - \sigma)$ patterns of the same array with random phase excitation for the special case of no mutuals. In this latter case the direction of the main beam appears to be random.

Computer program PLAN includes an option to compute the beam patterns without taking the mutuals into account. The impedance of an individual dipole is still accurately computed, i.e. mutuals between subsections on the same dipole are taken into account. However, mutual effects between dipoles are not taken into account. The matrix inversion then becomes very simple. Fig. 22a and b show broadside patterns of a 5 x 5 planar array with and without mutuals, respectively. Figs. 22 c, d show the endfire patterns (array scanned exactly to endfire) with and without mutuals, respectively. Note the significant differences in the sidelobe levels as computed with and without mutuals.

The beam patterns of a 9-element linear array were also studied as a function of σ_a, σ_p. Fig. 23 shows the sidelobe level of the array as a function of σ_a, σ_p. Note that sidelobe level increases monotonically with increasing σ_a, σ_p.

Figs 24-28 show the results of computation of some of the gain quantities G_0, G_1, G_2. Fig. 24 shows the gain G_0 of a linear array of halfwave dipoles with halfwave spacing (perpendicular line case) as a function of the number of dipoles. Computation is carried out with and without mutuals. Note that the gain with mutuals is always larger.

Figs. 25a and b show the ratio G_1/G_0 as a function of σ_p, σ_a for an eleven element linear array of halfwave spacing (perpendicular line case). Figs. 25a, b represent the same data plotted in different ways. Note that the ratio G_1/G_0 is approximately 0.2 in the worst case.

Figs. 26a, b show the ratio G_1/G_0 as a function of σ_p, σ_a for an eleven element linear array of halfwave dipoles with 0.6λ spacing (parallel line case). Figs. 26a, b represent the same data plotted in different ways. The data of figs. 25 and 26 differ because (1) the array is slightly larger and (2) the mutuals are different in the parallel line case. Note that the ratio G_1/G_0 is less than 0.2 in the worst case.

Computations of G_1/G_0 were not carried out for a planar array because of the difficulty in locating the position of the beam maximum, which can occur anywhere in space. However, using the array factor principle, one may deduce approximately the corresponding ratio G_1/G_0 for an 11 x 11 element planar array by multiplying the appropriate factors of figs. 25 and 26. Thus, the worst case value of G_1/G_0 would be approximately 0.04 for the 11 x 11 planar array. This represents a gain degradation of about 14 dB for the quantity G_1.

Fig. 27a, b show the ratio G_2/G_0 as a function of σ_p, σ_a for an eleven element linear array of halfwave dipoles with halfwave spacing (perpendicular line case). Figs 27 a, b show the same data plotted in different ways. Note that the ratio G_2/G_0 is approximately 0.3 for the worst case. This would imply a ratio of 0.09 or a gain degradation for G_2 of approximately 10.5 dB for an 11 x 11 element planar array.

Figs. 28a, b show the ratios G_1/G_0 and G_2/G_0 as a function of array size, for a linear array of halfwave dipoles with halfwave spacing (perpendicular line case). Computations have been carried out both with and without mutuals. Note that the gain with mutuals is larger in every case. Note that G_1/G_0 decreases to very small values in the random case. The corresponding ratios for a planar array can be approximately determined by squaring the data of figs. 28 a,b. For a 3600-element array (60 by 60), gain degradation for G_1/G_0 is in excess of 30 dB and gain degradation for G_2/G_0 is in excess of 20 dB for the worst case. Thus, gain degradation due to phase and amplitude errors can be a significant factor in determining harmonic levels in the far field.

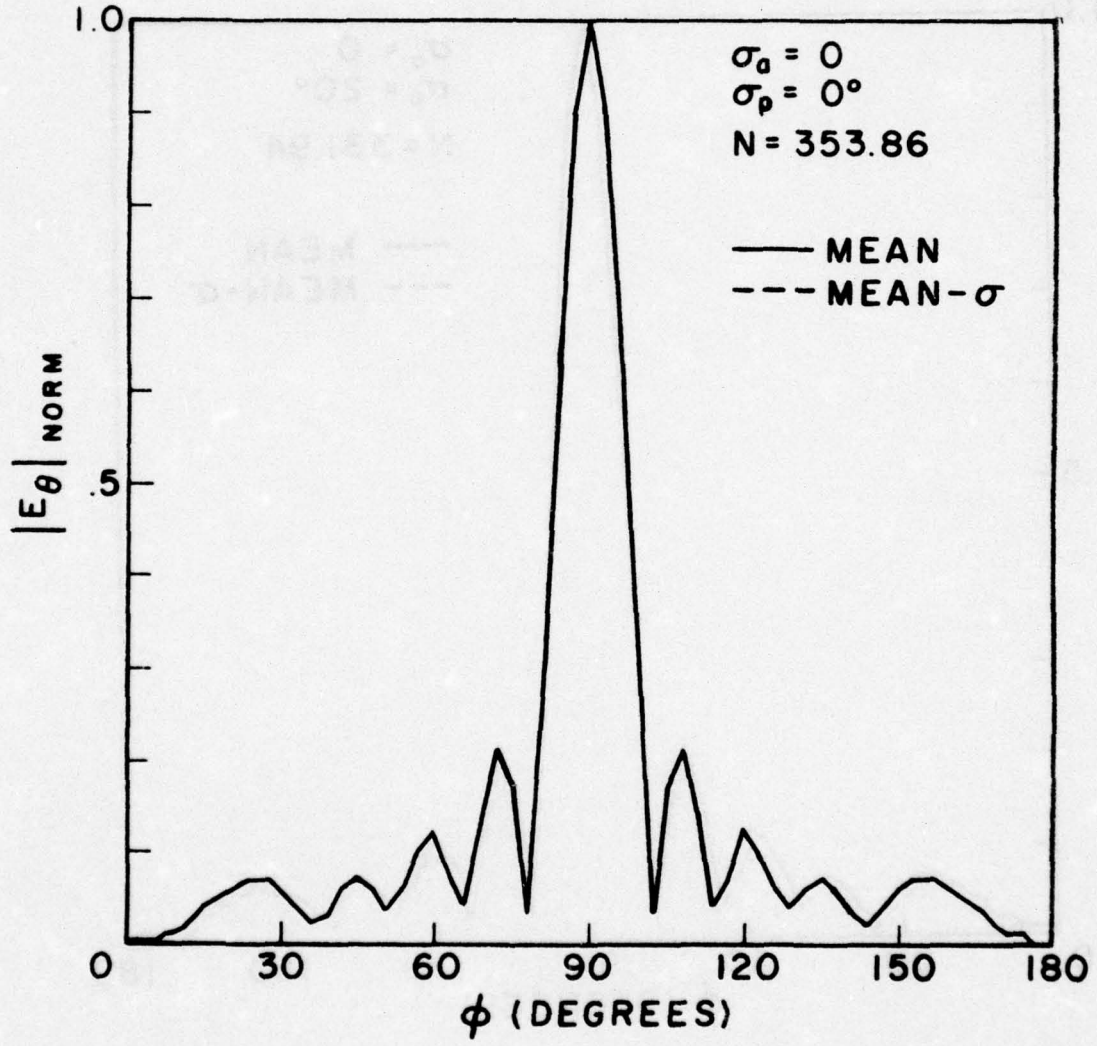

Fig. 15. Mean and (M-σ) broadside beam patterns (in the principal H-plane) of a 10 x 10 planar array of dipoles at fundamental frequency ($L = 0.5\lambda$, $S_x = 0.5\lambda$, $S_z = 1.0\lambda$, $a = 0.0005\lambda$)

(a) $\sigma_a = \sigma_p = 0$

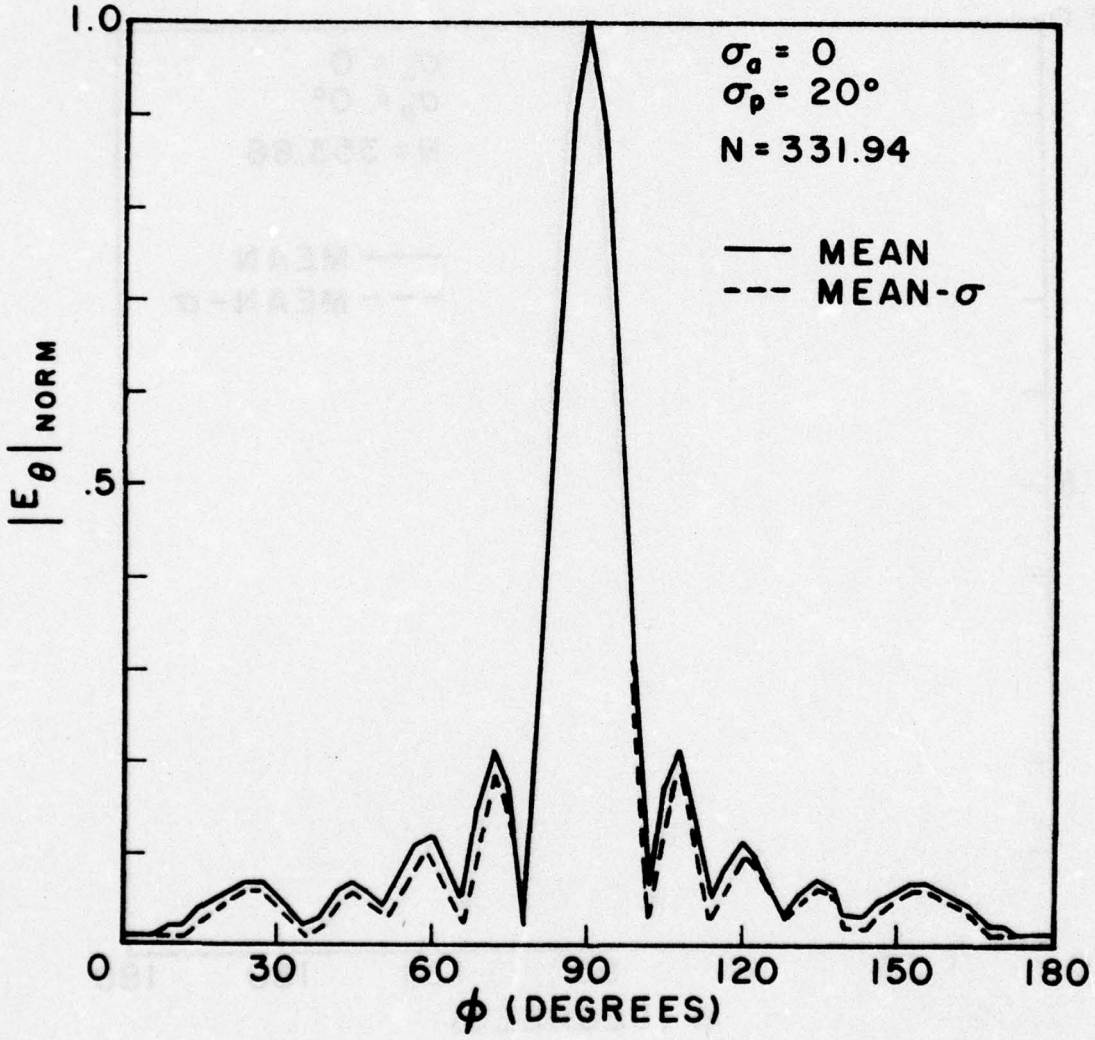

Fig. 15. Mean and (M-σ) broadside beam patterns (in the principal H-plane) of a 10 x 10 planar array of dipoles at fundamental frequency ($L = 0.5\lambda$, $S_x = 0.5\lambda$, $S_z = 1.0\lambda$, $a = 0.0005\lambda$)

(b) $\sigma_a = 0$, $\sigma_p = 20°$

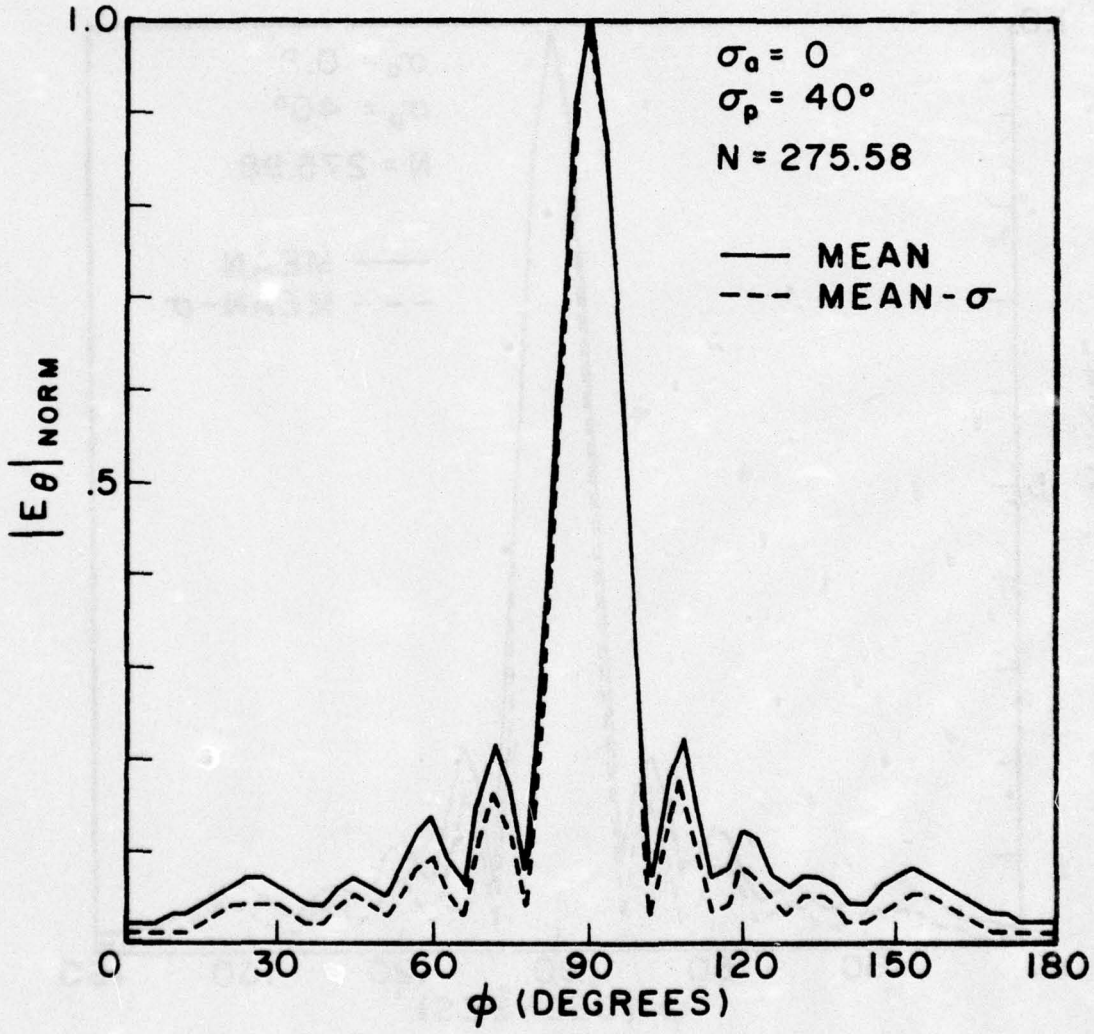

Fig. 15. Mean and (M-σ) broadside beam patterns (in the principal H-plane) of a 10 x 10 planar array of dipoles at fundamental frequency ($L = 0.5\lambda$, $S_x = 0.5\lambda$, $S_z = 1.0\lambda$, $a = 0.0005\lambda$)

(c) $\sigma_a = 0$, $\sigma_p = 40°$

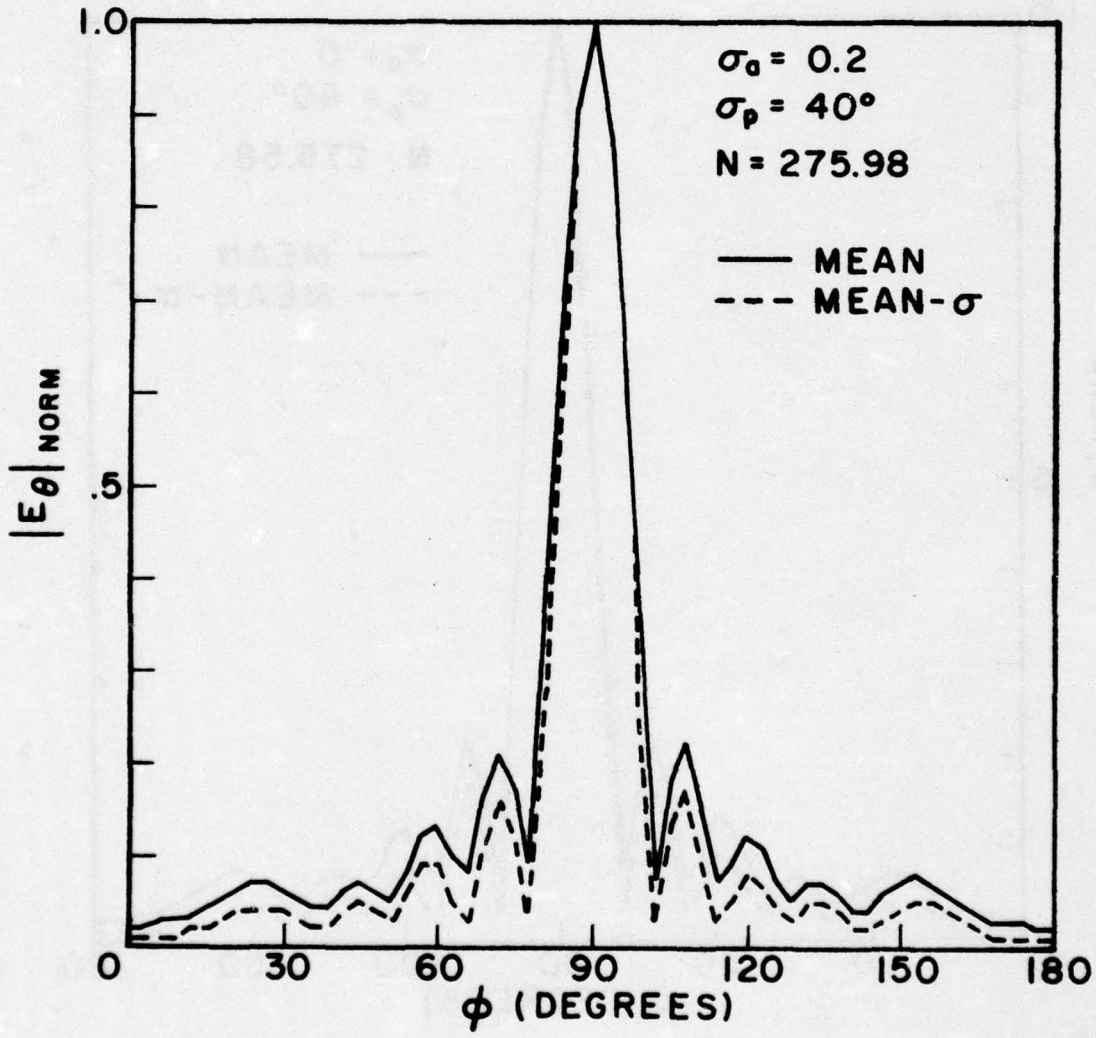

Fig. 15. Mean and (M-σ) broadside beam patterns (in the principal H-plane) of a 10 x 10 planar array of dipoles at fundamental frequency (L = 0.5λ, S_x = 0.5λ, S_z = 1.0λ, a = 0.0005λ)

(d) σ_a = 0.2, σ_p = 40°

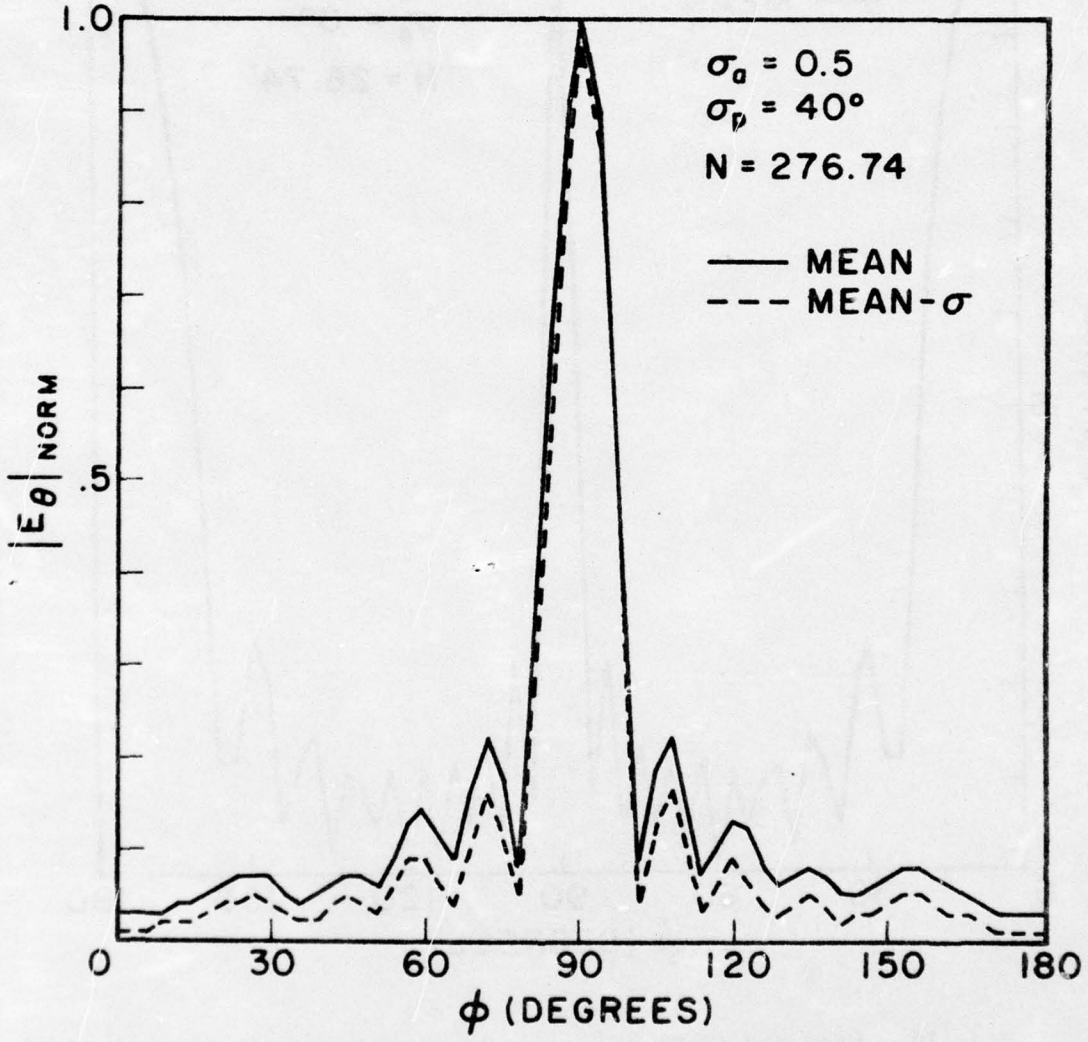

Fig. 15. Mean and (M-σ) broadside beam patterns (in the principal H-plane) of a 10 x 10 planar array of dipoles at fundamental frequency (L = 0.5λ, S_x = 0.5λ, S_z = 1.0λ, a = 0.0005λ)

(e) σ_a = 0.5, σ_p = 40°.

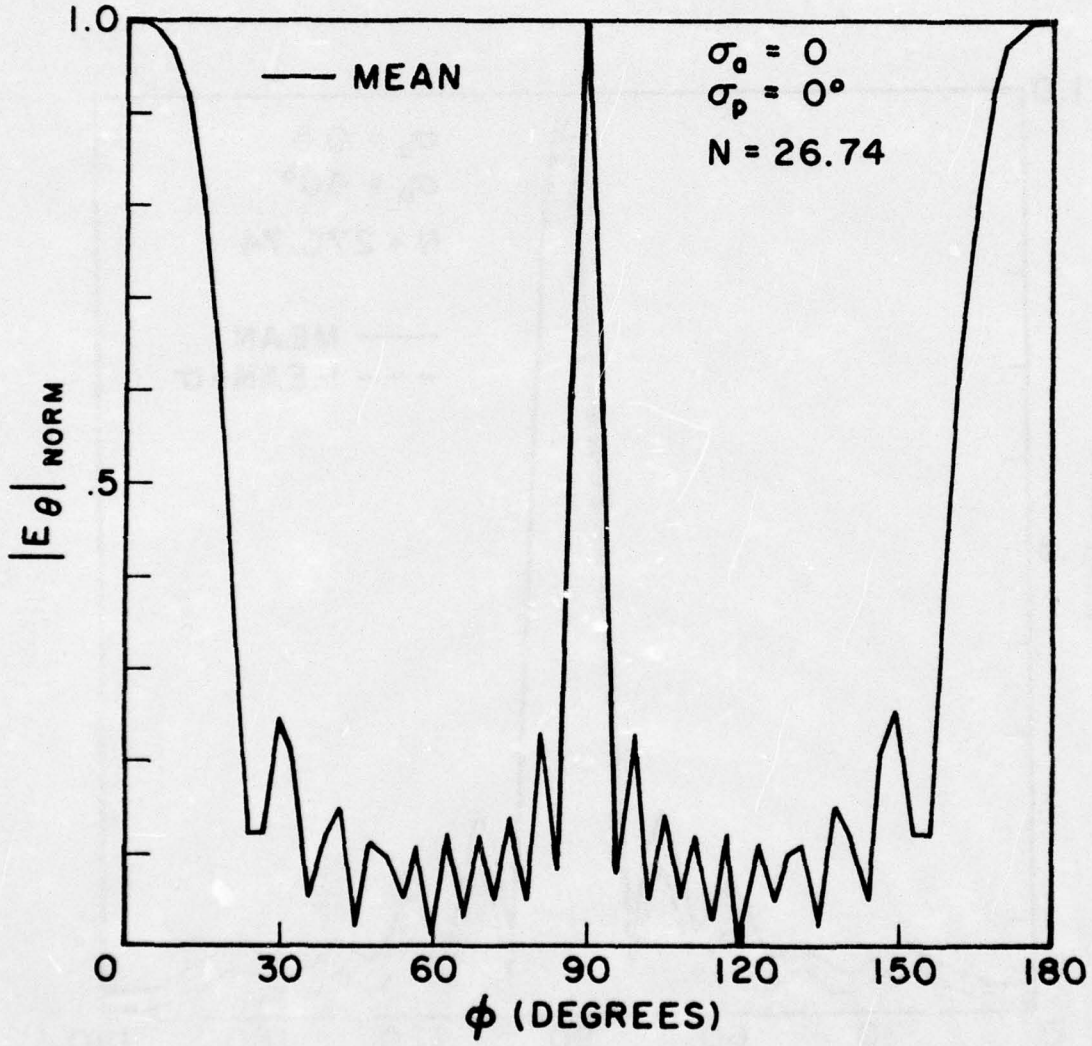

Fig. 16. Mean and (M-σ) broadside beam patterns (in the principal H-plane) of a 10 x 10 planar array of dipoles at second harmonic ($L = 1.0\lambda$, $S_x = 1.0\lambda$, $S_z = 2.0\lambda$, $a = 0.001\lambda$)

(a) $\sigma_a = \sigma_p = 0$

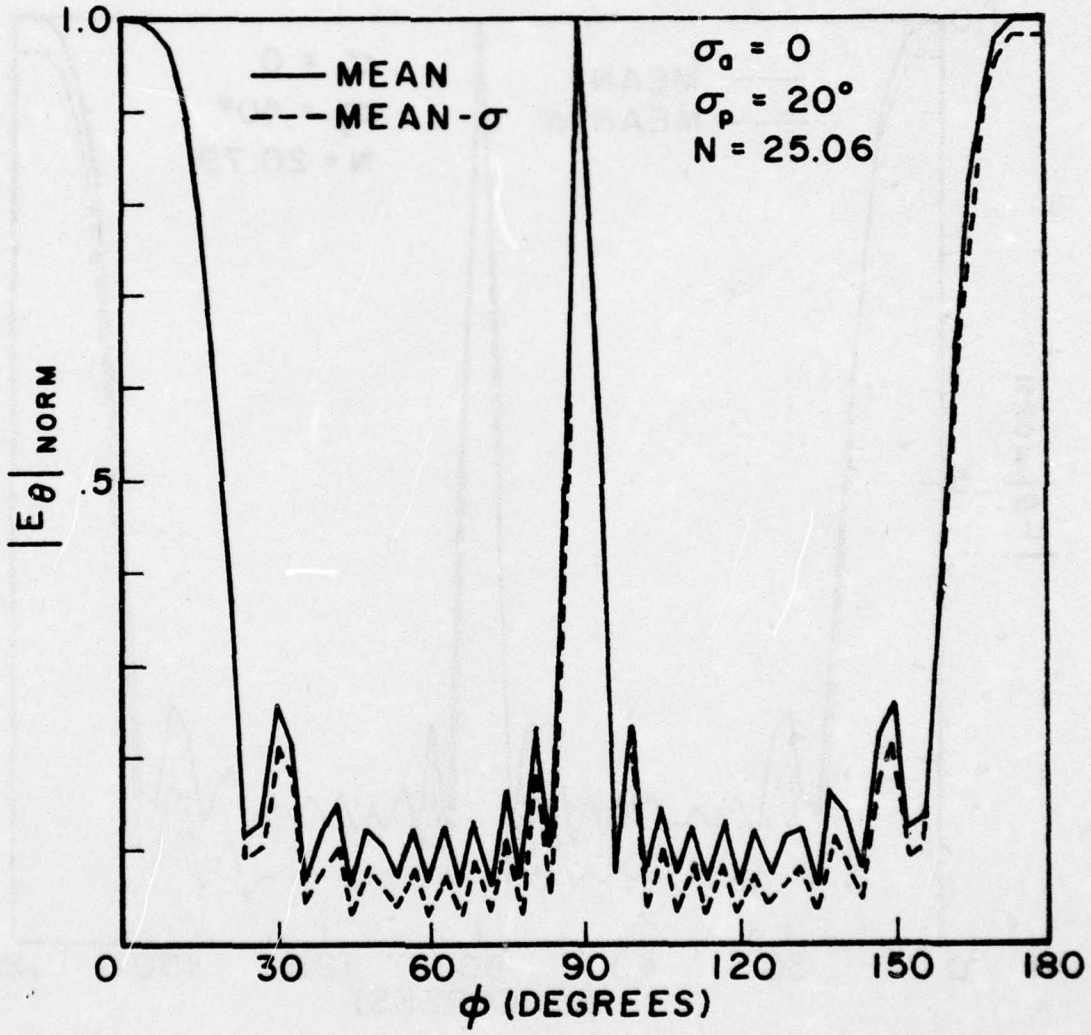

Fig. 16. Mean and (M-σ) broadside beam patterns (in the principal H-plane) of a 10 x 10 planar array of dipoles at second harmonic ($L = 1.0\lambda$, $S_x = 1.0\lambda$, $S_z = 2.0\lambda$, $a = 0.001\lambda$) (b) $\sigma_a = 0$, $\sigma_p = 20°$

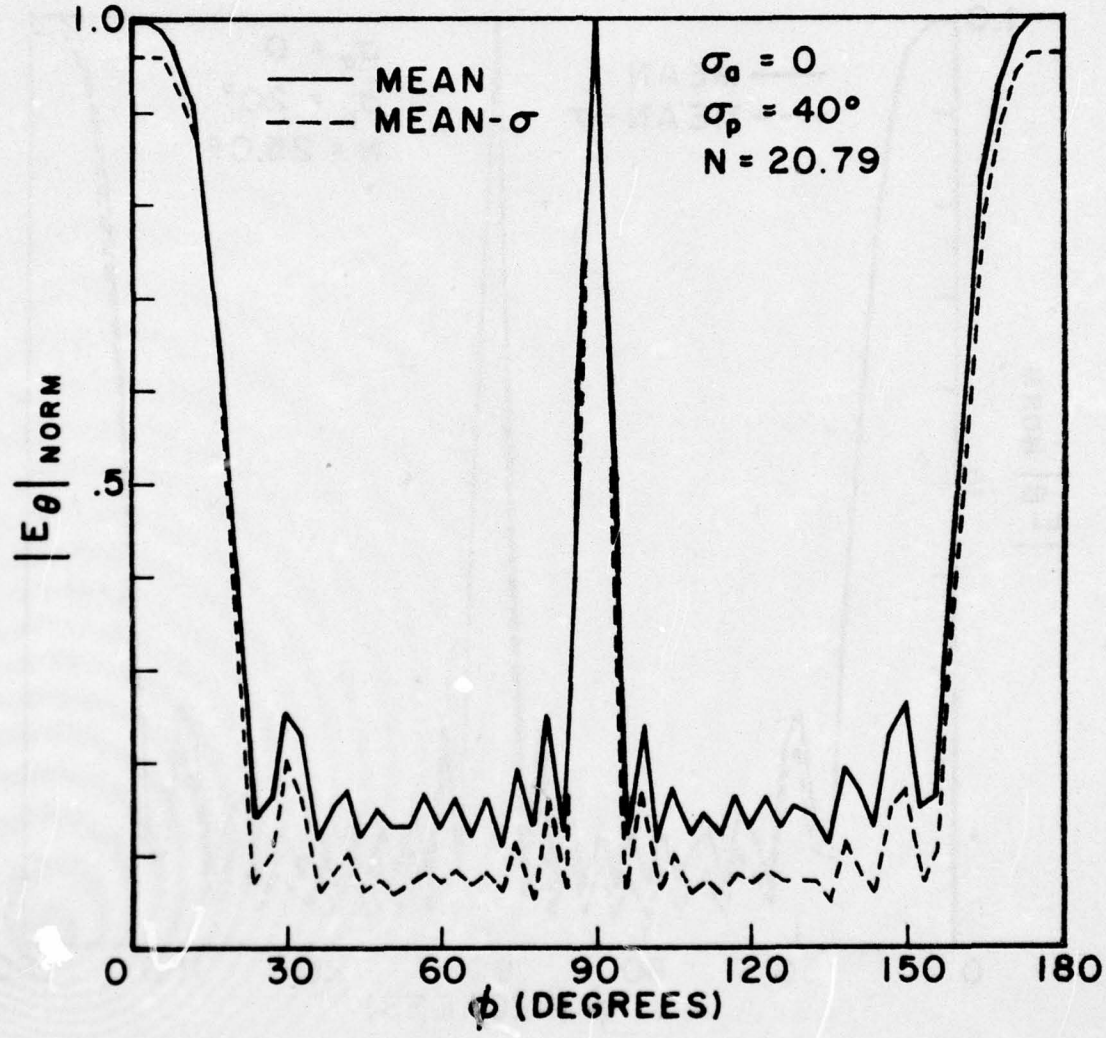

Fig. 16. Mean and (M-σ) broadside beam patterns (in the principal H-plane) of a 10 x 10 planar array of dipoles at second harmonic ($L = 1.0\lambda$, $S_x = 1.0\lambda$, $S_z = 2.0\lambda$, $a = 0.001\lambda$)

(c) $\sigma_a = 0$, $\sigma_p = 40°$

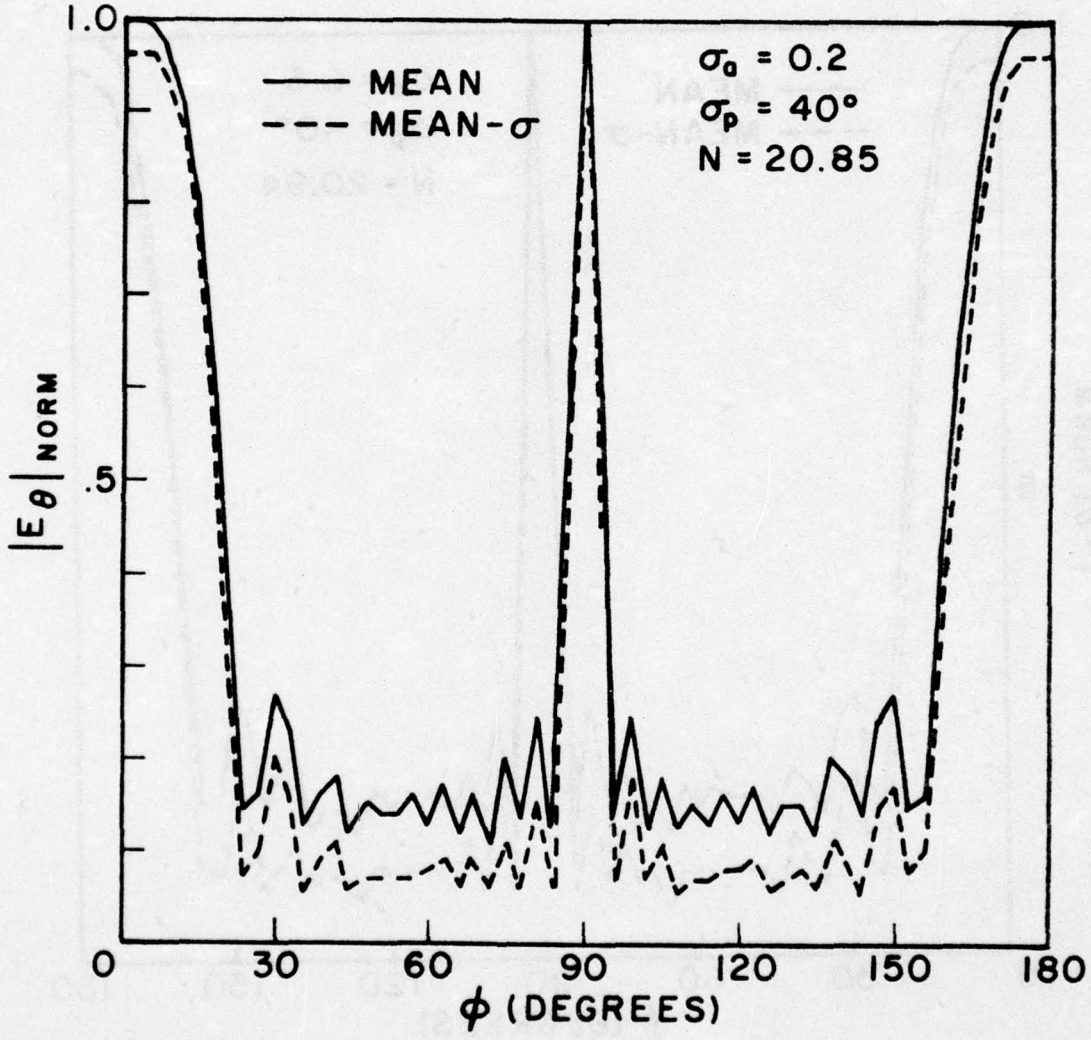

Fig. 16. Mean and (M-σ) broadside beam patterns (in the principal H-plane) of a 10 x 10 planar array of dipoles at second harmonic ($L = 1.0\lambda$, $S_x = 1.0\lambda$, $S_z = 2.0\lambda$, $a = 0.001\lambda$) (d) $\sigma_a = 0.2$, $\sigma_p = 40°$

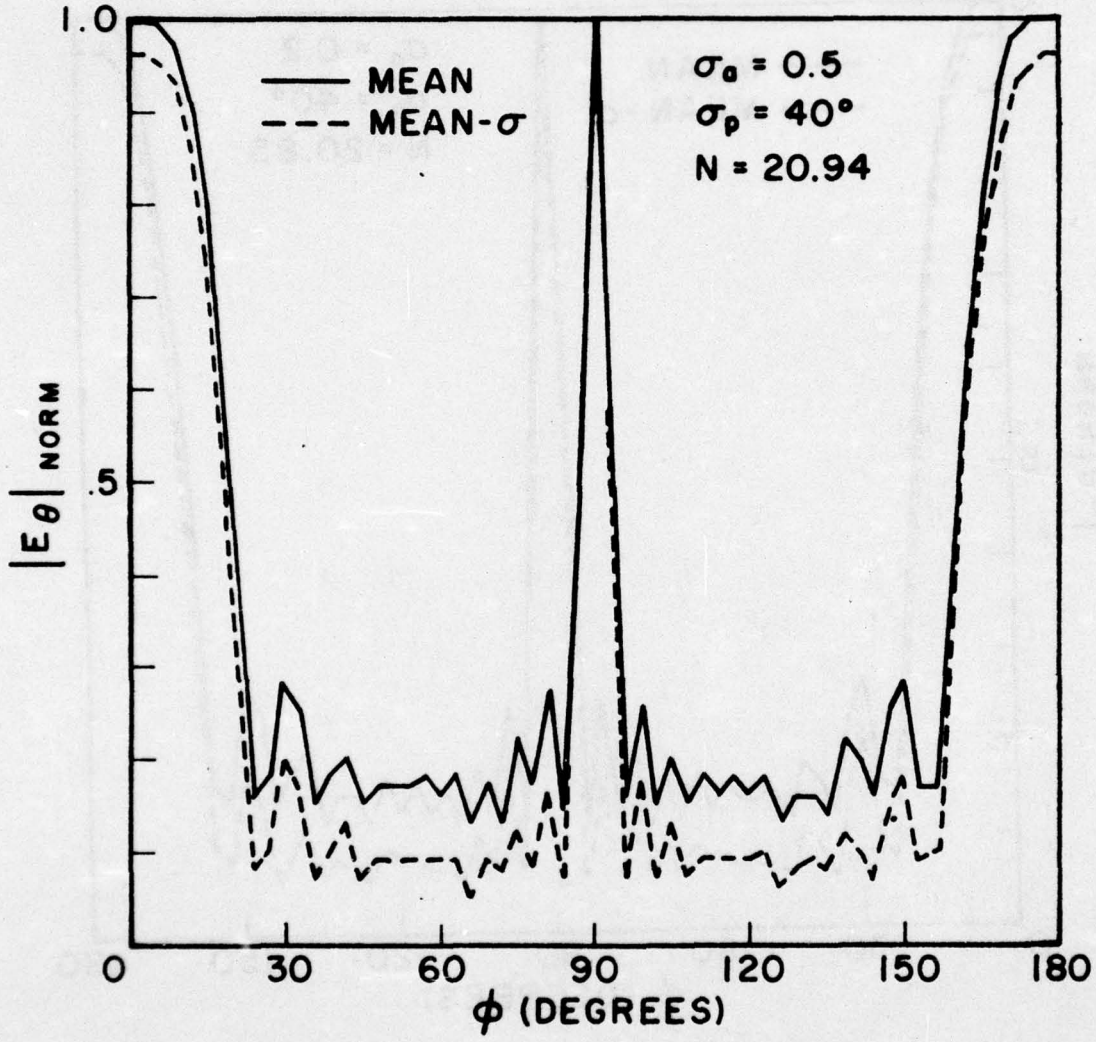

Fig. 16. Mean and (M-σ) broadside beam patterns (in the principal H-plane) of a 10 x 10 planar array of dipoles at second harmonic (L = 1.0λ, S_x = 1.0λ, S_z = 2.0λ, a = 0.001λ)
(e) σ_a = 0.5, σ_p = 40°

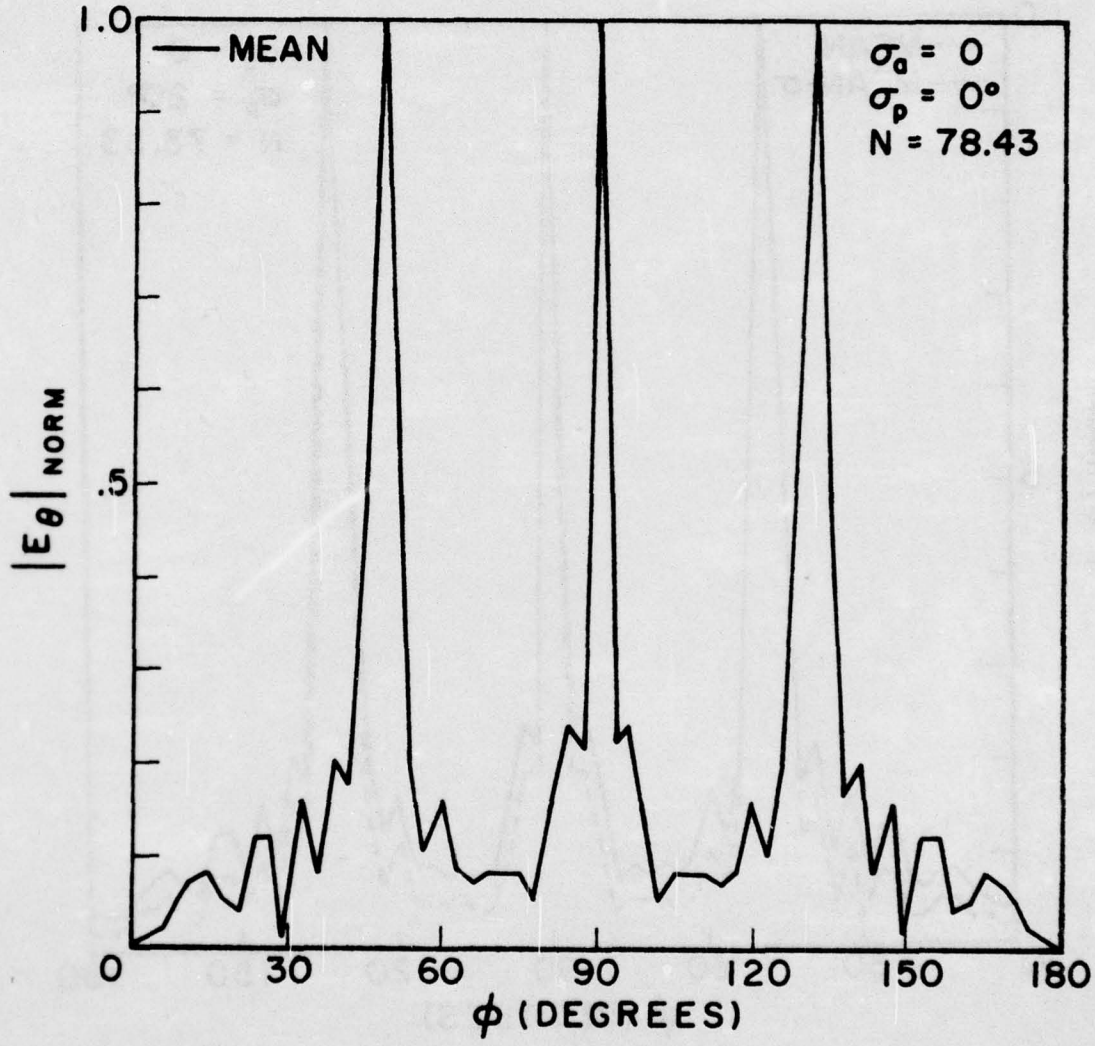

Fig. 17. Mean and (M-σ) broadside beam patterns (in the principal H-plane) of a 10 x 10 planar array of dipoles at third harmonic ($L = 1.5\lambda$, $S_x = 1.5\lambda$, $S_z = 3.0\lambda$, $a = 0.0015\lambda$).
(a) $\sigma_a = \sigma_p = 0$

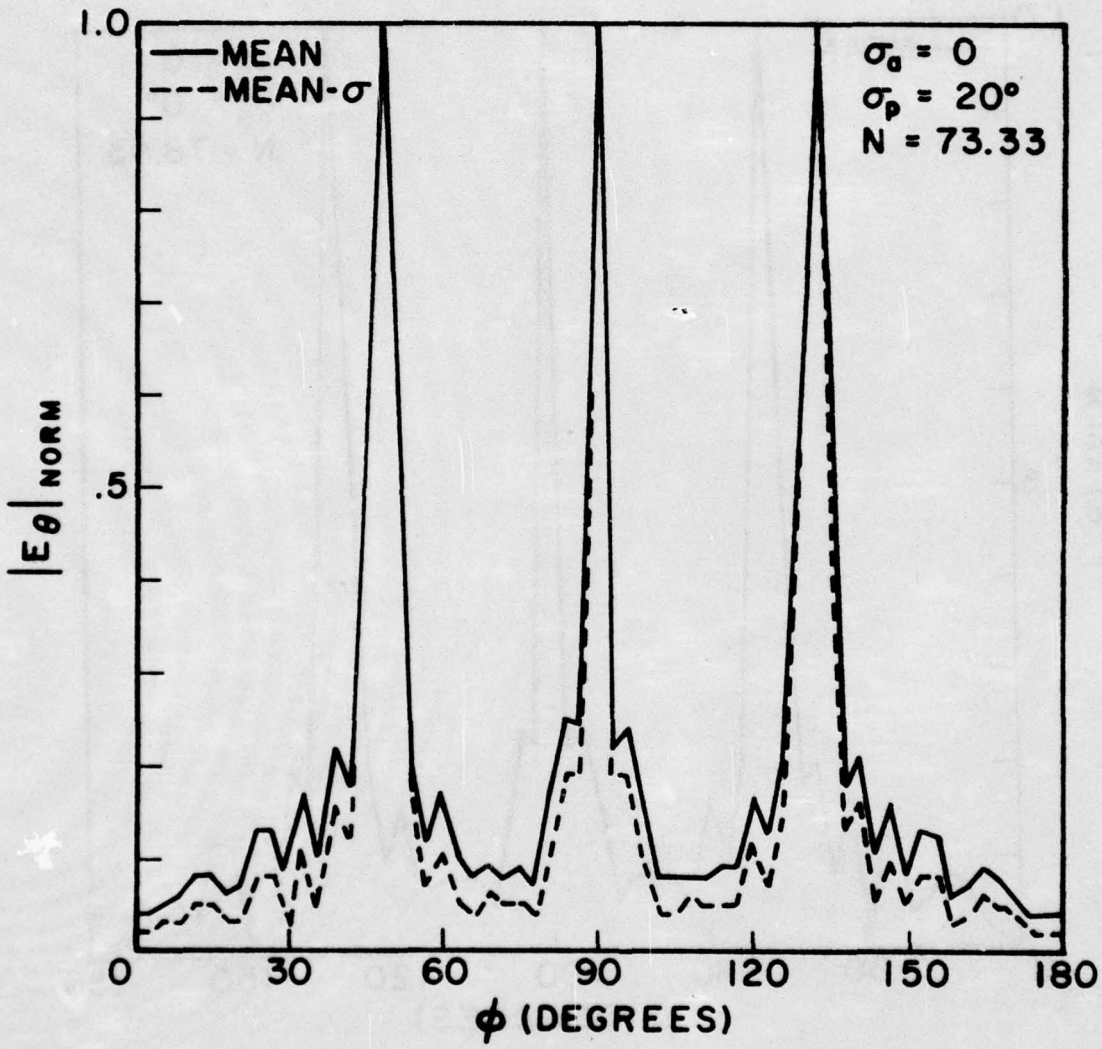

Fig. 17. Mean and (M-σ) broadside beam patterns (in the principal H-plane) of a 10 x 10 planar array of dipoles at third harmonic ($L = 1.5\lambda$, $S_x = 1.5\lambda$, $S_z = 3.0\lambda$, $a = 0.0015\lambda$). (b) $\sigma_a = 0$, $\sigma_p = 20°$

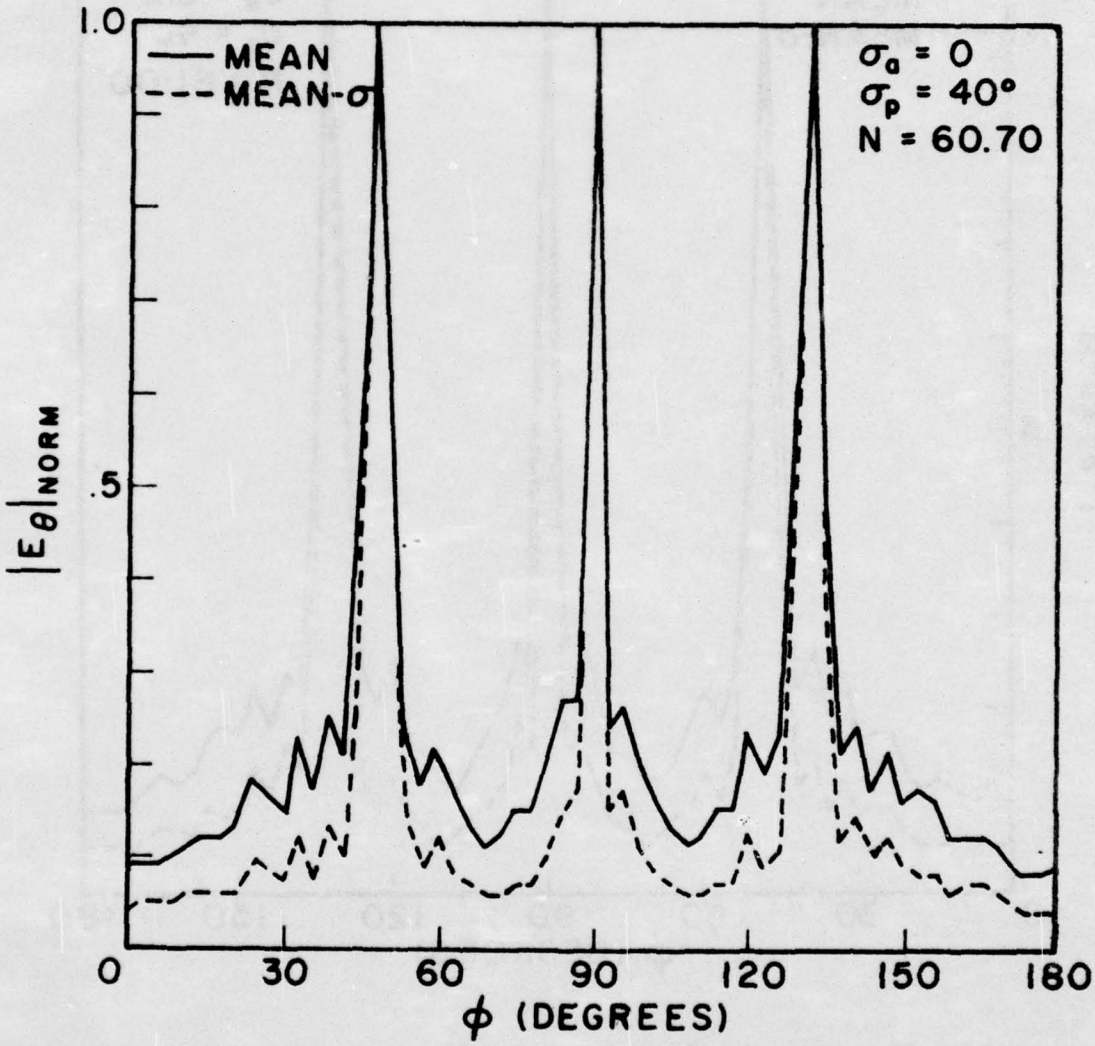

Fig. 17. Mean and (M-σ) broadside beam patterns (in the principal H-plane) of a 10 x 10 planar array of dipoles at third harmonic ($L = 1.5\lambda$, $S_x = 1.5\lambda$, $S_z = 3.0\lambda$, $a = 0.0015\lambda$).

(c) $\sigma_a = 0$, $\sigma_p = 40°$

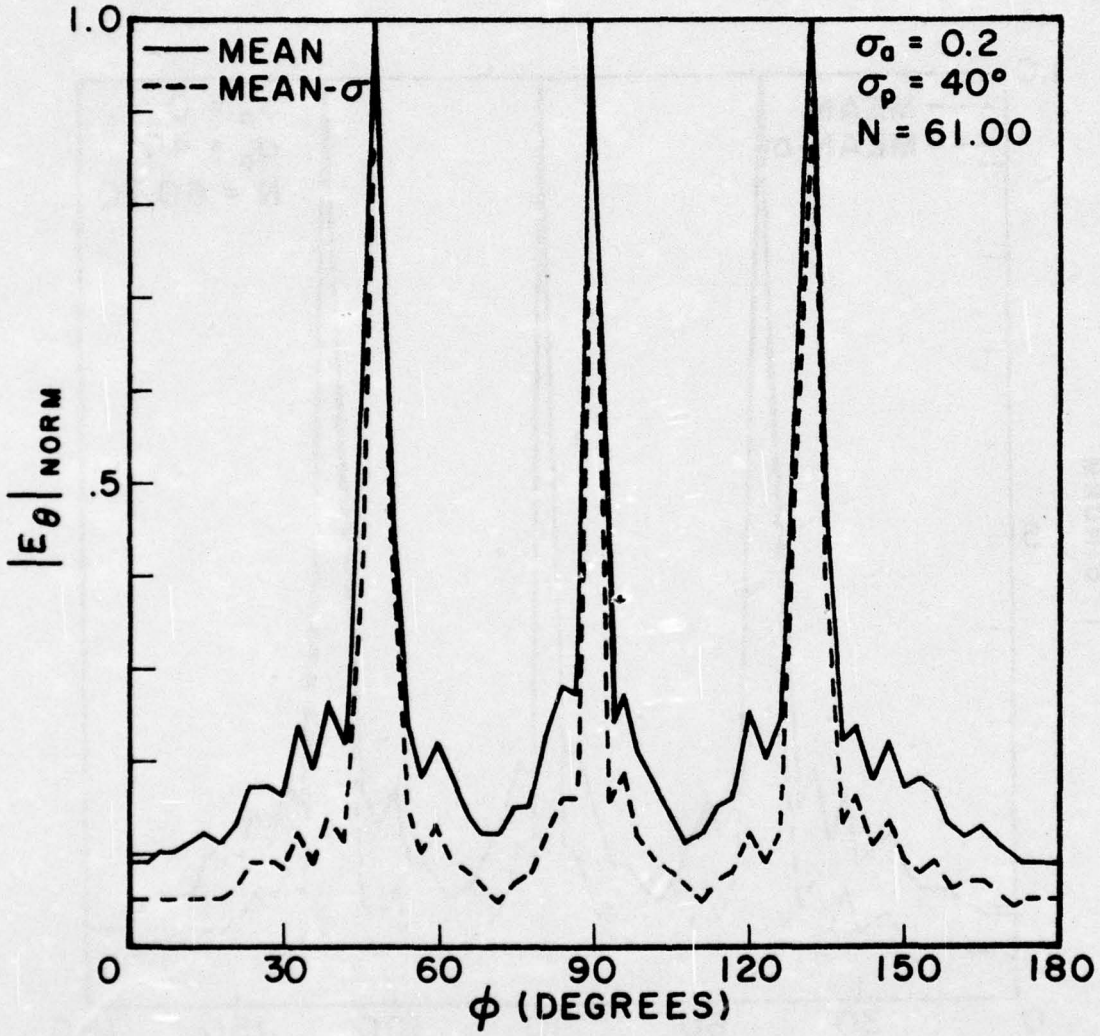

Fig. 17. Mean and (M-σ) broadside beam patterns (in the principal H-plane) of a 10 x 10 planar array of dipoles at third harmonic ($L = 1.5\lambda$, $S_x = 1.5\lambda$, $S_z = 3.0\lambda$, $a = 0.0015\lambda$).
(d) $\sigma_a = 0.2$, $\sigma_p = 40°$

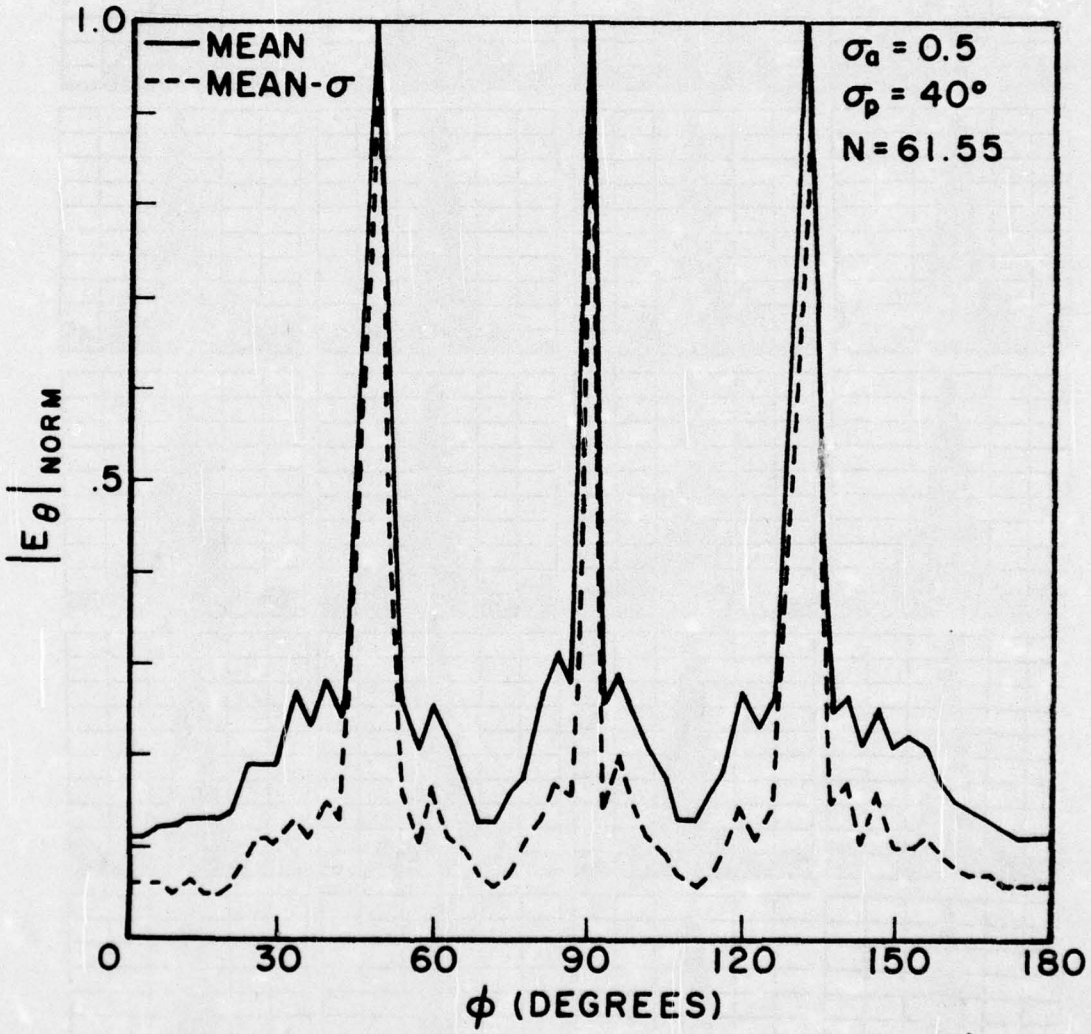

Fig. 17. Mean and (M-σ) broadside beam patterns (in the principal H-plane) of a 10 x 10 planar array of dipoles at third harmonic ($L = 1.5\lambda$, $S_x = 1.5\lambda$, $S_z = 3.0\lambda$, $a = 0.0015\lambda$).

(e) $\sigma_a = 0.5$, $\sigma_p = 40°$.

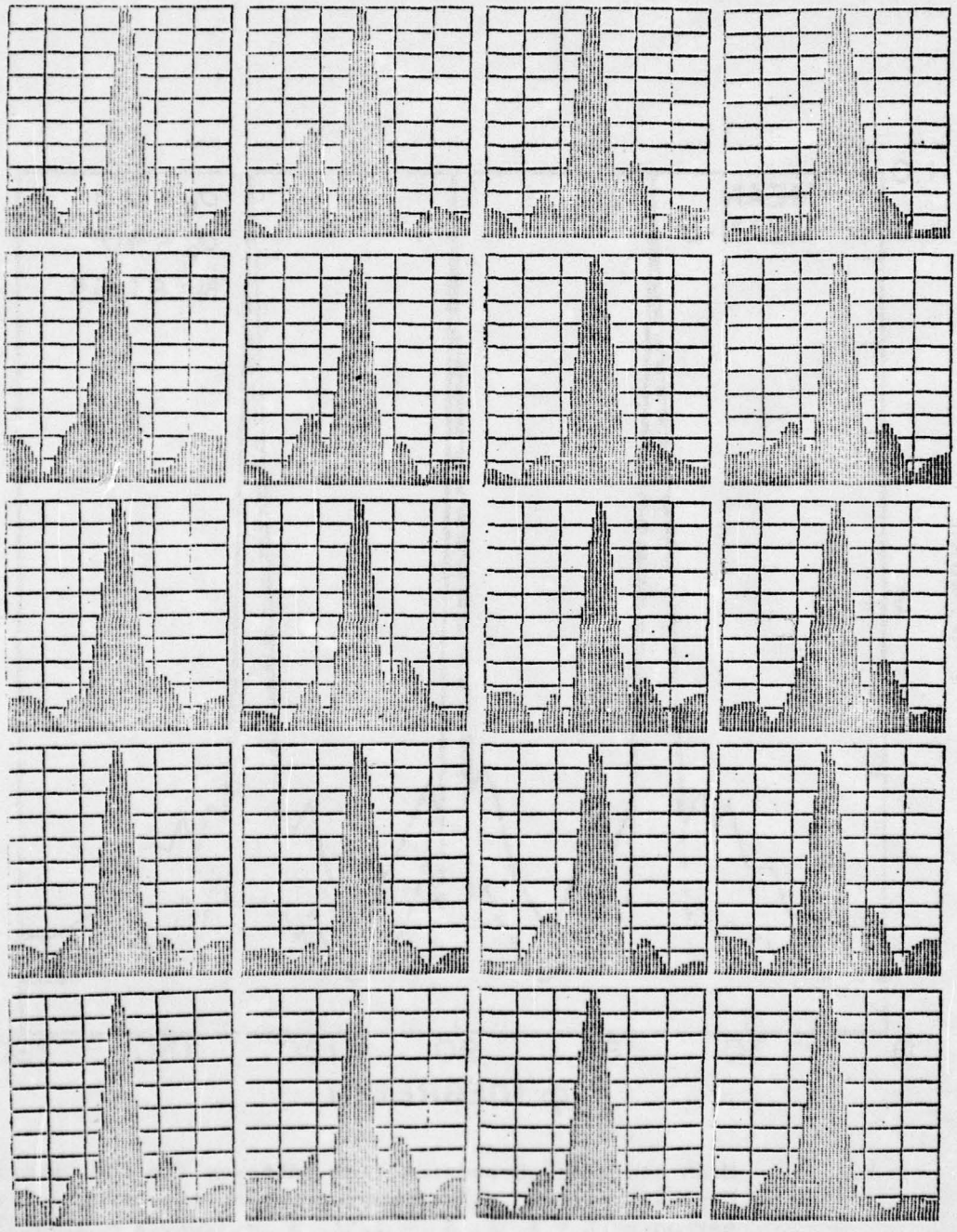

Fig. 18. Individual and mean broadside beam patterns (in the principal H-plane) of a 5 x 5 planar array of dipoles at fundamental frequency ($L = 0.5\lambda$, $S_x = 0.5\lambda$, $S_z = 1.0\lambda$, $a = 0.0005\lambda$, $\sigma_a = 0.5$, $\sigma_p = 40°$)

(a) Individual (sample) patterns.

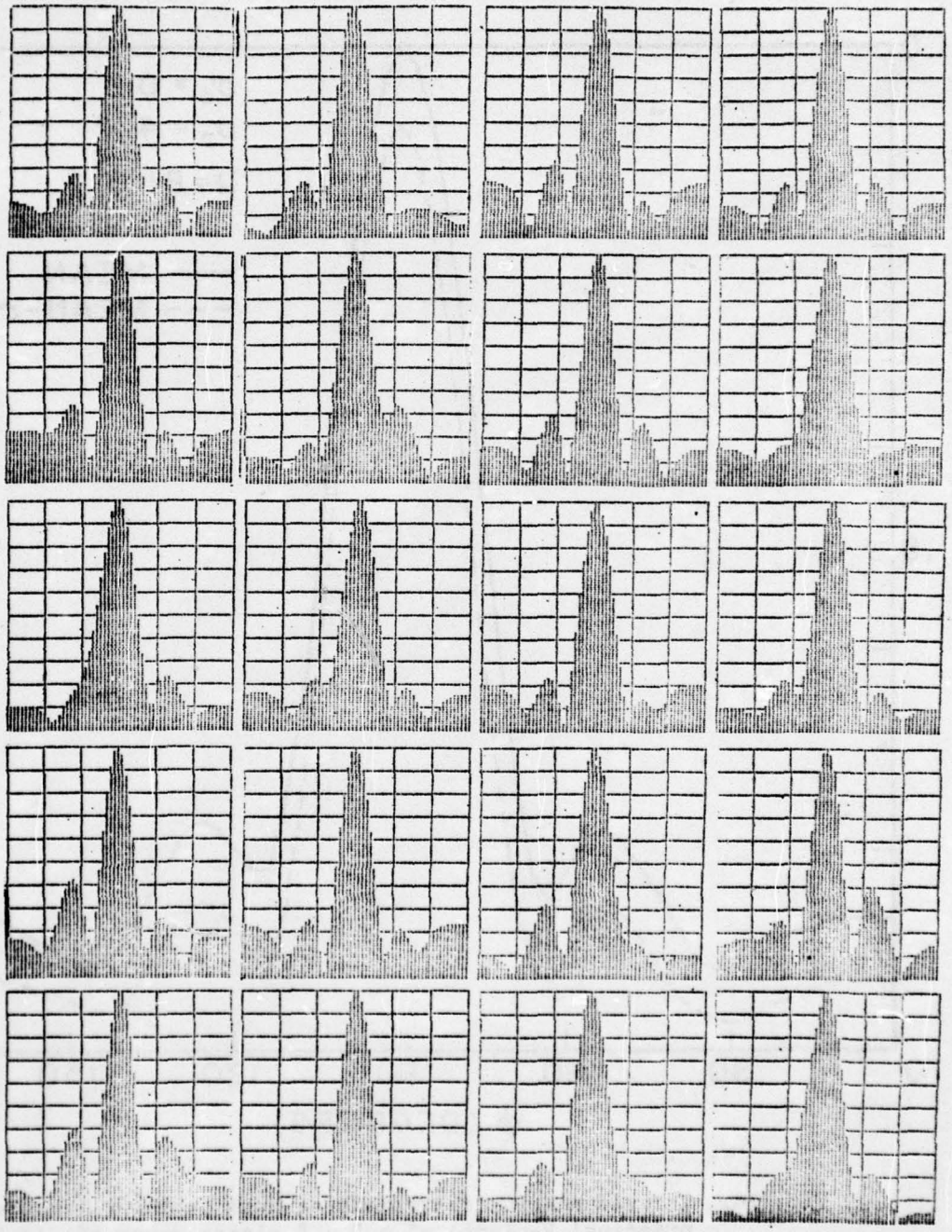

Fig. 18. Individual and mean broadside beam patterns (in the principal H-plane) of a 5 x 5 planar array of dipoles at fundamental frequency ($L = 0.5\lambda$, $S_x = 0.5\lambda$, $S_z = 1.0\lambda$, $a = 0.0005\lambda$, $\sigma_a = 0.5$, $\sigma_p = 40°$)

(b) Individual (sample) patterns

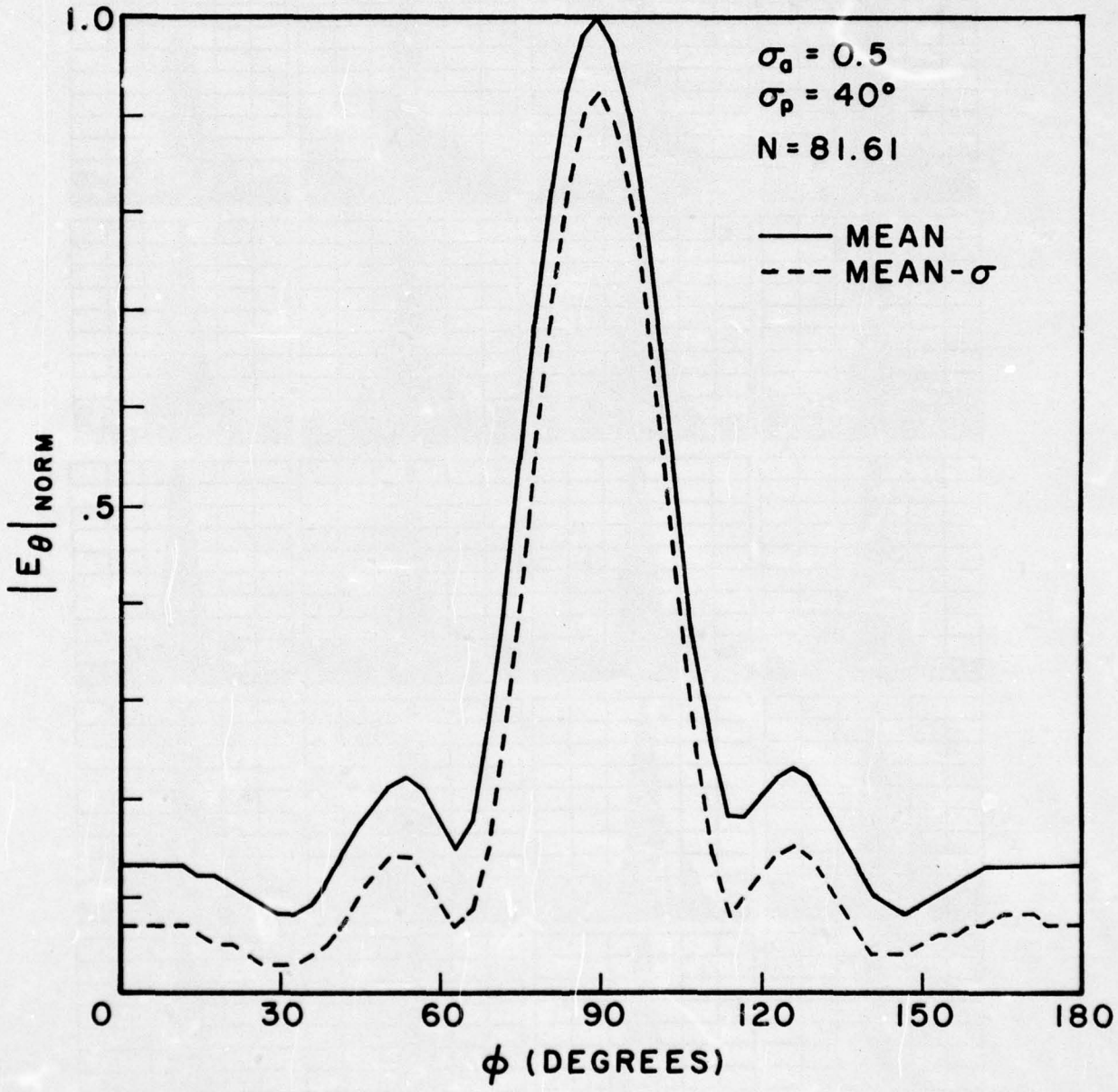

Fig. 18. Individual and mean broadside beam patterns (in the principal H-plane) of a 5 x 5 planar array of dipoles at fundamental frequency ($L = 0.5\lambda$, $S_x = 0.5\lambda$, $S_z = 1.0\lambda$, $a = 0.0005\lambda$, $\sigma_a = 0.5$, $\sigma_p = 40°$)

(c) Mean and M-σ patterns.

AD-A032 131 SYRACUSE UNIV N Y DEPT OF ELECTRICAL AND COMPUTER E--ETC F/G 9/5
SOLID STATE ARRAY STUDIES RELEVANT TO OTP REGULATIONS. PART 2. --ETC(U)
AUG 76 A T ADAMS, P HSI, A FARRAR F30602-75-C-0121
UNCLASSIFIED RADC-TR-76-241-PT-2 NL

2 OF 2
AD
A032131

END

DATE
FILMED
1-77

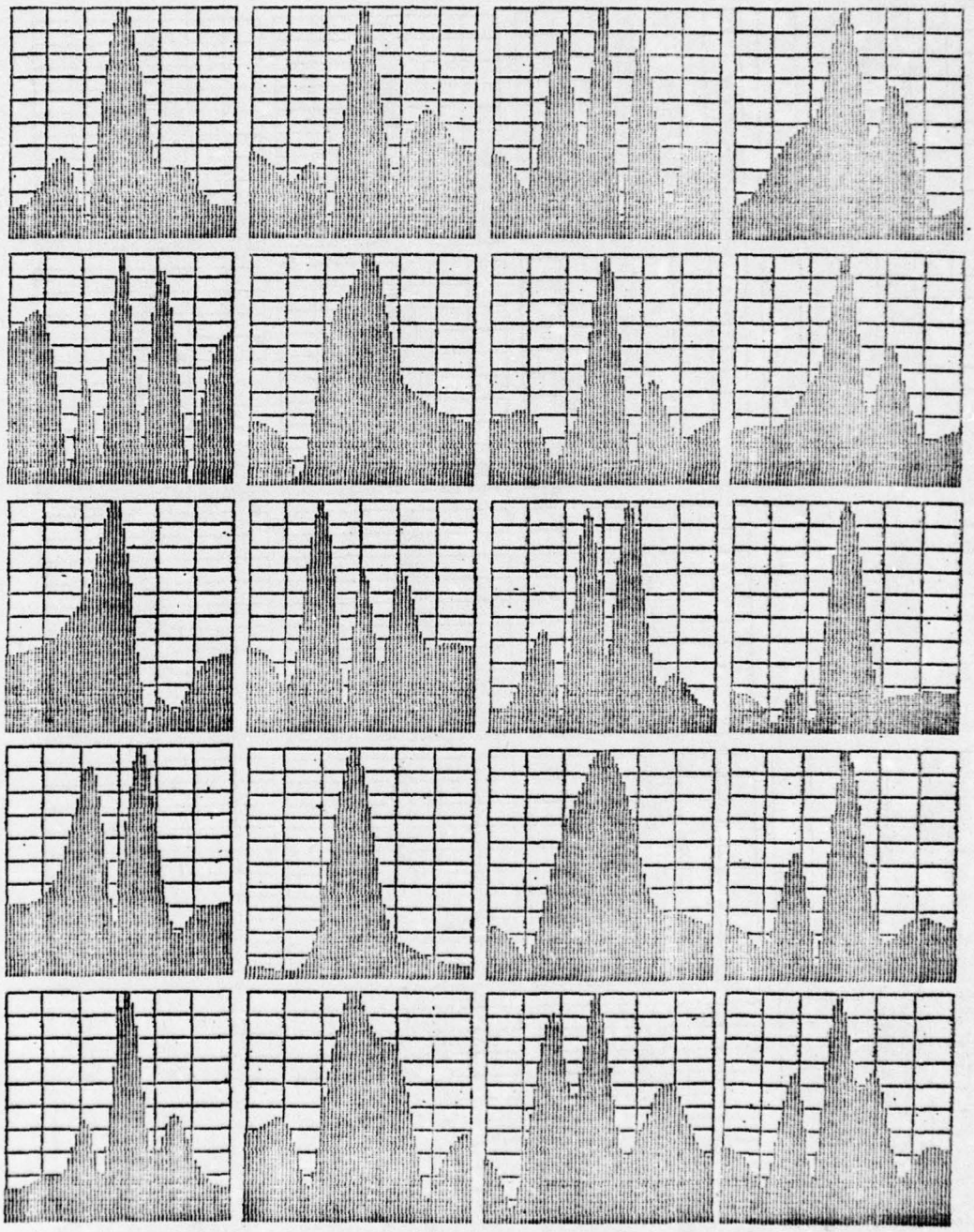

Fig. 19. **Individual and mean broadside bean patterns (in the principal H-plane) of a 5 x 5 planar array of dipoles at fundamental frequency ($L = 0.5\lambda$, $S_x = 0.5\lambda$, $S_z = 1.0\lambda$ $a = 0.0005\lambda$, $\sigma_a = 3.0$, $\sigma_p = 40°$)**

(a) Individual (sample) patterns

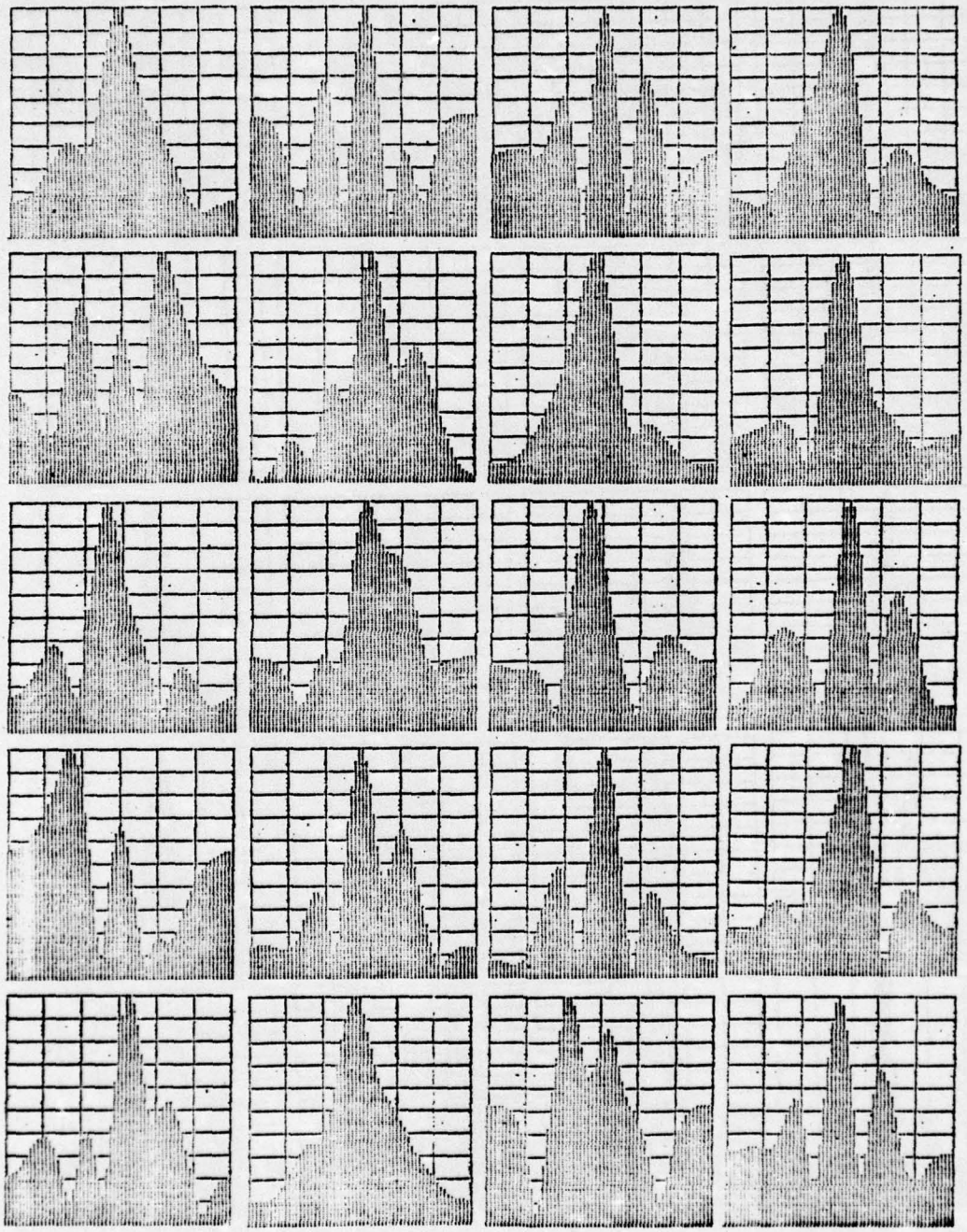

Fig. 19. Individual and mean broadside bean patterns (in the principal H-plane) of a 5 x 5 planar array of dipoles at fundamental frequency ($L = 0.5\lambda$, $S_x = 0.5\lambda$, $S_z = 1.0\lambda$ $a = 0.0005\lambda$, $\sigma_a = 3.0$, $\sigma_p = 40°$)

(b) Individual (sample) patterns

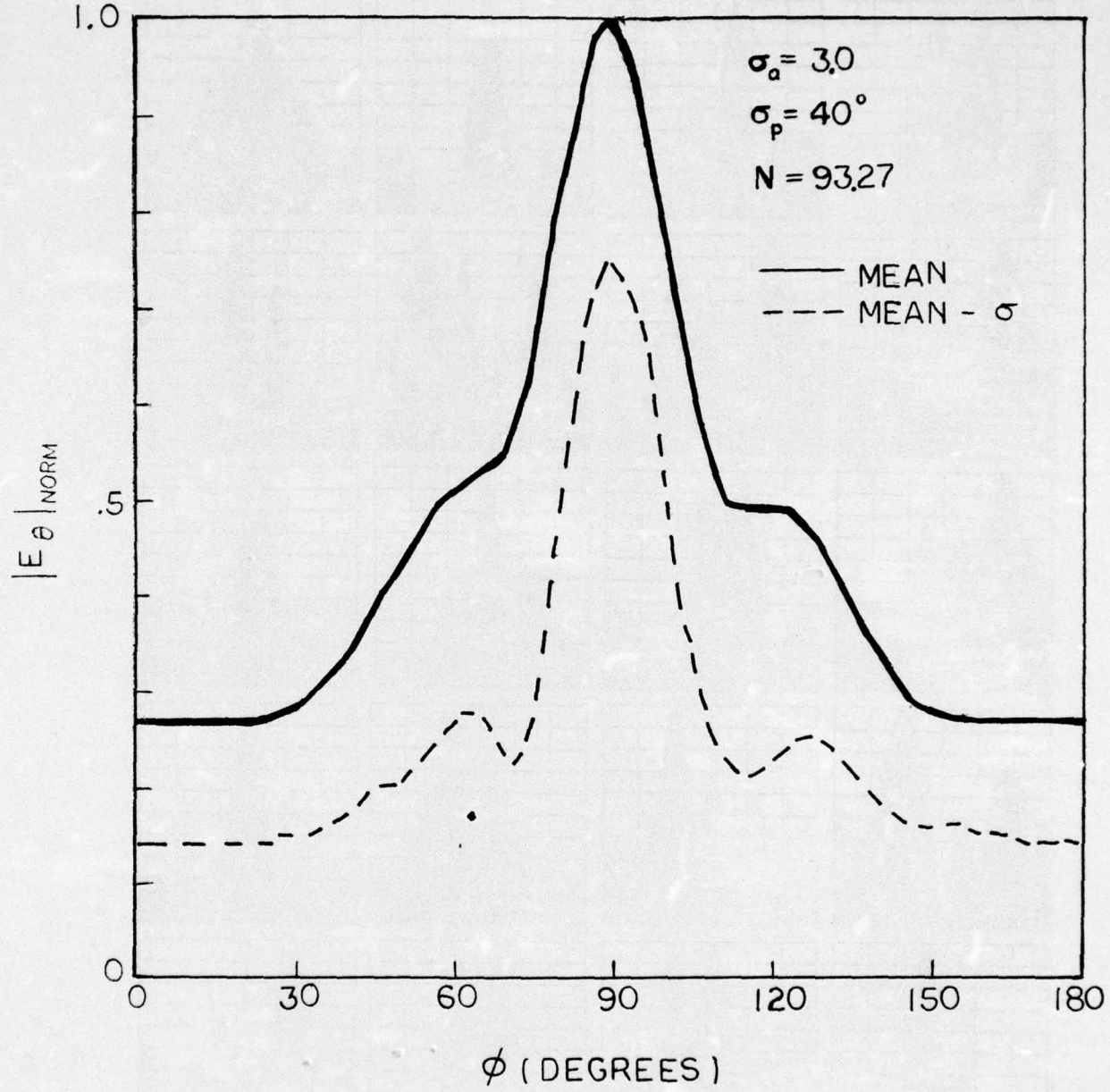

Fig. 19. Individual and mean broadside bean patterns (in the principal H-plane) of a 5 x 5 planar array of dipoles at fundamental frequency ($L = 0.5\lambda$, $S_x = 0.5\lambda$, $S_z = 1.0\lambda$ $a = 0.0005\lambda$, $\sigma_a = 3.0$, $\sigma_p = 40°$)

(c) Mean and (M-σ) patterns.

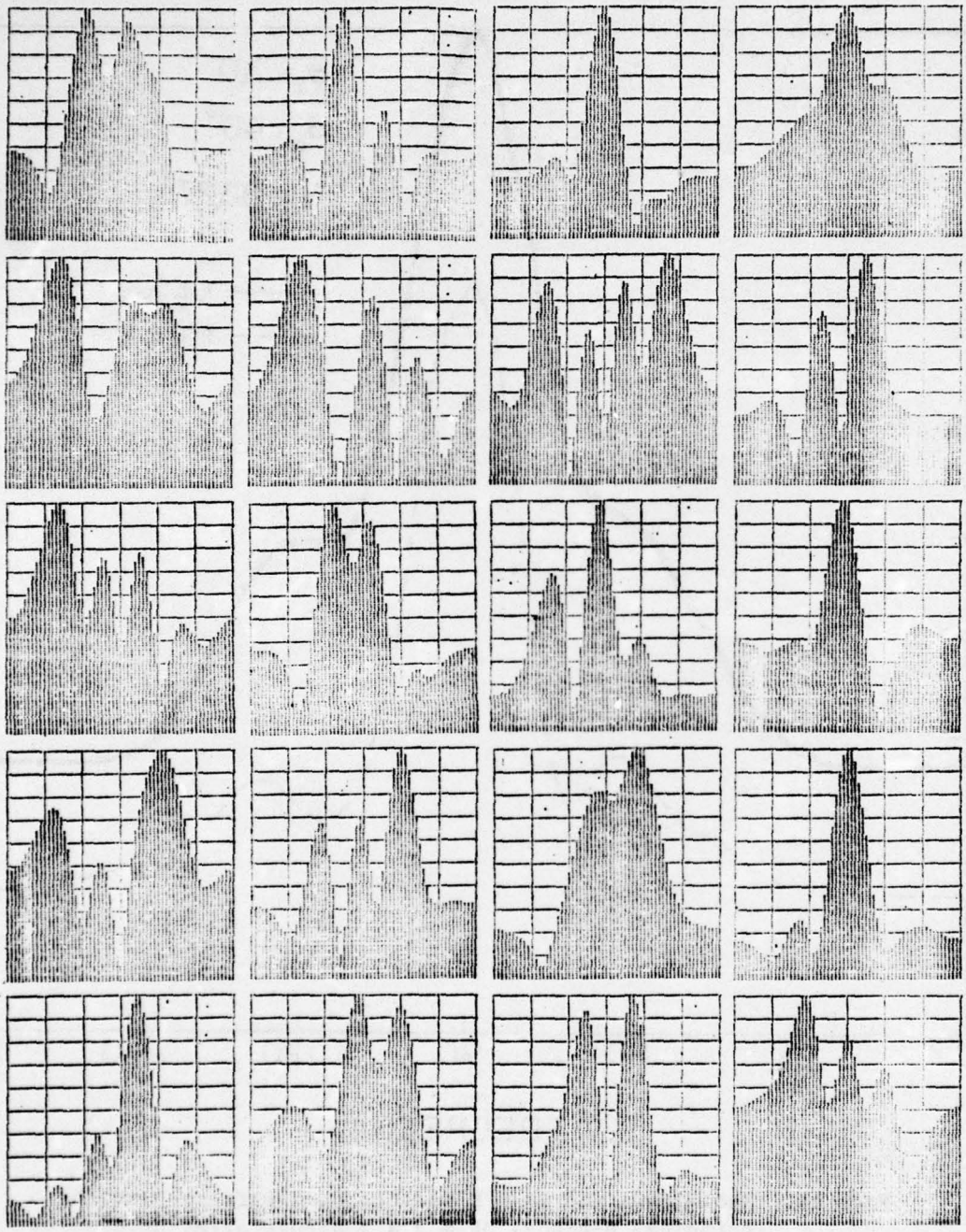

Fig. 20. Individual and broadside mean beam patterns (in the principal H-plane) of a 5 x 5 planar array of dipoles at fundamental frequency ($L = 0.5\lambda$, $S_x = 0.5\lambda$, $S_z = 1.0\lambda$, $a = 0.0005\lambda$, $\sigma_a = 0.5$, $\sigma_p = 180°$)

(a) Individual (sample) patterns

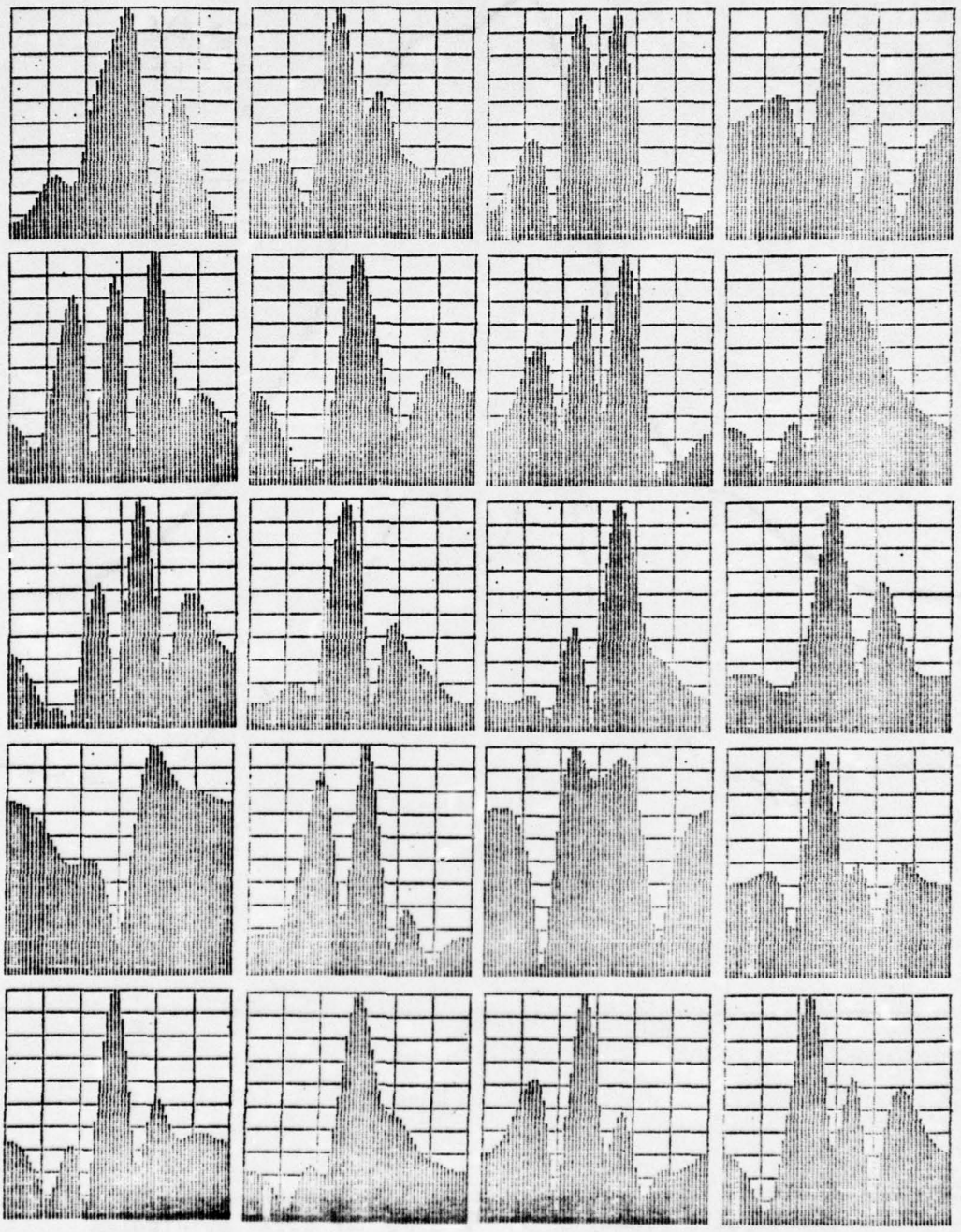

Fig. 20. Individual and broadside mean beam patterns (in the principal H-plane) of a 5 x 5 planar array of dipoles at fundamental frequency ($L = 0.5\lambda$, $S_x = 0.5\lambda$, $S_z = 1.0\lambda$, $a = 0.0005\lambda$, $\sigma_a = 0.5$, $\sigma_p = 180°$)

(b) Individual (sample) patterns

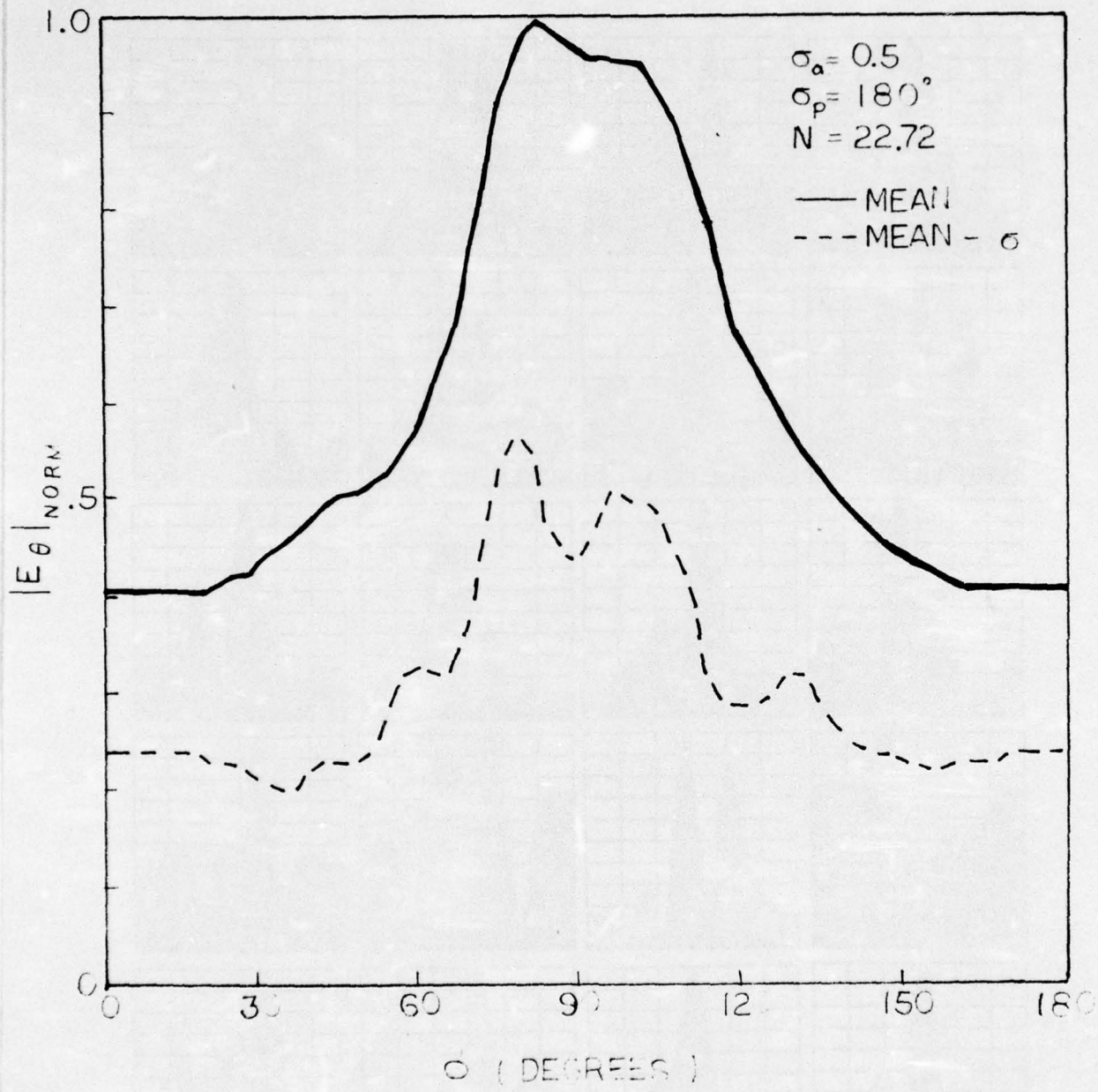

Fig. 20. Individual and broadside mean beam patterns (in the principal H-plane) of a 5 x 5 planar array of dipoles at fundamental frequency ($L = 0.5\lambda$, $S_x = 0.5\lambda$, $S_z = 1.0\lambda$, $a = 0.0005\lambda$, $\sigma_a = 0.5$, $\sigma_p = 180°$)

(c) Mean and (M-σ) patterns.

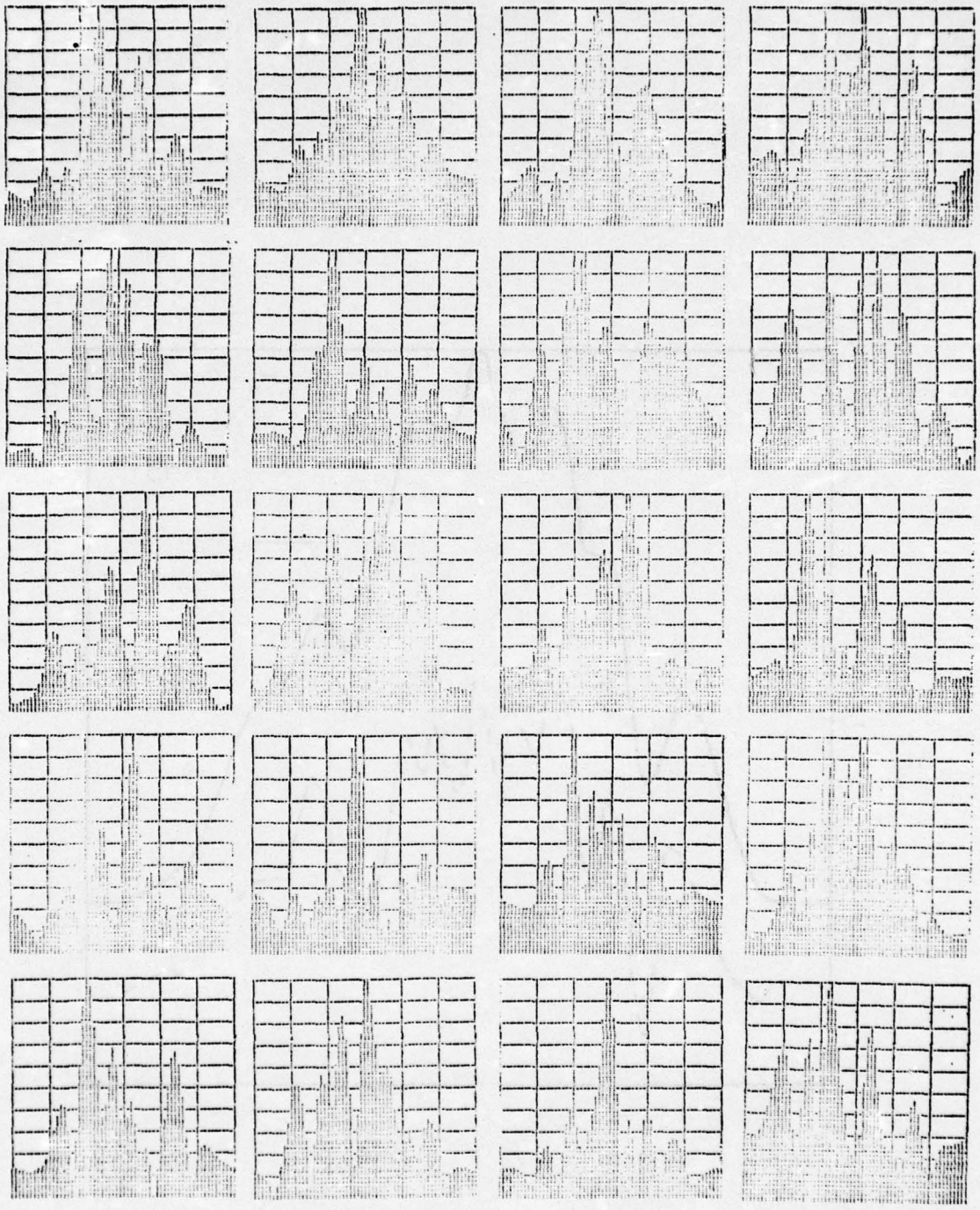

Fig. 21. Individual and mean broadside patterns (in the principal H-plane) of an eleven element linear array of dipoles at fundamental frequency ($L = 0.5\lambda$, $S_x = 0.5\lambda$, $a = 0.005\lambda$, $\sigma_a = 0$, $\sigma_p = \infty$(random))

(a) Individual (sample) patterns

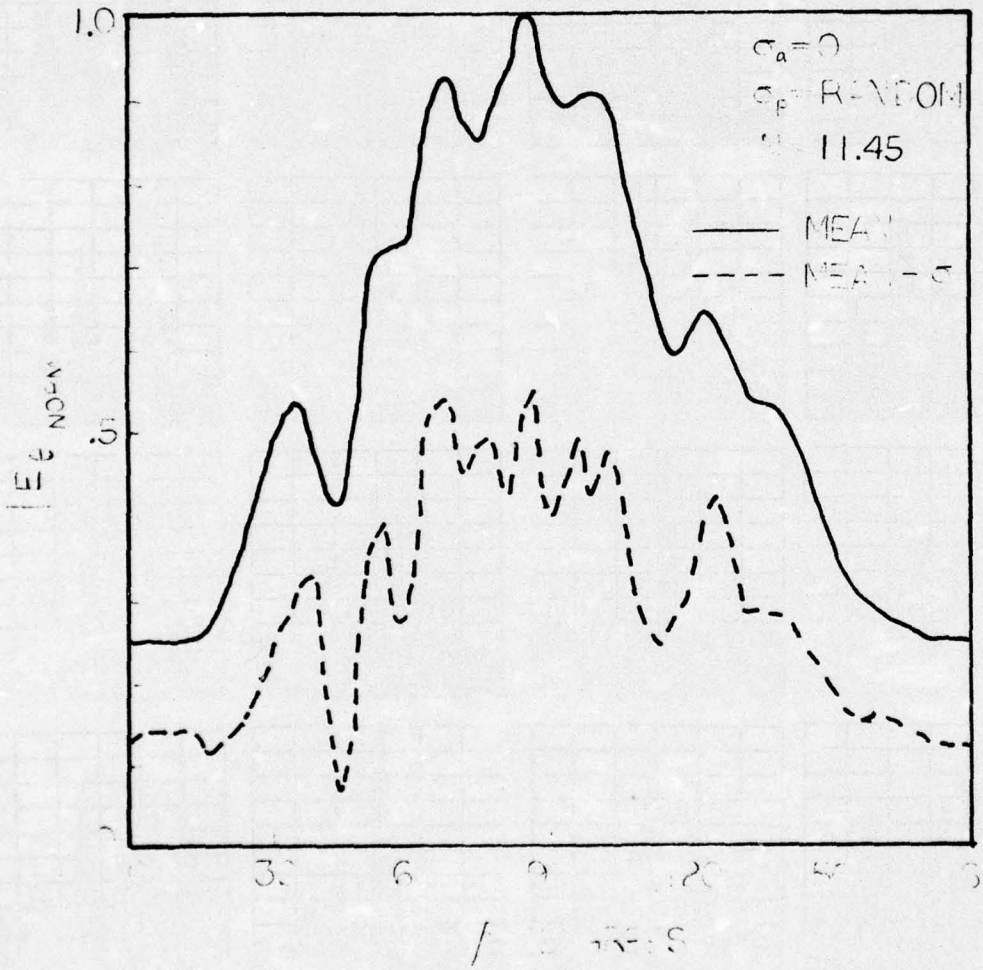

Fig. 21. Individual and mean broadside patterns (in the principal H-plane) of an eleven element linear array of dipoles at fundamental frequency ($L = 0.5\lambda$, $S_x = 0.5\lambda$, $a = 0.005\lambda$, $\sigma_a = 0$, $\sigma_p = \infty$(random))

(b) Mean and (n-σ) patterns with mutuals

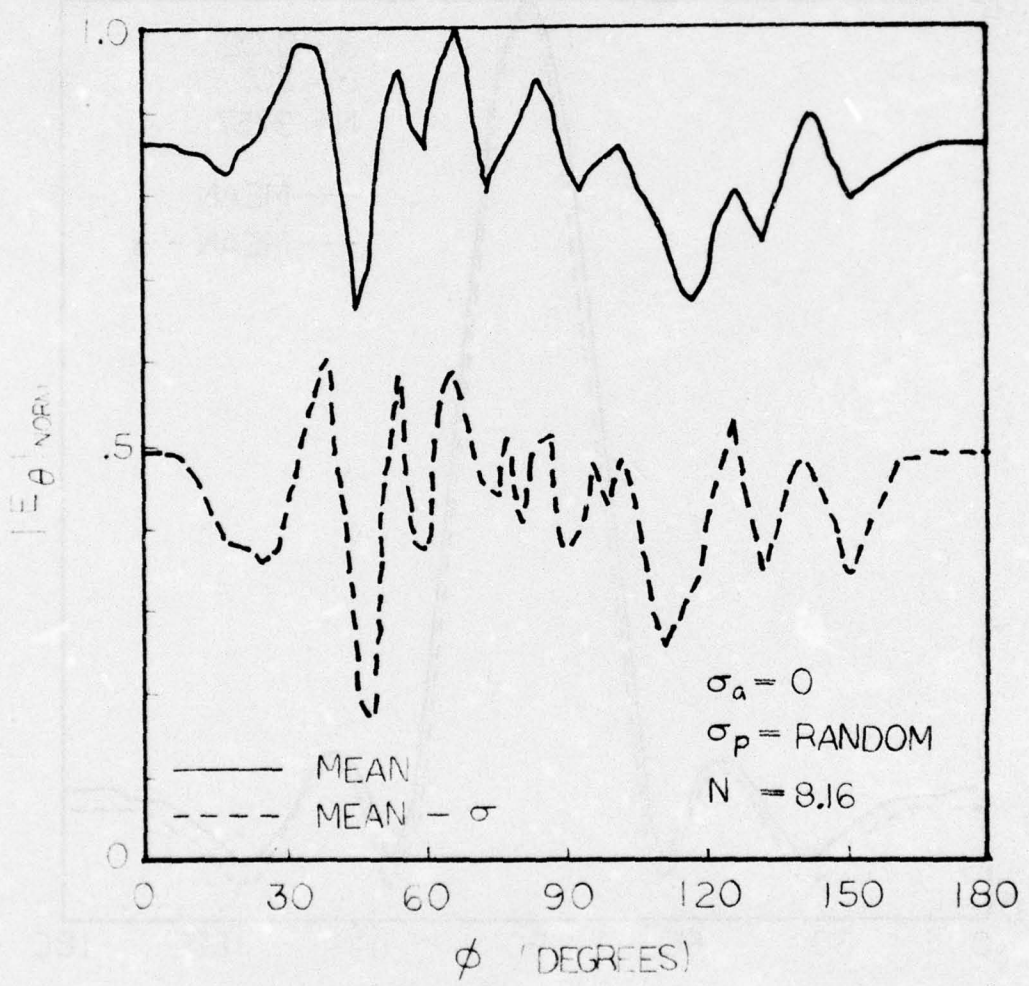

Fig. 21. Individual and mean broadside patterns (in the principal H-plane) of an eleven element linear array of dipoles at fundamental frequency ($L = 0.5\lambda$, $S_x = 0.5\lambda$, $a = 0.005\lambda$, $\sigma_a = 0$, $\sigma_p = \infty$(random))

(c) Mean and (n-σ) patterns without mutuals.

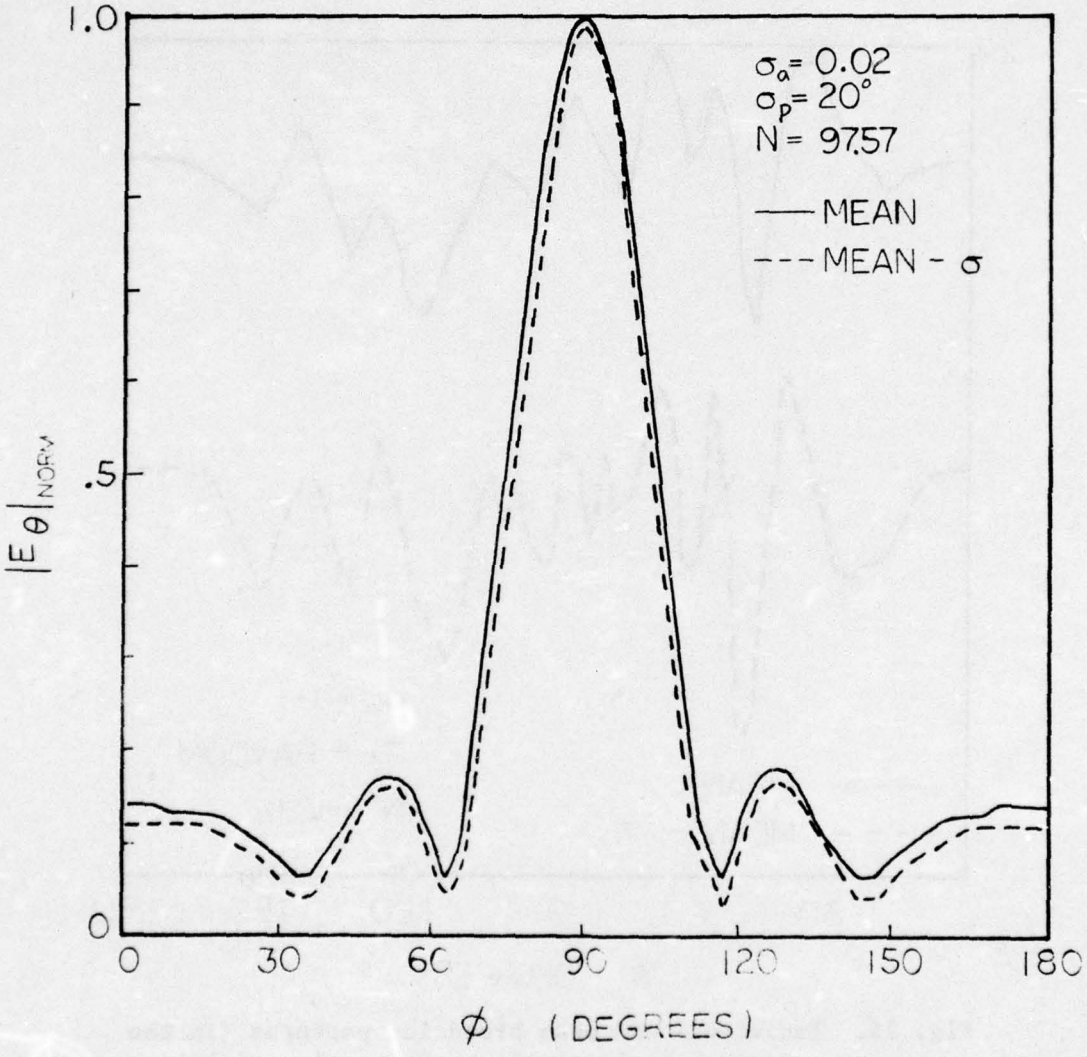

Fig. 22. Mean and (M-σ) beam patterns (in the principal H-plane) of a 5 x 5 planar array of dipoles at fundamental frequency ($L = 0.5\lambda$, $S_x = 0.5\lambda$, $S_z = 1.0\lambda$, $a = 0.0005\lambda$, $\sigma_a = 0.02$, $\sigma_p = 20°$)

(a) Broadside patterns - with mutuals

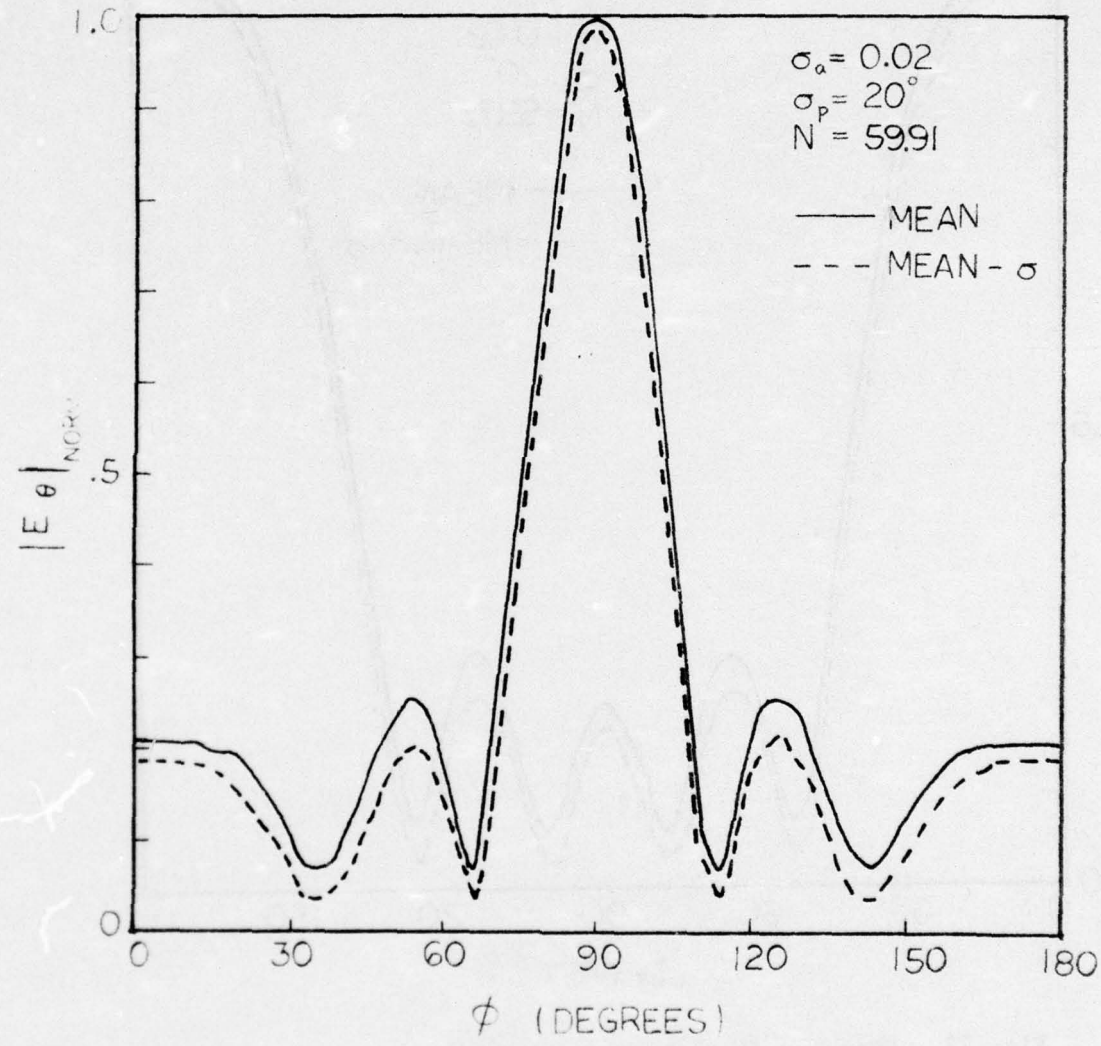

Fig. 22. Mean and (M-σ) beam patterns (in the principal H-plane) of a 5 x 5 planar array of dipoles at fundamental frequency ($L = 0.5\lambda$, $S_x = 0.5\lambda$, $S_z = 1.0\lambda$, $a = 0.0005\lambda$, $\sigma_a = 0.02$, $\sigma_p = 20°$)

(b) Broadside patterns - without mutuals

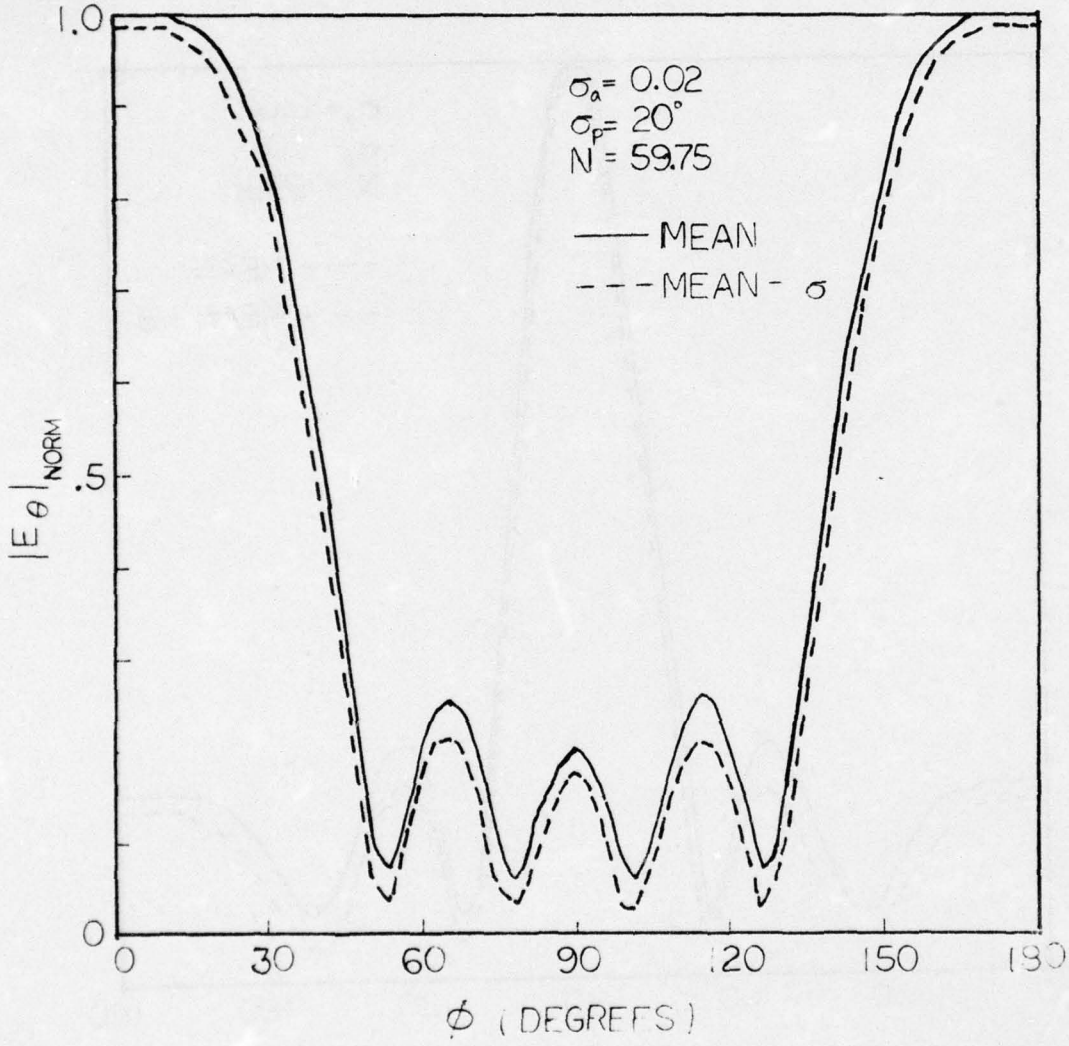

Fig. 22. Mean and (M-σ) beam patterns (in the principal H-plane) of a 5 x 5 planar array of dipoles at fundamental frequency (L = 0.5λ, S_x = 0.5λ, S_z = 1.0λ, a = 0.0005λ, σ_a = 0.02, σ_p = 20°)

(c) Endfire patterns - with mutuals

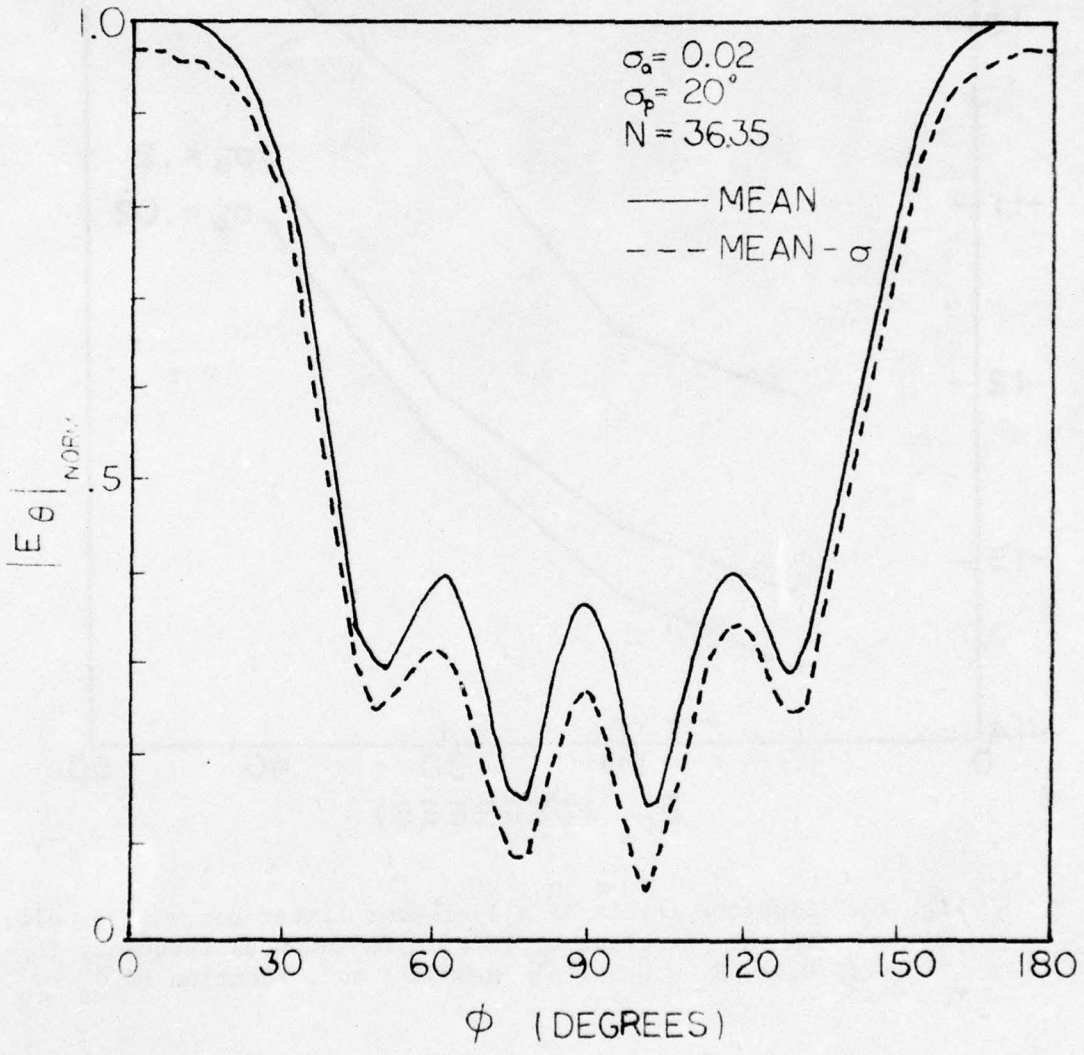

Fig. 22. Mean and (M-σ) beam patterns (in the principal H-plane) of a 5 x 5 planar array of dipoles at fundamental frequency ($L = 0.5\lambda$, $S_x = 0.5\lambda$, $S_z = 1.0\lambda$, $a = 0.0005\lambda$, $\sigma_a = 0.02$, $\sigma_p = 20°$)

(d) Endfire patterns - without mutuals.

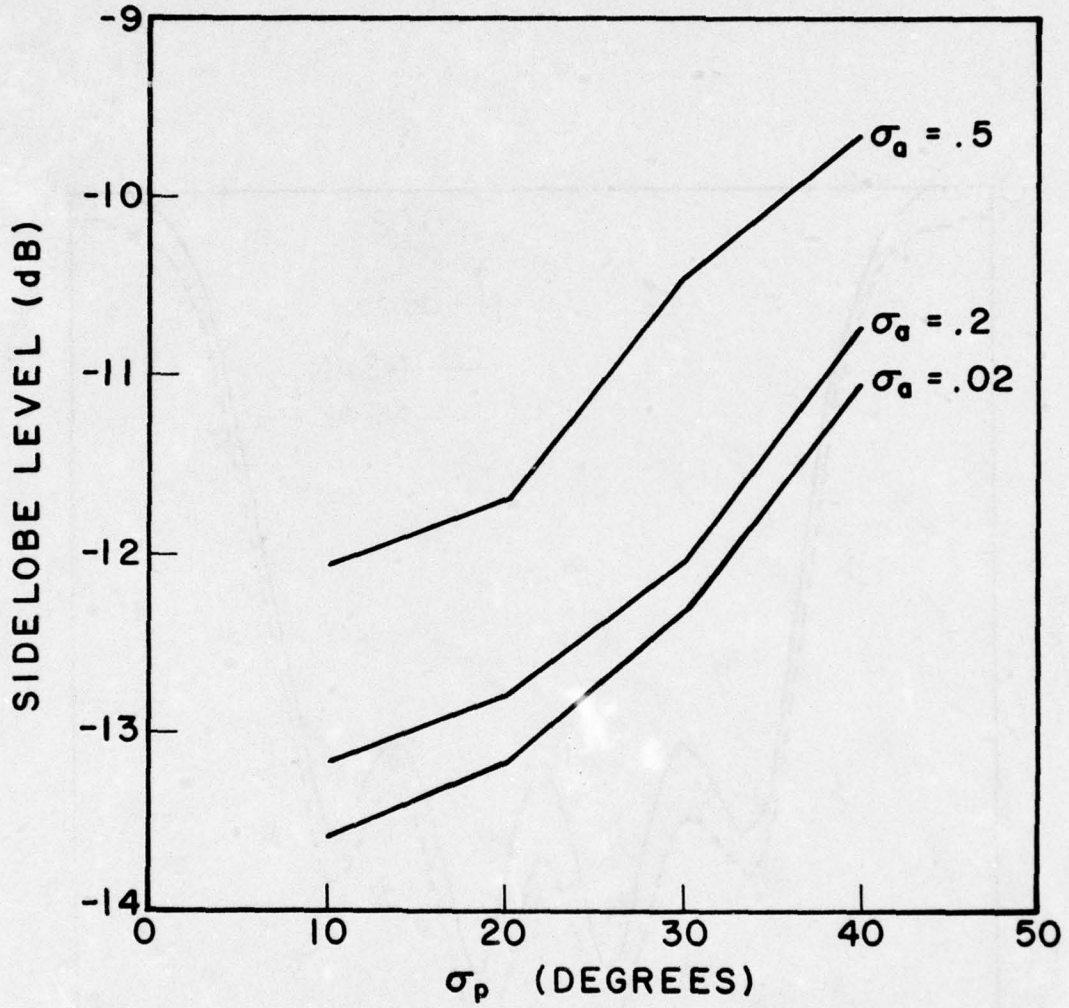

Fig. 23. Sidelobe levels of a 9-element linear array of dipoles in the principal H-plane at fundamental frequency (L = 0.5λ, S_x = 0.5λ, a = 0.0005λ) as a function of σ_a. σ_p.

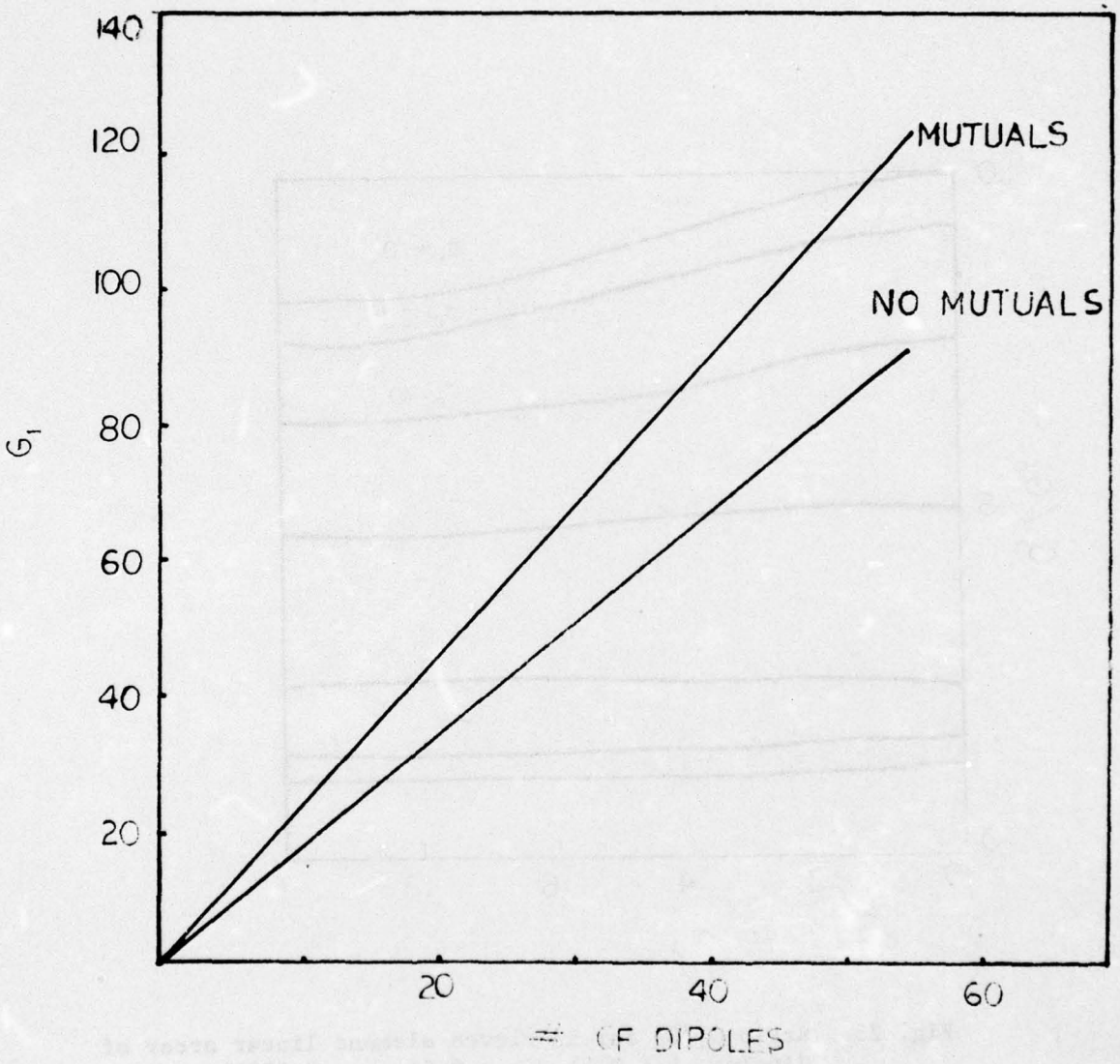

Fig. 24. Gain G_o for a uniformly-excited linear array of dipoles ($L = 0.5\lambda$, $S_x = 0.5\lambda$, $a = 0.005\lambda$) with and without mutuals as a function of the number of dipoles.

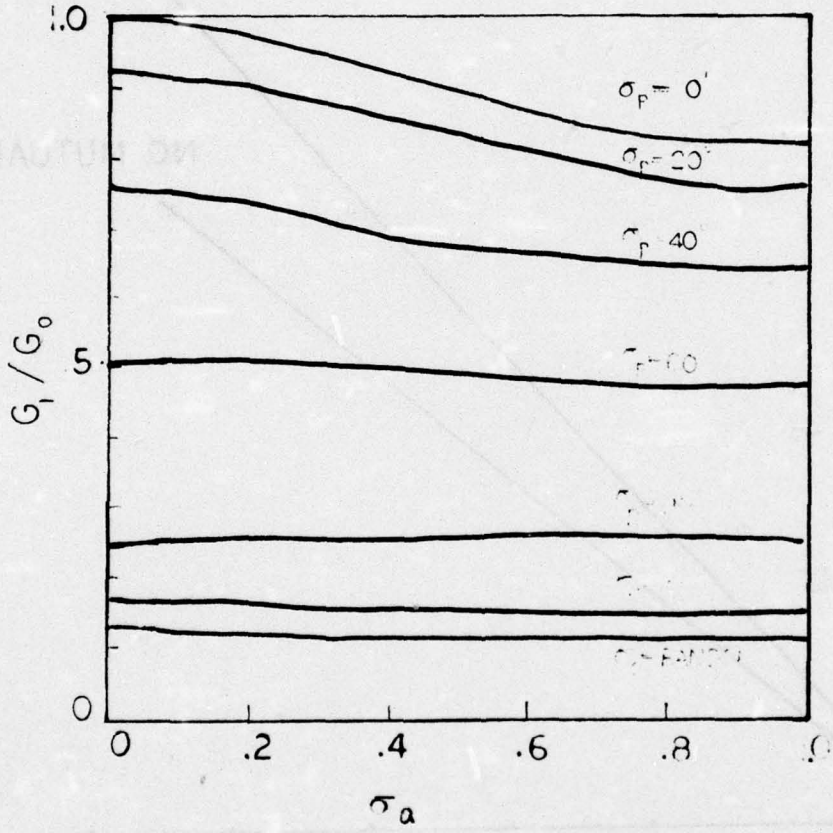

Fig. 25. Ratio G_1/G_0 for an eleven element linear array of dipoles ($L = 0.5\lambda$, $S_x = 0.5\lambda$, $a = 0.005\lambda$)

(a) as a function of σ_a, σ_p

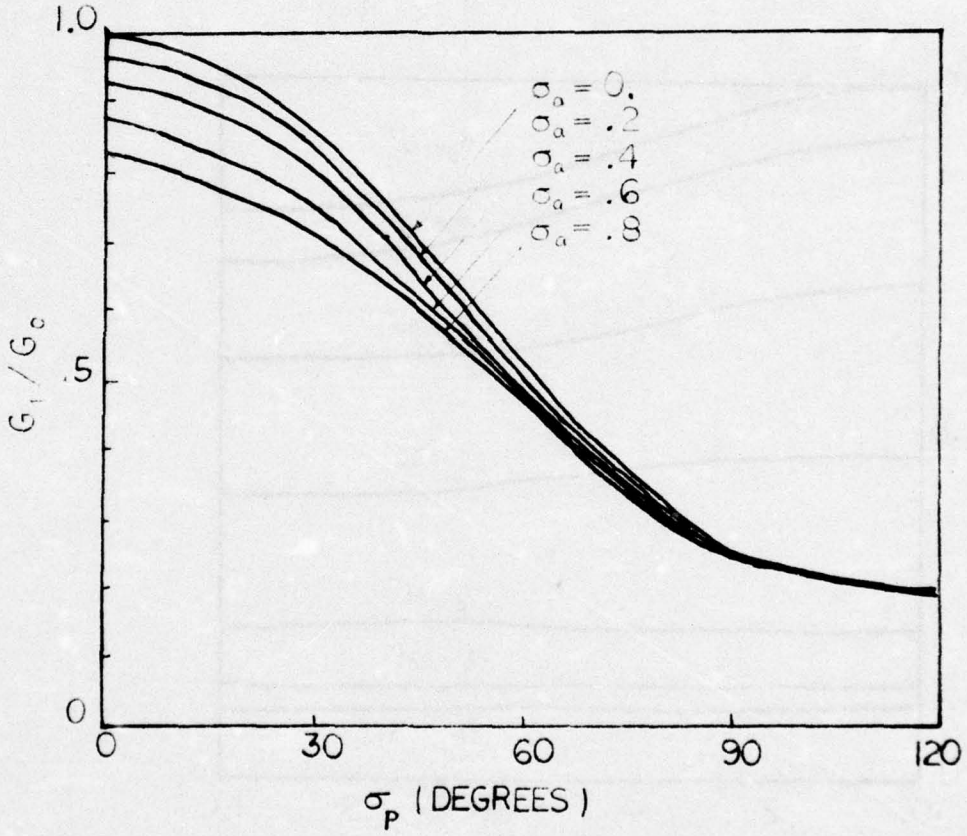

Fig. 25. Ratio G_1/G_0 for an eleven element linear array of dipoles ($L = 0.5\lambda$, $S_x = 0.5\lambda$, $a = 0.005\lambda$)

(b) as a function of σ_p, σ_a.

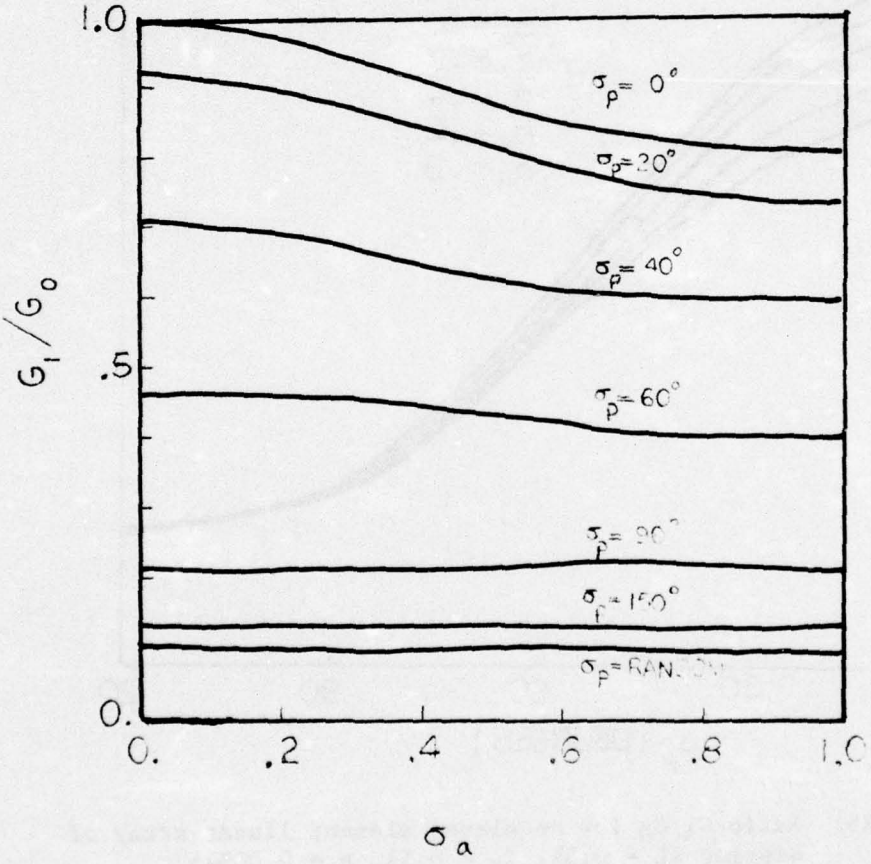

Fig. 26. Ratio G_1/G_0 for an eleven element linear array of dipoles ($L = 0.5\lambda$, $S_z = 0.6\lambda$, $a = 0.005\lambda$)

(a) as a function of σ_a, σ_p

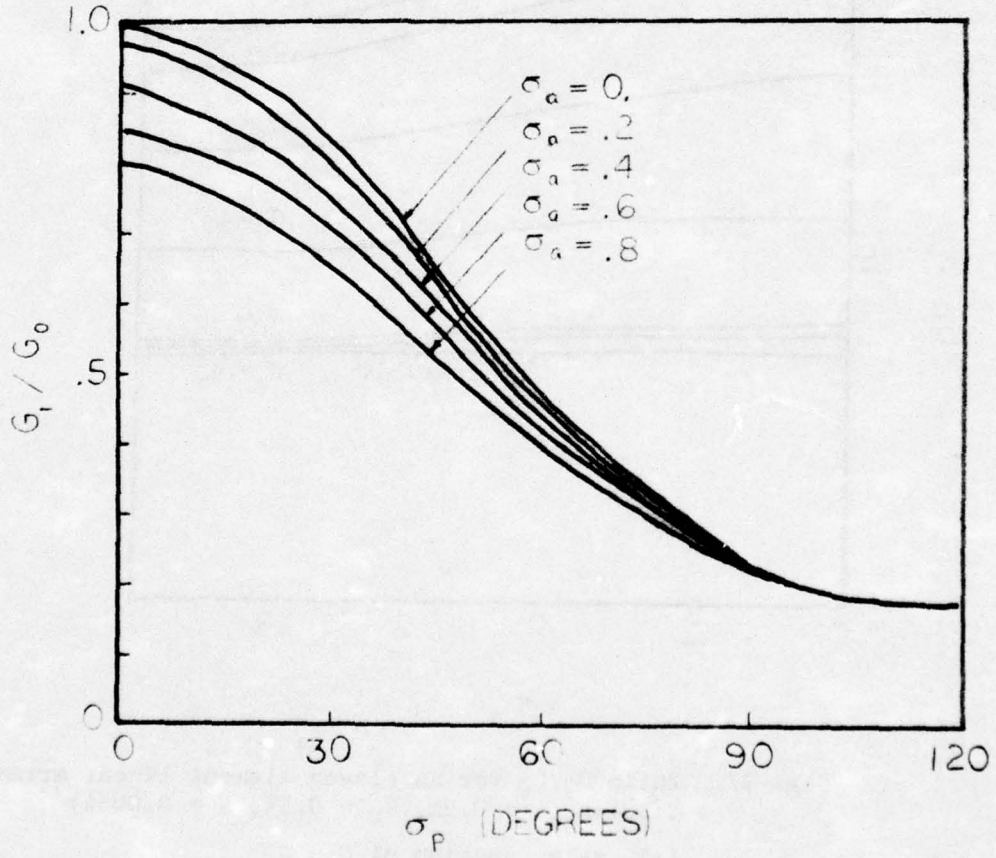

Fig. 26. Ratio G_1/G_0 for an eleven element linear array of dipoles ($L = 0.5\lambda$, $S_z = 0.6\lambda$, $a = 0.005\lambda$)

(b) as a function of σ_p, σ_a.

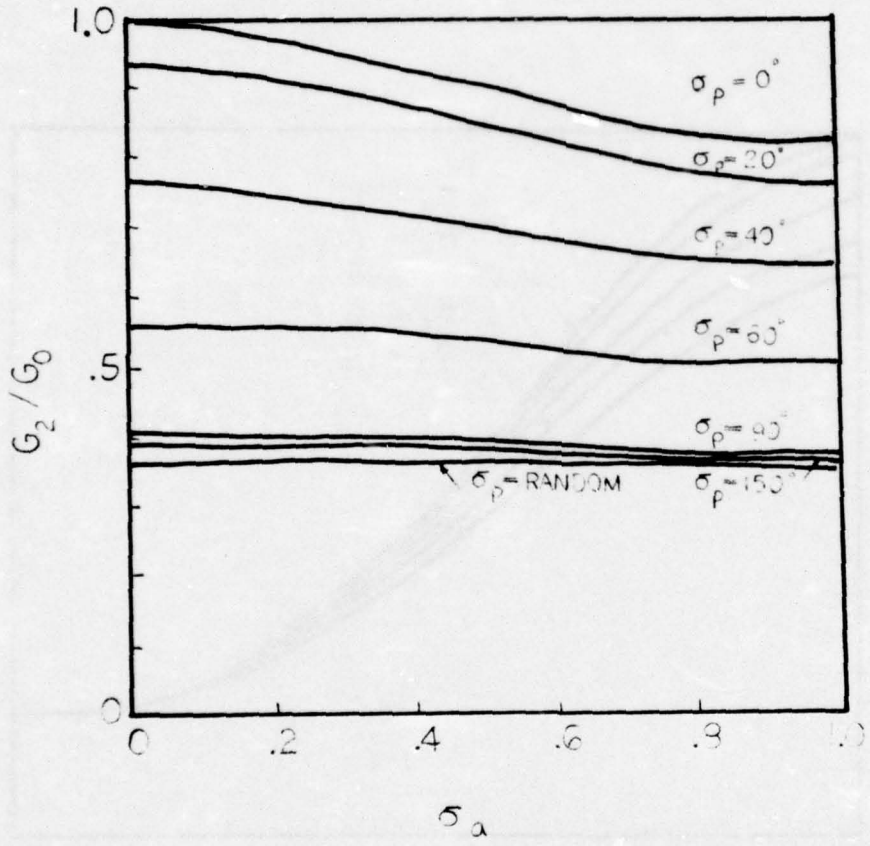

Fig. 27. Ratio G_2/G_0 for an eleven element linear array of dipoles ($L = 0.5\lambda$, $S_x = 0.5\lambda$, $a = 0.005\lambda$)

(a) as a function of σ_a, σ_p

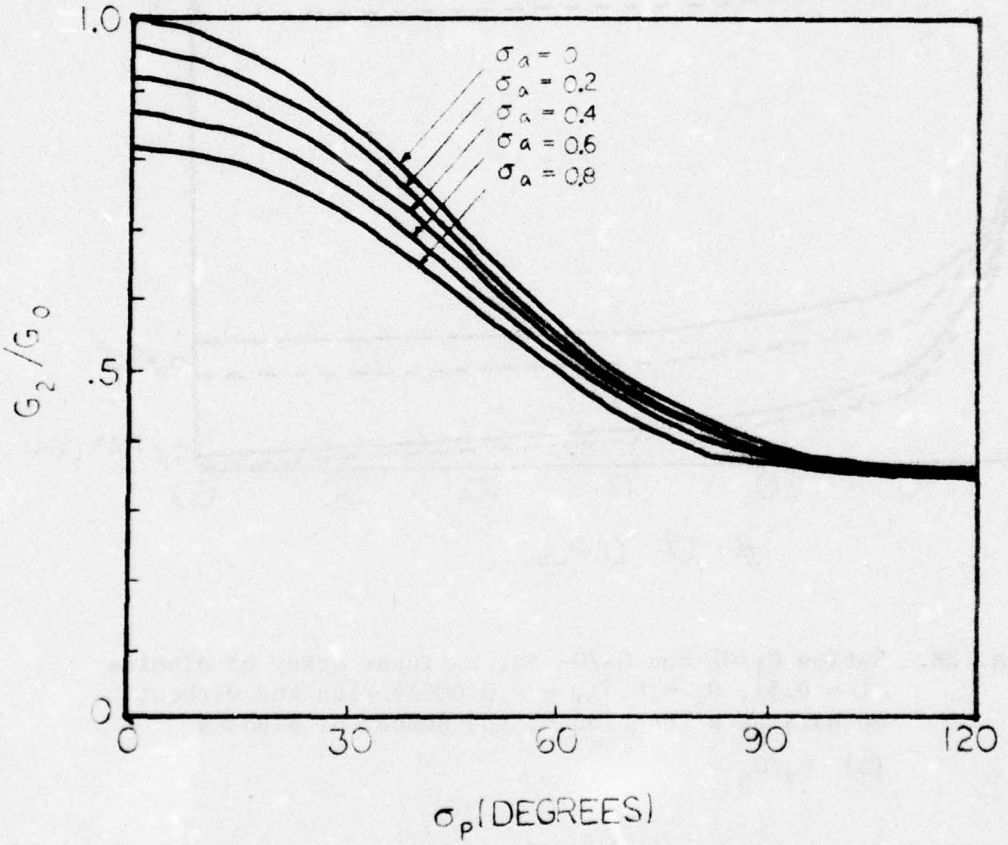

Fig. 27. Ratio G_2/G_0 for an eleven element linear array of dipoles ($L = 0.5\lambda$, $S_x = 0.5\lambda$, $a = 0.005\lambda$)

(b) as a function of σ_p, σ_a.

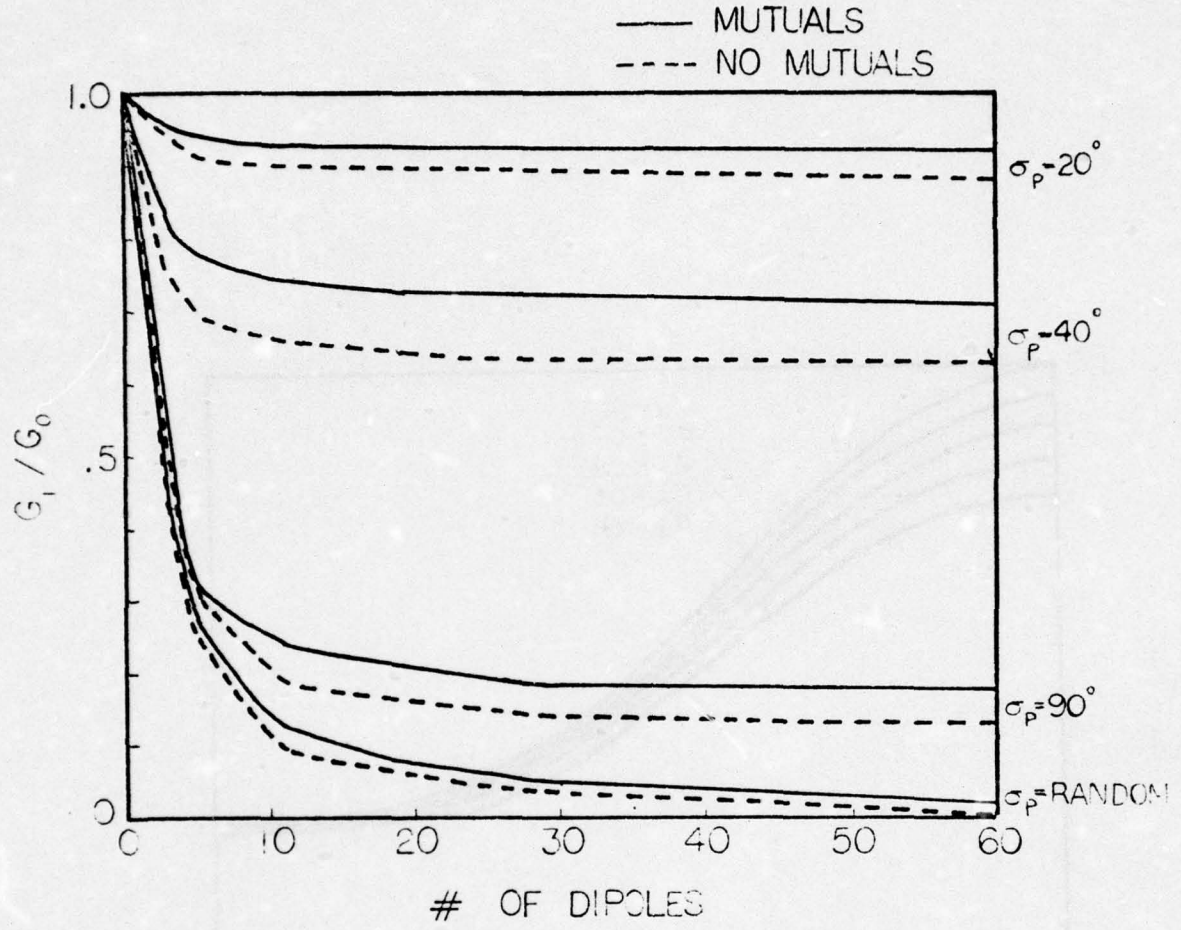

Fig. 28. Ratios G_1/G_0 and G_2/G_0 for a linear array of dipoles ($L = 0.5\lambda$, $S_x = 0.5\lambda$, $a = 0.005\lambda$) with and without mutuals as a function of the number of dipoles

(a) G_1/G_0

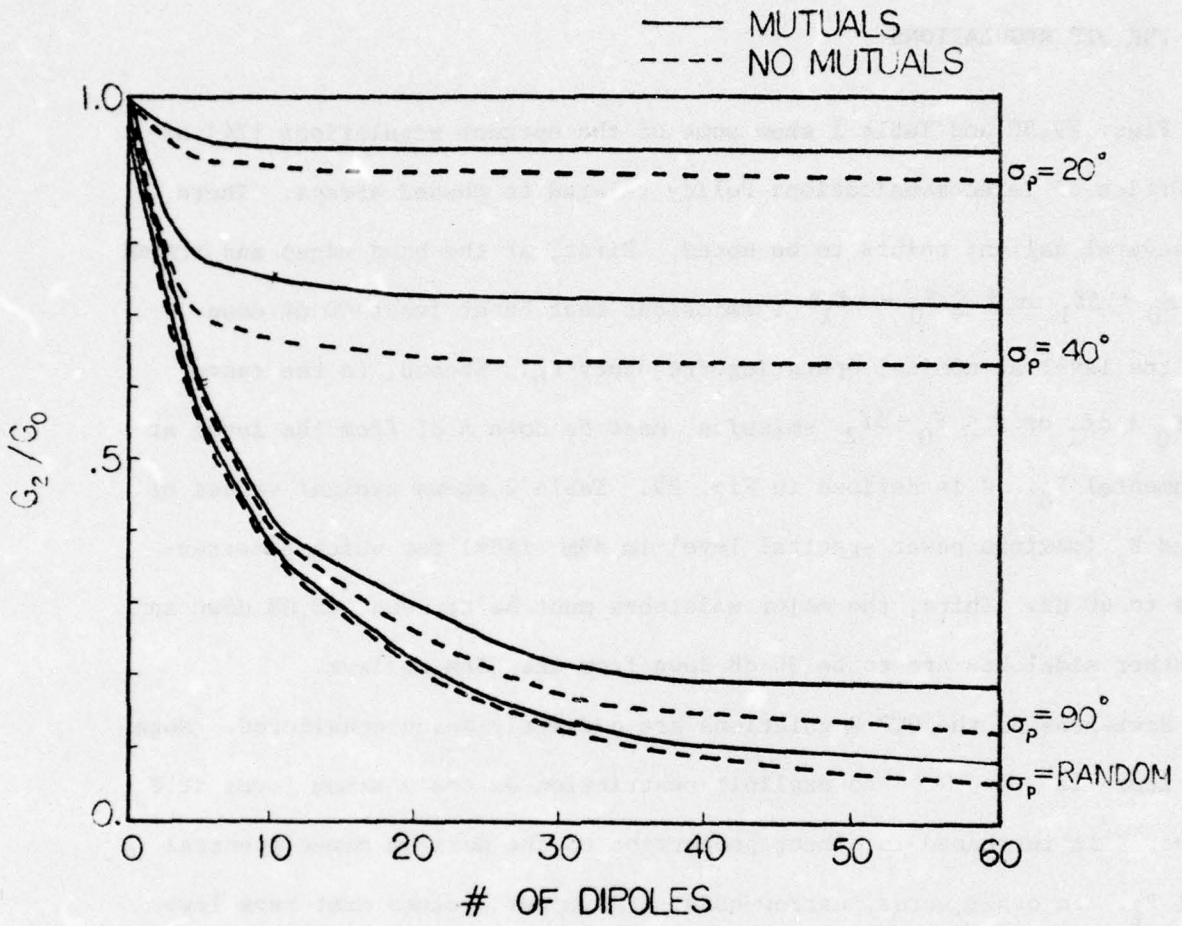

Fig. 28. Ratios G_1/G_0 and G_2/G_0 for a linear array of dipoles ($L = 0.5\lambda$, $S_x = 0.5\lambda$, $a = 0.005\lambda$) with and without mutuals as a function of the number of dipoles

(b) G_2/G_0

6 APPLICATION OF THE OTP REGULATIONS

6.1 THE OTP REGULATIONS

Figs. 29,30 and Table 1 show some of the current regulations [24] of the Office of Telecommunications Policy related to phased arrays. There are several salient points to be noted. First, at the band edges and beyond ($f \geq F_0 + \Delta f_1$ or $f \leq F_0 - \Delta f_1$) , emissions must be at least 40 dB down from the level at nominal operating frequency F_0. Second, in the range $f \geq F_0 + \Delta f_2$ or $f \leq F_0 - \Delta f_2$ emissions must be down S dB from the level at fundamental F_0. S is defined in Fig. 29. Table 2 shows typical values of F_0 and P_t (maximum power spectral level in dBm /KHz) for which S corresponds to 60 dB. Third, the major sidelobes must be at least 20 dB down and all other sidelobes are to be 30 dB down from the beam maximum.

Revisions of the OTP Regulations are currently being considered. Note that there is no explicit restriction on the maximum level at F_0, however S is increased in direct proportion to the maximum power spectral level P_t. In other words, narrow-band, high-power systems must have lower relative levels for harmonic and spurious emissions. The level S may be changed somewhat in future revised regulations. In the discussions of this chapter, the level S is assumed to be about 60 dB, corresponding to the cases shown in Table 2. Cases falling outside this range will be discussed separately.

RADAR EMISSION BANDWIDTH AND EMISSION LEVELS

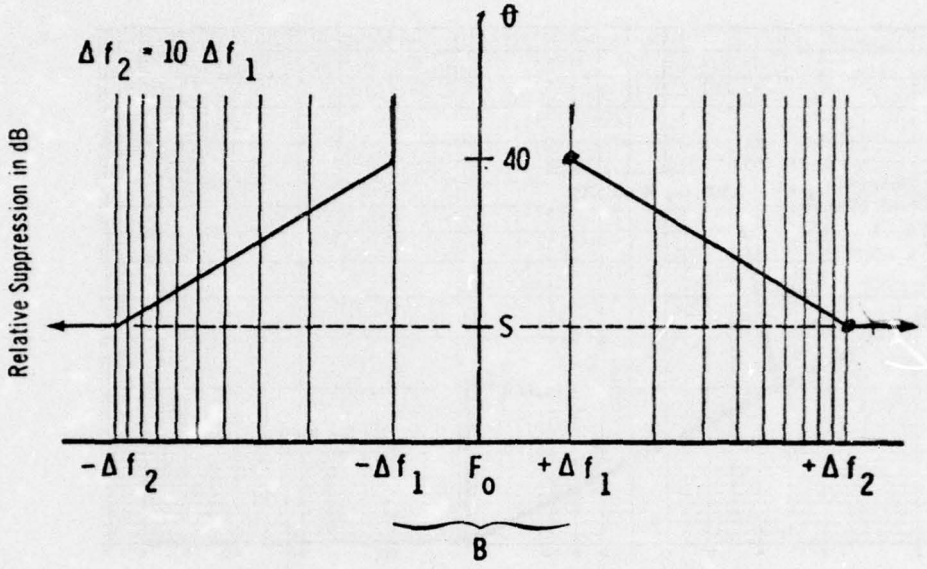

Definition of S:

$$S = P_t - 20 \log F_0 + 100 > 40 \text{ dB}$$

Sidelobe Level Requirements:

Major sidelobes - 20 dB

All other sidelobes - 30 dB

Fig. 29. **OTP Regulations on Emission Levels and Sidelobe Levels.**

DEPENDENCE OF WEIGHTING FACTOR k UPON K

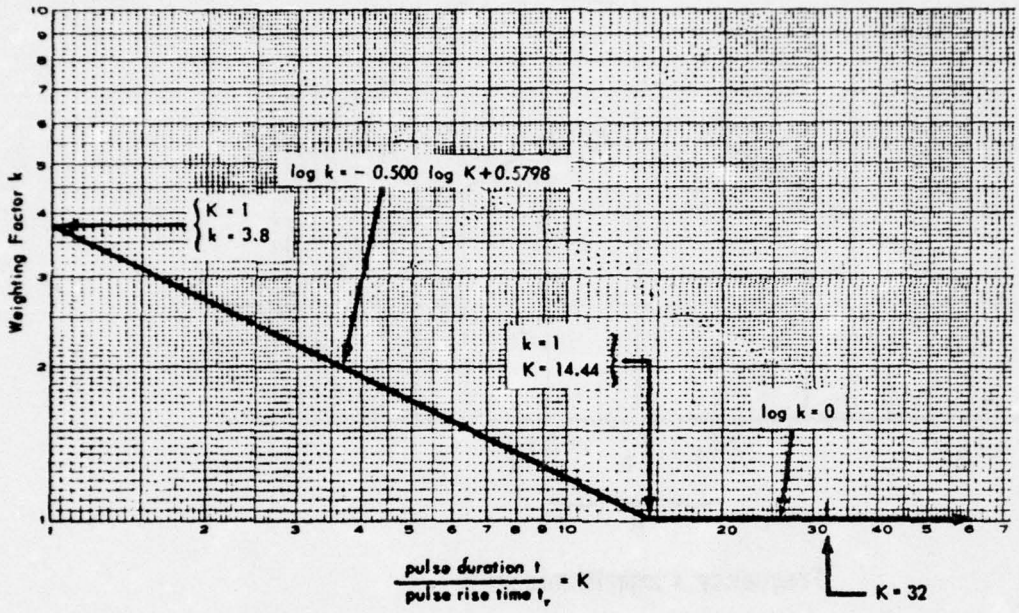

Fig. 30. Weighting Factor k (OTP Regulations).

TABLE 1

BANDWIDTH DEFINITIONS FOR OTP REGULATIONS

$$B = \frac{2kK}{t} \leq \frac{64}{t}$$ (For conventional pulse and pulse doppler radars).

$$= \frac{2kK}{t} + M \leq \frac{64}{t} + M$$ (For "modified" pulse radars such as pulse compression, chirp, etc.).

B = emission bandwidth in MHz

t = pulse duration in microseconds

t_r = pulse rise time

$K = t/t_r$

BM = bandwidth due to pulse modification in MHz

k = weighting factor for K (see Fig. 30)

$B = 2\Delta f_1 = \Delta f_2/5$

TABLE 2

VALUES OF F_0, P_t CORRESPONDING TO S = 60 dB

F_0 (MHz)	P_t (dBm/KHz)
100	0
1000	20
10,000	40

How does one demonstrate fulfillment of the requirements? This question has not been completely resolved at the present time. Two possibilities are (1) measurement of emission levels at the device or at antenna terminals, or (2) measurement or computation of emission levels in the far field of the array. Each possibility has some advantages and disadvantages. Technique (1) is clearly a simpler measurement (if only a few devices or terminal pairs are tested), whereas technique (2) addresses a more fundamental quantity, i.e., emission levels in the field. Our results show that in general, harmonic levels in the field will be significantly lower than those measured at the device, because of gain degradation and reflection coefficient. In other words, the array has a significant effect in reducing harmonic levels. Either technique should take into account beam scanning and operating frequency variation, since Part I [1] of the final report has shown that the levels of fundamental and harmonics are all highly dependent on load conditions which, of course, vary with frequency and scan angle.

Now let us consider some of the points noted previously concerning Fig.29 . The first point is concerned with the emissions at band edges. The emissions at band edges ($F_0 \pm \Delta f_1$) must be down at least 40 db down from the fundamental. Now the emission characteristics over the bandwidth B of the system ($F_0 - \Delta f_1 \leq f \leq F_0 + \Delta f_1$) and at band edges depend of course on the details of the particular pulse shape used. One assumes that this requirement can be met; the restrictions which it places on the radar system will, of course, depend on the particular system.

The second point raised concerns the levels at $F_0 - \Delta f_2$ and beyond, which must be down at least S dB from the fundamental. This requirement will be applicable in most cases to the 2nd and 3rd harmonics ($2F_0$ and $3F_0$, respectively). For instance, the bandwidth of the bipolar transistor modules treated is less than 12%. Thus, f_1 would be less than 0.06 F_0, Δf_2 would be less than o.6 F_0 and both 2nd and 3rd harmonics would lie outside the region ($F_0 - \Delta f_2 \leq f \leq F_0 + \Delta f_2$). In these cases, then, 2nd and 3rd harmonic levels must be at least 60 db below fundamental level. This requirement is discussed in sections 6.2 and 6.3.

The third point raised concerns the sidelobe level. The first three sidelobes must be at least 20 db down and all others at least 30 db down from beam pattern maximum. This requirement is principally a problem of proper array design. One can of course produce sidelobes which are sufficiently low by proper amplitude taper. The effect of random variations in amplitude and phase can be predicted using the computer program of this report. Then the taper can be overdesigned to take into account such random variations. The variations of impedance with scan angle may have a significant effect. As the beam is scanned and the load presented at the output of the solid state device varies, the fundamental output will vary as pointed out in Part I. These effects must also be taken into account in considering the desired taper. The expected variation of amplitude and phase could be used as a statistical input to the computer program of this report. In other words, the expected variation of amplitude and phase could be used to determine an equivalent σ_a and σ_p. Then one could observe expected variations in sidelobe level and overdesign accordingly.

In summary, the sidelobe level requirement is considered to be an array design problem which can be adequately treated by the usual design techniques, supplemented by the computer program of this report. In addition, the requirement that emissions at the band edges be 40 db down from fundamental is considered to be primarily a pulse design problem.

Thus, our attention is focussed on the remaining requirement that emissions outside the range ($F_0 - \Delta f_2 \leq f \leq F_0 + \Delta f_2$) be S db down from the fundamental. In most cases, this requirement will apply to the 2nd and 3rd harmonics, since bandwidth B will in most cases be less than $0.20\ F_0$ and $F_0 + \Delta f_2$ will thus be less than $2F_0$.

6.2 SUMMARY AND DISCUSSION OF EXPERIMENTAL RESULTS

Table 3 lists approximate levels of 2nd and 3rd harmonics of the microwave solid state devices tested with matched load. In parenthesis, the range of levels encountered with a VSWR of 3.0 and varying angle of reflection coefficient is also tabulated. The data of Table 3 is extracted from Table 6.1 of Part I of Ref. [1].

It should be noted that several additional TRAPATT devices showed 2nd harmonic levels in the range 22-27 db under matched conditions (see Part I). The reasons for the superior performance of the type 3 circuit are also outlined in Part I.

For the moment, we will assume that S = 60 dB and that both 2nd and 3rd harmonics must satisfy this requirement. First, consider the 3rd harmonic levels listed in Table 3. The S-band Bipolar transistor modules and the improved (circuit 3 type) TRAPATT device have third harmonic levels which are lower than -60 db relative to fundamental. The L-band modules have higher levels of third harmonic. One module has levels at match lower than -60 db and the other has levels at match of -54 db. The worst case is -47 db under a VSWR of 3.0. These third harmonic levels are, of course, very encouraging. It is believed that very little effort has been made to reduce 2nd or 3rd harmonics to levels as low as -60 db and it therefore seems likely that with improved design 3rd harmonic levels can be reduced to less than -60 db at the device itself.

TABLE 3

SECOND AND THIRD HARMONIC LEVELS OF

SOME MICROWAVE SOLID STATE DEVICES*

L BAND MODULES

2^{nd} Harmonic

-50 db (-47 to -65 db)

-54 db (-47 to -67 db)

3^{rd} Harmonic

-54 db (-50 to -57 db)

-61 db (-58 to -66 db)

S BAND MODULES

2^{nd} Harmonic

-40 db (-38 to -43 db)

-37 db (-34 to -41 db)

3^{rd} Harmonic

<-60 db (<-60db)

<-60 db (<-60 db)

TRAPATT DEVICE

2^{nd} Harmonic

-51 db

3^{rd} Harmonic

<-60 db

*Figures not in parentheses indicate levels with VSWR = 1.0 (matched). Figures in parentheses indicate levels with VSWR = 3.0 and variable angle of reflect. coeff.

Now consider the 2nd harmonic levels listed in Table 3. Under conditions of match, these vary from -50 to -54 db for the L-band modules, -37 to -40 db for the S-band modules, and are -51 db for the improved (type #3) TRAPATT device. The L-band modules and TRAPATT device are thus within better than 10 db of -60 db at match and the S-band modules are within 23 db of -60 db at match. The worst cases under a VSWR of 3.0 is -47 db for the L-band and -34 db for the S-band modules. Clearly, these devices require some improvement in regard to 2nd harmonic levels. It may be possible to significantly lower these levels by design procedures. Some suggestions are made in Part I for appropriate design improvements. Again, since so little attention has been given to lowering harmonics below -60 db, it seems likely that some improvement can be obtained. Since the worst case for L-band modules and the improved TRAPATT device is only 13 db away from the -60 db level, we conclude that the l-band modules and the improved TRAPATT device (circuit type #3) are strong candidates for array elements in view of the OTP regulations. The worst case for the S-band bipolar modules is 27 dB away from the -60 db level. Clearly, some significant improvement is required here. It should be noted, however, that there is less design experience with the S-band modules than with the L-band modules. If the 2nd harmonic levels of the S-band modules cannot be improved sufficiently, it may be necessary to add a 2nd harmonic filter to each module. This might be a reasonable solution. A microstrip filter should not greatly increase cost and size.

In conclusion, the 2nd and 3rd harmonic levels are encouragingly low for most devices. The -60 db levels are not satisfied in all cases at the device itself. However, many of the levels are close to the -60 db levels required and it seems likely that modest improvements in design should permit most of these devices to satisfy OTP regulations at the array terminals. The S-band bipolar modules require significant improvement in 2nd harmonic levels and an additional filter may possibly be required. Thus, we conclude that of the solid state devices tested, the L-band bipolar modules and the improved TRAPATT devices are strong candidates for array elements and that the S-band bipolar modules are also viable candidates.

For those radar systems for which $S \leq 60$ dB, then, one expects that with some improvement in design, the OTP regulations can be satisfied at the antenna terminals. In addition, a significant gain degradation is expected at harmonic frequencies, as noted in chapter 5.

A point should be made here concerning those radar systems for which $S > 60$ dB. For such systems, the design problems and especially the measurement problems may be quite severe. However, the additional effect of the array in reducing harmonic levels may be predictable by using the program of this report, and in some cases this effect may be sufficient to reduce the emission in the field to the required levels. The effect of the array is discussed in Section 6.3.

6.3 EFFECTS OF THE ARRAY ON FAR FIELD LEVELS OF HARMONICS

The result of computation of Chapter 5 have shown that the array has a significant effect upon harmonic levels in the field. In particular, if phase and amplitude are highly random at harmonics, then there will be a significant degradation of gain as indicated by figs. 24-28.

In addition to the gain degradation, an array of halfwave dipoles will usually be well matched at fundamental F_0, highly mismatched at 2nd harmonic $2F_0$, and fairly well matched at 3rd harmonic $3F_0$. Fig. 31 shows the reflection factor $1 - |\Gamma|^2$ (where Γ is the reflection coefficient at antenna terminals), for a dipole of length L and diameter D, fed with a transmission line of characteristic impedance of 50 ohms. The data were computed by the method of moments. Note that there is a significant reflection loss, of the order of 10 dB or greater in some cases, at 2nd harmonic ($L = 1.0\lambda$). The effect of this reflection factor is complex. The load presented to the solid state device at F_0 is different from that at $2F_0$ and one can determine the corresponding harmonic levels only by test, in general. In some cases, however, experiments have shown [1] that the levels generated depend primarily on the load presented at fundamental frequency. In such cases, one can then use the reflection factor at 2nd harmonic directly.

Thus, there are three principal effects of the array on harmonic levels. The first is a degradation of gain due to phase and amplitude errors at harmonic frequencies, the second is an increased electrical array size at

harmonic frequencies, and the third is a reflection factor at harmonic frequencies. We expect that in most cases the overall effect will be a significant reduction in the ratio of maximum harmonic to maximum fundamental levels. In other words, we expect that the ratios of maximum harmonic to maximum fundamental levels will be considerably lower in the field than at the device itself (or at the antenna terminals).

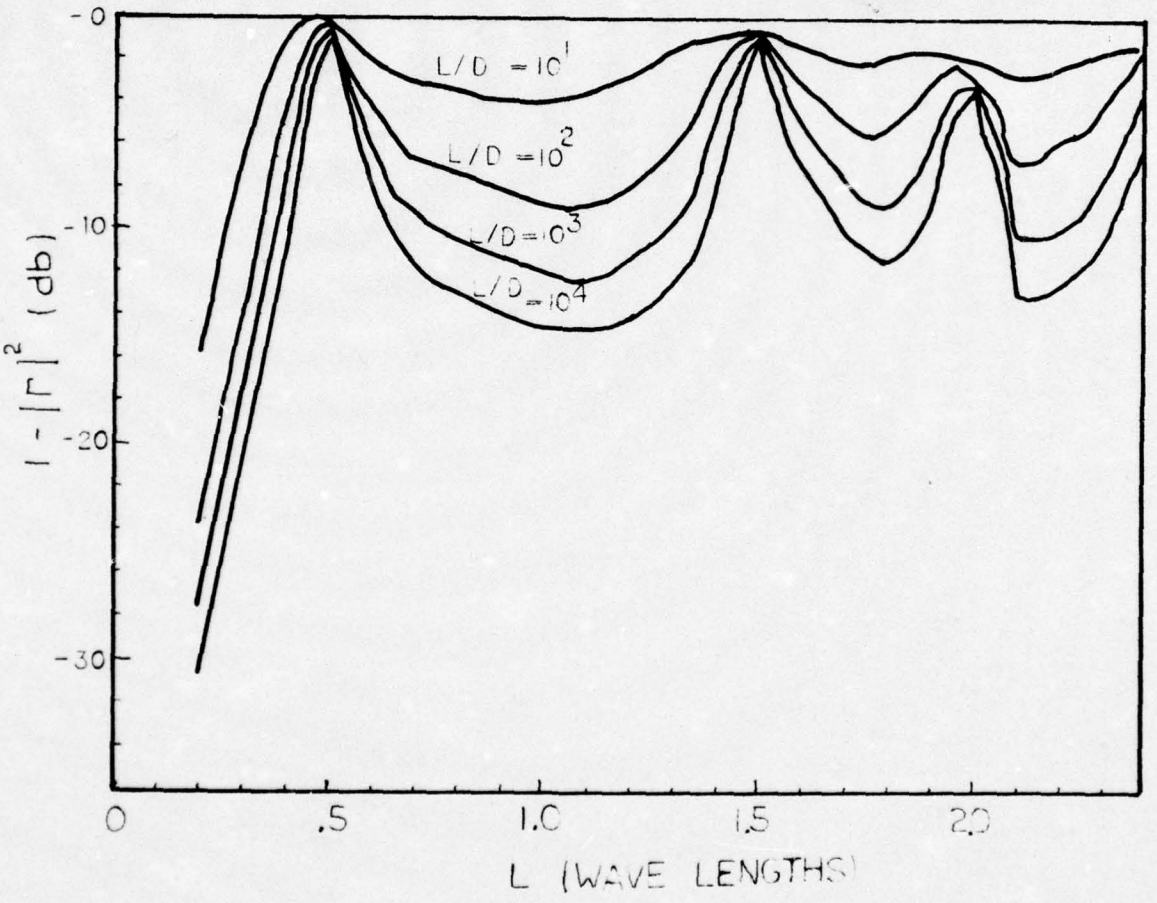

Fig. 31. Reflection Loss for a centerfed dipole of length L, diameter D, fed by a 50 ohm transmission line, as a function of antenna length.

7. CONCLUSIONS

The application of the OTP Regulations to Solid State Arrays has been considered. In part I [1] of this final report, typical emission levels of some solid state devices are reported. Using this data, as summarized in table 3 of part II, it is concluded that the devices tested (Bipolar transistors and TRAPATT devices) are reasonable candidates for array elements, assuming that the level S is approximately 60 dB. For S levels in excess of 60dB, significant development and experimental problems are anticipated if measurements are to be made at the antenna terminals. However, the array itself is significant help here because of gain degradation and reflection loss at harmonic frequencies. A computer program has been prepared to analyze random effects in planar arrays of dipoles. Typical results indicate that the array has a significant effect in reducing the ratio of harmonic to fundamental levels. If this factor is taken into account the solid state devices become even stronger candidates for array elements in view of the OTP regulations.

REFERENCES

[1] D. Griffin, A.T. Adams, P. Hsi, and A. Farrar, "Solid State Array Studies Relevant to OTP Regulations, Part I: Evaluation of Amplitude and Phase Characteristics of Microwave Solid State Amplifiers; Part II Computation of Random Effects in Planar Arrays," RADC-TR-76-241, Pt 1 & 2, dated August 1976.

[2] T. Tseng, D.K. Cheng, "Gain Optimization for Arbitrary Antenna Arrays Subject to Random Fluctuations," IEEE Trans. on Antennas and Propagation, Vol. AP-15, No. 3, May 1967, pp. 356-366.

[3] C.A. Greene, R.T. Moller, "The Effect of Normally Distributed Random Phase Errors on Synthetic Array Gain Patterns," IRE Trans. on Military Electronics, April 1962, pp. 130-139.

[4] J. Ruze, "The Effect of Aperture Errors on the Antenna Radiation Pattern," Nuovo Cim., Vol. 9, Suppl. No. 3, 1952, pp. 364-380.

[5] J. Ruze, "Antenna Tolerance Theory - A Review," Proc. IRE, Vol. 54, No. 4, 1966, p. 633.

[6] Y.S. Shifrin, Statistical Antenna Theory, Golern Press, Boulder, Colorado, 1971.

[7] T. Maher and K.K. Cheng, "Random Removal of Radiators from Large Linear Arrays," IEEE Trans. on Antennas and Propagation, Vol. AP-11, No. 2, March 1963, pp. 106-112.

[8] R.F. Harrington, "Matrix Methods for Field Problems," Proc. of the IEEE Vol. 35, No. 2, Feb. 1967, pp. 136-149.

[9] R.F. Harrington Field Computation by Moment Methods, Macmillan Co., New York, 1968.

[10] Random Number Generating and Testing, IBM Manual 020-8011.

[11] System /360 Scientific Subroutinge Package (360A-CM-03X), Version III, H20-0166-5.

[12] J.H. Richmond, "Coupled Linear Antenna with Skew Orientation," IEEE Trans. on Antennas and Propagation, Vol. AP-18, No. 5, Sept. 1970, pp. 694-696.

[13] B.J. Strait, T. Sarkar and D.C. Kuo, "Special Programs for Analysis of Radiation by Wire Antennas," Scientific Report No. 1, on Contract No. F19628-73-C-0047, AFCRL-TR-73-0399, Syracuse University, Syracuse, N.Y., June 1973.

References (Continued)

[14] O. Toeplitz, "Zur Theorie der Quadratischen Formen von unendlichvielen Variabeln," Nachr. Ges. Wiss. Gottingen, Math. Phys. Kl., 1910, pp. 489-506.

[15] W.F. Trench, "An Algorithm for the Inversion of Finite Toeplitz Matrices," J. Soc. Indust. Appl. Math. Vol. 12, No. 3, Sept. 1964, pp. 515-522.

[16] S. Zohar, "Toeplitz Matrix Inversion; the Algorithm of W.F. Trench," J. Ass. Comput. Mach., Vol. 16, No. 4, Oct. 1969, pp. 592-601.

[17] D.H. Preis, "The Toeplitz Matrix: Its Occurrence in Antenna Problems and a Rapid Inversion Algorithm," IEEE Trans. on Antennas and Propagation, Vol. AP-20, No. 2, March 1972, pp. 204-205.

[18] D.H. Sinnott, "Matrix Analysis of Linear Antenna Arrays of Equally Spaced Elements," IEEE Trans. on Antennas and Propagation, Vol. AP-21, No. 3, May 1973, pp. 385-386.

[19] D.H. Sinnott, "Matrix Analysis of Linear Antenna Arrays of Equally Spaced Elements," WRE-Technical Note-622 (AP), Weapons Research Establishment, Dept. of Defense, Salisbury, South Australia, May 1972.

[20] D.C. Kuo, H.H. Chao, J.R. Mautz, B.J. Strait, and R.F. Harrington, "Analysis of Radiation and Scattering by Arbitrary Configurations of Thin Wires," (Program Description) IEEE Trans. on Antennas and Propation, Vol. AP-20, No. 6, Nov. 1972, pp. 814-815.

[21] D.E. Warren, T.E. Baldwin, and A.T. Adams, "Near Electric and Magnetic Fields of Wire Antennas," (Program Description), IEEE Trans. on Antennas and Propagation, Vol. AP-22, No. 2, March 1974, p. 364. *Program and description on deposit:* ASIS-NAPS *Document No.* NAPS-02221.

[22] A.T. Adams, "Method of Moments Applications - Vol. I. An Introduction to the Method of Moments," RADC-TR-73-217, Nov. 1974, **AD# A002820.**

[23] K.S. Miller, Multidimensional Gaussian Distributions. John Wiley and Sons, Inc., New York, 1964, p. 23.

[24] The Office of Telecommunications Policy Manual of Regulations and Procedures for Radio Frequency Management, Section 5.3.2, "Radar Spectrum Engineering Criteria," Revision 1/73 (current OTP Regulations),

Appendix A

The Matrix Inversion Routine for the Impedance Matrix of a Planar Array

The algorithm used in this program to obtain the inverse of a block-Toeplitz matrix is based on D.H. Sinnott's implementation [19] and can be summarized as follows:

For a given block-Toeplitz matrix:

$$[Z] = \begin{bmatrix} \underset{\sim}{Z}_0 & \underset{\sim}{Z}_1 & \cdots & \underset{\sim}{Z}_N \\ \underset{\sim}{Z}_1 & \underset{\sim}{Z}_0 & & \underset{\sim}{Z}_{N-1} \\ \vdots & \vdots & & \vdots \\ \underset{\sim}{Z}_N & \underset{\sim}{Z}_{N-1} & \cdots & \underset{\sim}{Z}_0 \end{bmatrix} \qquad \text{(A-1)}$$

where each submatrix $\underset{\sim}{Z}_i$ is of order n. Then inversion matrix [Y] can be partitioned in the same fashion.

$$[Y] = \begin{bmatrix} Y_{00} & Y_{01} & \cdots & Y_{0N} \\ Y_{10} & Y_{11} & & \\ \vdots & & & \vdots \\ Y_{N0} & \cdots & \cdots & Y_{NN} \end{bmatrix} \qquad \text{(A-2)}$$

The inversion routines are:

$$(1)\ \psi^{(0)} = Z_0^{-1} Z_1, \quad \Delta^{(-1)} = Z_0^{-1} \qquad \text{(A-3)}$$

$$(2)\ \Delta^{(m-1)} = [I_N - (\psi_{m-1}^{(m-1)})^2]^{-1}\ \Delta^{(m-2)} \qquad \text{for } m = 1, \ldots, N-1 \qquad \text{(A-4)}$$

$$(3)\ \psi_m^{(m)} = -\Delta^{(m-1)} \{ \sum_{s=0}^{m-1} \psi_s^{(m-1)T} Z_{m-s} - Z_{m+1} \} \qquad \text{(A-5)}$$

$$(4)\quad \underset{\sim}{\psi}_r^{(m)} = \underset{\sim}{\psi}_r^{(m-1)} - \underset{\sim}{\psi}_{m-r-1}^{(m-1)}\,\underset{\sim}{\psi}_m^{(m)} \qquad 0 \le r \le m-1 \qquad \text{(A-6)}$$

$$(5)\quad \underset{\sim}{Y}_{00} = \underset{\sim}{\Delta}^{(n-1)} \qquad \text{(A-7)}$$

$$(6)\quad \underset{\sim}{Y}_{r0} = -\underset{\sim}{\psi}_{r-1}^{(n-1)}\,\underset{\sim}{\Delta}^{(n-1)} \qquad 1 \le r \le N \qquad \text{(A-8)}$$

$$(7)\quad \underset{\sim}{Y}_{rs} = \underset{\sim}{Y}_{r-1,s-1} + \underset{\sim}{\psi}_{r-1}^{(n-1)}\underset{\sim}{\Delta}^{(n-1)}\underset{\sim}{\psi}_{s-1}^{(n-1)T} - \underset{\sim}{\psi}_{n-r}^{(n-1)}\underset{\sim}{\Delta}^{(n-1)}\underset{\sim}{\psi}_{n-s}^{(n-1)T} \qquad \text{(A-9)}$$
$$1 \le r,s \le N$$

where $\underset{\sim}{\psi}_i^{(j)}$, $\underset{\sim}{\Delta}^{(i)}$ are square matrix of order n.

The computer storage requirement for this algorithm is:

$Z((N + 1) \times n^2)$

$\psi(2N \times n^2)$

$\Delta(2n^2)$

$Y(\frac{1}{4}(N + 1)^2 \times n^2)$

Since matrices $\underset{\sim}{\psi}_i$ are intermediate data, and are calculated iteratively in Eq. (1) to (4), i.e. $\underset{\sim}{\psi}_0^{(0)}$, $\underset{\sim}{\psi}_1^{(1)}$, $\underset{\sim}{\psi}_0^{(1)}$, $\underset{\sim}{\psi}_2^{(2)}$, $\underset{\sim}{\psi}_1^{(2)}$, $\underset{\sim}{\psi}_0^{(2)}$ .... , they can be stored alternately in two disc files A and B instead of in computer memory. i.e.

$\underset{\sim}{\psi}_0^{(0)}$ → disc A

$\underset{\sim}{\psi}_1^{(1)}$, $\underset{\sim}{\psi}_0^{(1)}$ → disc B

$\underset{\sim}{\psi}_2^{(2)}$, $\underset{\sim}{\psi}_0^{(2)}$, $\underset{\sim}{\psi}_1^{(2)}$ → disc A

$\underset{\sim}{\psi}_3^{(3)}$

$\underset{\sim}{\psi}_0^{(3)}$ → disc B

$\underset{\sim}{\psi}_1^{(3)}$

$\underset{\sim}{\psi}_2^{(3)}$

This saves the storage requirement for the ψ array. In addition, since submatrices $\underset{\sim}{Y}_{ij}$ are only a function of $\underset{\sim}{\Delta}$ and $\underset{\sim}{\psi}$ in Eq. (5) and (6), it can be restored into the Z array if [Z] and [Y] are not subsequently required. Due to the effects of the zero's in the voltage excitation matrix as explained in section 2.6, only part of the [Y] matrix is computed, i.e. a condensed [Y] matrix. Hence, the size of the array [Y] is almost compatible with the Z array, which saves the storage requirement for [Y] array.

The resultant program needs computer storage:

$Z((N+1) \times n^2)$

$\Delta(2n^2)$, $ST(n^2)$, $PS1(n^2)$, $PS2(n^2)$

where ST, PS1, PS2 arrays are used as temporary storage. The computer storage requirement is cut down to only a small fraction of the original requirement.

In Eq. (5)-(6), submatrices $\underset{\sim}{Y}_{rs}$ are calculated subsequently from $\underset{\sim}{Y}_{r-1,s-1}$, $\underset{\sim}{\Delta}$, and $\underset{\sim}{\psi}$. Since there are only a few fixed columns of each submatrix $\underset{\sim}{Y}_{rs}$ required with respect to non-zero element in [V], once the fixed columns $\underset{\sim}{Y}_{r0}$ and $\underset{\sim}{Y}_{0r}$ submatrices are obtained for $0 \leq r \leq N$,

the fixed columns of all other submatrices $\underset{\sim}{Y}_{rs}$ can be determined without calculating the other elements of the submatrix.

The number of complex multiplications is approximated as $\frac{1}{2}(N+1)^2(n)^3$ for Eq. (1) - (4) and $\frac{1}{2}(N+1)^2(n)^3$ for Eq. (5)-(7). When taking advantage of the condensed [Y] matrix, the number of complex multiplications for Eq. (5)-(7) is about $\frac{1}{2}(N+1)n^3$, which is relatively small compared with $\frac{1}{2}(N+1)^2n^3$, hence it can be neglected. The resultant program needs about one-half the complex multiplication required by the original one. A typical example of comparison between three matrix inversion routines is shown below.

For a block-Toeplitz matrix of size

$(N+1)xn = 1400$ - order of the entire matrix

$N+1 = 20$ - order of the matrix in terms of blocks

$n = 70$ - order of submatrix

Computer memory required is listed below (in units of million words)

Gauss-Jordan	Sinnott	Improved
1.98	1.57	0.24

The number of complex multiplications (in units of million) are:

Gauss-Jordan	Sinnott	Improved
1870	187	98

Appendix B

Computer Program PLAN Listing

```
C
C      ***** COMPUTER PROGRAM - PLAN *****
C
C                            - BY PETER HSI
C                            - NOV. 10, 1975
C
C      * ANALYSIS OF THE FIELD PATTERN AND GAIN DEGREGATION
C      * OF A GIVEN PLANAR ARRAY DUE TO RANDOM NOISE EXIST
C      * ON EACH DIPOLE
C
C      *DEFINITION- M1=#OF EXPANSION FUNCTIONS ON EACH DIPOLE
C                   M2=#OF COLUMNS IN PLANAR ARRAY
C                   M3=#OF ROWS IN PLANAR ARRAY
C                   HL=DIPOLE LENGTH(IN WAVE LENGTH)
C                   AK=DIPOLE RADIUS(IN WAVE LENGTH)
C                   SX=X-DIRECTION SPACING BETWEEN DIPOLES
C                   SY=Y-    "            "          "
C                   SZ=Z-    "            "          "
C                   JF=FREQUENCY MODE; 1-FUNDAMENTAL
C                                      2-SECOND HARMONIC
C                                      ETC.
C                   NW=MAX.(M2,M3)
C                   NP=MIN.(M2,M3)*M1
C                   NNN=TOTAL # OF FAR FIELF POINTS
C
C      *STORAGE REQUIREMENT-
C                   Z(NW*NP**2) OR Z(0.5*M1*(M2*M3)**2)
C                   CUR,CUR2,CC,DD(M1*M2*M3)
C                   HX,HY,HZ,V,VP,(M2*M3)
C                   TE,TEE,PH,PHH,TOT1,TOT2,TOT3,TOT4,(NNN)
C                   AA,BP ST1,ST2,ST3,ST4,(NNN)
C                   Z2(M1**2)
C                   TWO DISC FILES FOR TEMPARARY STORAGE
C
      COMPLEX Z(5000),Z2(50)
      COMPLEX ZZ
      COMPLEX CUR(300),CUR2(300),V(100),VP(100)
      DIMENSION HX(100),HY(100),HZ(100)
      DIMENSION TOT1(180),TOT2(180),TOT3(180),TOT4(180),
     $TE(180),PH(180),TEE(180),PHH(180),ST1(180),ST2(180)
      DIMENSION ST3(180),ST4(180),G1(100),G2(100)
      COMMON AA(180),BB(180)
      LOGICAL IOP(10),Y
      DIMENSION Y2(180),YMIN(3),YMAX(3),YCHAR(3),DUMY(180)
      COMPLEX CC(300),DD(300),EE
      DATA (YCHAR(I),I=1,3)/1H*,1H$,1H#/
      KI=07
      CALL FLGBDF(5,Y)
      CALL OPTION(IOP)
      CALL ARRAY(HX,HY,HZ,HL,AK,DZ,M1,M2,M3)
```

```
      M23=M2*M3
      CALL IMPD(M1,M2,M3,DZ,AK,HX,HY,HZ,Z)
      NW=M3
      IF(M3.LT.M2) NW=M2
      NB=M2*M3/NW
      NP=M1*NB
      L=0
      K=(M1/2)*NP
      DO 82 I=1,NW
      DO 83 J=1,NP
      L=L+1
      K=K+1
      CC(L)=Z(K)
83    CONTINUE
82    K=K+NP*(NP-1)
      IF(IOP(1)) GO TO 111
      KKK=NP*NP*NW
      PRINT 61
61    FORMAT(///1X,'GENERALIZED IMPEDANCE MATRIX',//)
      PRINT 60,(Z(I),I=1,KKK)
60    FORMAT(1X,10F11.6)
111   CONTINUE
      CALL LINVRT(Z,NW,NP,NB)
      NH=(NW+1)/2
      MP=NP*NB
      MPN=MP*NW
      NPT=NH*NB*NW*NP
      IF(IOP(2)) GO TO 100
      PRINT 91
91    FORMAT(///1X,'COMPACT ADMITTANCE MATRIX',//)
      PRINT 60, (Z(I),I=1,NPT)
100   CONTINUE
      REWIND KI
      DO 90 LL=1,NH
      DO 90 J=1,NB
      DO 90 I=1,NW
      DO 90 K=1,NP
      L=(I-1)*MP+(LL-1)*MPN+(J-1)*NP+K
      ZZ=Z(L)
      WRITE(KI) ZZ
90    CONTINUE
      IF(IOP(3)) GO TO 300
      CALL NOMUL(M1,DZ,AK,Z2)
      NN2=M1*M1
      PRINT 71
71    FORMAT(///1X,'SELF-IMPEDANCE (NO MUTUAL EFFECT)',//)
      PRINT 60, (Z2(I),I=1,NN2)
      CALL LINEQ(Z2,M1)
      PRINT 81
81    FORMAT(///1X,'SELF-ADMITTANCE (NO MUTUAL EFFECT)',//)
      PRINT 60,(Z2(I),I=1,NN2)
```

```
      DO 33 I=1,NN2
33    Z2(I)=Z2(I)*0.01
300   ENDFILE KI
      L=0
      M123=M1*M2*M3
      K=0
      DO 92 I=1,NW
      DO 93 J=1,NP
      L=L+1
      K=K+1
93    DD(L)=Z(K)
92    K=K+NP*(NE-1)
      EE=CMPLX(0.,0.)
      DO 94 I=1,M123
      EE=EE+CC(I)*DD(I)
94    CONTINUE
      PRINT 96,EE
      WRITE(2,96) EE
96    FORMAT(///1X,'CHECK FOR MATRIX INVERSION',2F12.6//)
      TP=6.2831853
      REW IND KI
      DO 66 I=1,NPT
      READ(KI) ZZ
66    Z(I)=ZZ*0.01
7     READ 40,AM1,AM2,SD1,SD2,IT,JT
      IF(Y) CALL EXIT
823   FORMAT(///1X,'  # OF ITERATIONS = ',I10,//)
      WRITE(2,19) AM1,AM2,SD1,SD2
      PRINT 707
707   FORMAT(//,1X,'UNIFORM EXCITATION APPLIED -',//)
      PRINT 19,AM1,AM2,SD1,SD2
      SD2=SD2*TP/360.
40    FORMAT(4F10.5,2I5)
      PRINT 823, IT
      DO 250 I=1,M23
250   VP(I)=CMPLX(1.0,0.0)
      IF(IOP(4)) GO TO 301
      CALL TAPER(VP,M1,M2,M3,HX,HY,HZ)
301   CONTINUE
      DO 201 J=1,JT
      IX=13579
      READ 80,NP,NT,NY,NK,NS,NJ
80    FORMAT(6I5)
      AVG1=0.
      AVG2=0.
      DO 50 I=1,180
      TOT1(I)=0.0
      TOT2(I)=0.0
      TOT3(I)=0.0
      TOT4(I)=0.0
      TEE(I)=0.0
      PHH(I)=0.0
      TE(I)=0.0
50    PH(I)=0.0
```

```
      DO 1000 K=1,IT
      CALL VOLT('V',VP,M2,M3,IX,AM1,AM2,SD1,SD2)
      CALL MULT(Z,V,CUR,M1,M2,M3)
      CALL FAR(CUR,NP,NT,NY,NK,NS,NJ,HX,HY,HZ,NNN,DZ,
     1PH,TE,TOT1,TOT2,M23,M1,V,AVG1)
      IF(ICP(5)) GO TO 101
      PRINT 13,K
      NA=NP+1
      NB=NT+1
      NC=NK+1
      ND=NS+1
      LL=0
      BIG=0.
      DO 11 LY=NC,ND,NJ
      DO 11 LK=NA,NB,NY
      LL=LL+1
      ITH=LY-1
      IPC=LK-1
      PRINT 15,ITH,IPC,AA(LL),BB(LL)
      IF(AA(LL).GT.BIG) BIG=AA(LL)
11    CONTINUE
      DO 333 I=1,3
      YMAX(I)=1.0
333   YMIN(I)=0.0
      DO 334 I=1,NNN
334   AA(I)=AA(I)/BIG
      PRINT 16,BIG
      CALL GRPLOT(0,NNN,0,0.,3.,YCHAR,YMAX,YMIN,AA,DUMY,
     $DUMY,DUMY,DUMY,DUMY)
101   CONTINUE
      IF(ICP(3)) GO TO 1000
      CALL MULT3(Z2,V,CUR2,M1,M2,M3)
      CALL FAR(CUR2,NP,NT,NY,NK,NS,NJ,HY,HY,HZ,NNN,
     $DZ,PHH,TEE,TOT3,TOT4,M23,M1,V,AVG2)
1000  CONTINUE
      PRINT 166
166   FORMAT(///1X,' FAR FIELD PATTERN (E-FIELD)',//)
      CALL STDV(TOT1,TOT2,PH,TE,NP,NT,NY,NK,NS,NJ,ST1,ST2,IT,AVG1)
      IF(ICP(3)) GO TO 177
      PRINT 167
167   FORMAT(///1X,' FAR FIELD PATTERN (E-FIELD)',
     $' *** NO MUTUAL EFFECT TAKING INTO ACCOUNT'//)
      CALL STDV(TOT3,TOT4,PHH,TEE,NP,NT,NY,NK,NS,NJ,ST3,
     $ST4,IT,AVG2)
177   NC=0
178   CONTINUE
      DO 110 I=1, 3
      YMAX(I)=-1.E-36
 110  YMIN(I)=1.E36
      DO 120 I=1, NNN
      Y2(I)=TOT1(I)-ST1(I)
      YMAX(2)=AMAX1(YMAX(2),TOT1(I))
      YMIN(2)=AMIN1(YMIN(2),TOT1(I))
120   CONTINUE
 20   DO 170 I=1, NNN
      Y2(I)=Y2(I)/YMAX(2)
 170  TOT1(I)=TOT1(I)/YMAX(2)
```

```
      WRITE (6,19) AM1,AM2,SD1,SD2
      WRITE (6,16)
      DO 160 I=1, 2
      YMAX(I)=1.0
  160  YMIN(I)=0.0
      CALL GEPLOT(2,NNN,0,0.,3.,YCHAR,YMAX,YMIN,TOT1,Y2,
     &DUMY,DUMY,DUMY,DUMY)
      IF(N C.EQ.1) GO TO 201
      IF(IOP(3)) GO TO 201
      DO 77 I=1,NNN
      TOT1(I)=TOT3(I)
      ST1(I)=ST3(I)
   77 CONTINUE
      NO=1
      GO TO 178
   10  FORMAT(  2X , 18F6.3//)
   12  FORMAT(6I12)
   15 FORMAT(1X,2I10,1P2E30.6)
   13 FORMAT(//1X,'INDIVIDUAL PATTERN #',I10,//,8X,
     1'THE',7X,'PHI',20X,'E-FIELD',20X,'GAIN',//)
   14  FORMAT(2X 1P3E14.5)
   16  FOR MAT(1H1)
   9   FORM AT(6F12.6)
   18  F ORMAT(1H1// 22HNORMALIZATION FACTOR = 1PE14.6)
   19  FO RMAT(//12HMEAN VOLTAGE 9X 1H= 1PE14.6/10HMEAN PHASE
     1 11X 1H= 1PE14.6/16HVOLTAGE VARIANCE 5X 1H=1PE14.6/
     2 14HPHASE VARIANCE 7X 1H= 1PE14.6)
  201 CONTINUE
   30 GO TO 7
      END


      SUBROUTINE ARRAY(HX,HY,HZ,HL,AK,DZ,M1,M2,M3)
C     READ IN ARRAY DATA
      DIMENSION HX(1),HY(1),HZ(1)
      TP=6.2831853
      READ 10,M2,M3,SX,SY,SZ,HL,AK
      READ 10,JF,M1
   10 FORMAT(2I5,5F10.5)
      M23=M2*M3
      PRINT 30,M2,M3
      WRITE(2,30) M2,M3
   30 FORMAT(///1X,' ******  PLANAR ARRAY PROGRAM   *****',///,
     $1X,'      PLANAR ARRAY OF',I5,' BY ',I2,'   DIPOLES',//)
      LL=0
      DO 20 I=1,M3
      DO 20 J=1,M2
      LL=LL+1
      HX(LL)=(J-1)*SX
      HY(LL)=(J-1)*SY
      HZ(LL)=(I-1)*SZ
   20 CONTINUE
```

```
      PRINT 112
  112  FORMAT(3X,'ELEMENT',15X,'LENGTH',12X,'X-COORDINATE',8X,
     1'Y-COORDINATE',8X,'Z-COORDINATE',8X,'RADIUS',///)
      PRINT 111,(I,HL,HX(I),HY(I),HZ(I),AK,I=1,M23)
  111  FORMAT(5X,I3,8X,5E20.7)
      DO 43 I=1,M23
      HX(I)=HX(I)*TP*FLOAT(JF)
      HY(I)=HY(I)*TP*FLOAT(JF)
      HZ(I)=HZ(I)*TP*FLOAT(JF)
  43  CONTINUE
      HL=HL*TP*FLOAT(JF)
      AK=AK*TP*FLOAT(JF)
      DZ=HL/FLOAT(M1+1)
      RETURN
      END


      SUBROUTINE OPTION(IOP)
C     DETERMINE OPTIONS BEING CHOSEN
      LOGICAL IOP(1)
      READ 10,IOPT
  10  FORMAT(I5)
      DO 20 N=1,10
      K=11-N
      INDEX=2**(K-1)
      IOP(K)=.TRUE.
      IF(IOPT.LT.INDEX) GO TO 20
      IOPT=IOPT-INDEX
      IOP(K)=.FALSE.
  20  CONTINUE
      RETURN
      END


      SUBROUTINE IMPD(M1,M2,M3,DZ,AK,HX,HY,HZ,Z)
C     GENERATE IMPEDANCE MATRIX BY BLOCK-TOEPLITZ PROPERTY
C     - RETURN WITH SUBMATRIXES Z0,Z1,Z2,...ETC.
      DIMENSION HX(1),HY(1),HZ(1)
      COMPLEX A(140),Z(1),ZMNG
      II=0
      IF(M3.LT.M2) GO TO 60
      M12=M1*M2
      DO 30 M=1,M3
      MM=1+(M-1)*M2
      DO 31 L=1,M2
      LL=(L-1)*M1
      ZM=HZ(L)
      ZN=HZ(MM)
      SD1=HX(L)-HX(MM)
      SD2=HY(L)-HY(MM)
      SD3=HZ(L)-HZ(MM)
```

```
      SD=SQRT(SD1*SD1+SD2*SD2+SD3*SD3)
      IF(SD.EQ.0.) SD=AK
      DO 21 I=1,M1
      A(LL+I)=ZMNG(ZM,ZN,DZ,DZ,SD)
      A(LL+I)=A(LL+I)*0.01
21    ZM=ZM+DZ
31    CONTINUE
      IF(M.EQ.1) GO TO 22
      DO 23 L=1,M2
      LL=(L-1)*(M1-1)
      KK=MM+L-1
      ZM=HZ(1)
      ZN=HZ(KK)+DZ
      SD1=HX(1)-HX(KK)
      SD2=HY(1)-HY(KK)
      SD3=HZ(1)-HZ(KK)
      SD=SQRT(SD1*SD1+SD2*SD2+SD3*SD3)
      DO 24 I=2,M1
      A(M12+LL+I-1)=ZMNG(ZM,ZN,DZ,DZ,SD)
      A(M12+LL+I-1)=A(M12+LL+I-1)*0.01
      ZN=ZN+DZ
24    CONTINUE
23    CONTINUE
22    MMM=M
      MM3=M3
      CALL BLK(M1,M2,MM3,MMM,A,Z)
30    CONTINUE
      GO TO 70
60    DO 40 M=1,M2
      LL=0
      DO 41 L=1,M3
      L1=M+(L-1)*M2
      ZM=HZ(L1)
      ZN=HZ(1)
      SD1=HX(L1)-HX(1)
      SD2=HY(L1)-HY(1)
      SD3=HZ(L1)-HZ(1)
      SD=SQRT(SD1*SD1+SD2*SD2+SD3*SD3)
      IF(SD.EQ.0.) SD=AK
      DO 42 I=1,M1
      LL=LL+1
      A(LL)=ZMNG(ZM,ZN,DZ,DZ,SD)*0.01
42    ZM=ZM+DZ
41    CONTINUE
      IF(M3.EQ.1) GO TO 90
      DO 50 L=2,M3
      L1=M+(L-1)*M2
      ZM=HZ(1)+DZ
      ZN=HZ(L1)
      SD1=HX(L1)-HX(1)
      SD2=HY(L1)-HY(1)
      SD3=HZ(L1)-HZ(1)
      SD=SQRT(SD1*SD1+SD2*SD2+SD3*SD3)
```

```
      IF(SD.EQ.0.) SD=AK
      DO 51 I=2,M1
      LL=LL+1
      A(LL)=ZMNG(ZM,ZN,DZ,DZ,SD)
      A(LL)=A(LL)*0.01
 51   ZM=ZM+DZ
 50   CONTINUE
 90   MMM=M
      MM2=M3
      CALL BLK2(M1,MM2,MMM,A,Z)
 40   CONTINUE
 70   RETURN
      END


      SUBROUTINE BLK(M1,M2,M3,M,A,B)
C     GENERATE A TOEPLITZ MATRIX BY 1-ST ROW &COLUMN
      COMPLEX A(1),B(1)
      M12=M1*M2
      M123=M12*M1
      M1234=M123*M2
      DO 100 N=1,M2
      DO 100 I=1,M2
      DO 100 J=1,M1
      DO 100 L=1,M1
      K1=(ABS(L-J)+1)+M1*ABS(I-N)
      IF(M.EQ.1) GO TO 15
      IF(L.LT.J) K1=K1+M12-(ABS(I-N)+1)
 15   K=L+M1*(I-1)+M12*(J-1)+M123*(N-1)+M1234*(M-1)
      B(K)=A(K1)
 100  CONTINUE
      DO 110 K=1,M12
      I=K+(M-1)*M1234
 110  CONTINUE
 12   FORMAT(2X,9F6.0)
      RETURN
      END


      FUNCTION  ZMNG(ZM1,ZN1,DZM,DZN,R)
C     COMPUTE MUTUAL IMPEDANCE BETWEEN TWO PARALLEL SEGMENTS
C     OF THIN WIRE DIPOLES - BY PIECE-WISE SINUSOIDAL
C     EXPANSION & WEIGHTING FUNCTIONS
      COMPLEX    ZMNG,CMPLX,CSQRT
      DIMENSION A(9),U(9),V(9),SU(9),SV(9),CU(9),CV(9),C(9),S(9),SP(9),
     1SN(9),CN(9),CP(9)
      N=1
      CC=2.0*COS(DZM)
      RR=R*R
```

```
      ZN=ZN1
      DO 1 I=1,3
      ZM=ZM1
      DO 2 J=1,3
      A(3*(I-1)+J)=ZN-ZM
2     ZM=ZM+DZM
1     ZN=ZN+DZN
6     DO 3 I=1,9
      IF (A(I) .LT. 0.0) GO TO 21
      U(I)=SQRT(RR+A(I)*A(I))+A(I)
      V(I)=RR/U(I)
      GO TO 22
21    V(I)=SQRT(RR+A(I)*A(I))-A(I)
      U(I)=RR/V(I)
22    CALL   SICI(SI,CI,U(I))
      SU(I)=SI
      CU(I)=CI
      CALL   SICI(SI,CI,V(I))
      SV(I)=SI
      CV(I)=CI
      SP(I)=SU(I)+SV(I)
      SN(I)=SU(I)-SV(I)
      CP(I)=CU(I)+CV(I)
      CN(I)=CU(I)-CV(I)
3     CONTINUE
      C(1)=COS(A(1))
      C(2)=COS(A(2))
      C(3)=COS(A(3))
      C(7)=COS(A(7))
      C(8)=COS(A(8))
      C(9)=COS(A(9))
      S(1)=SIN(A(1))
      S(2)=SIN(A(2))
      S(3)=SIN(A(3))
      S(7)=SIN(A(7))
      S(8)=SIN(A(8))
      S(9)=SIN(A(9))
      RL=C(1)*(CP(1)-CP(4))-S(1)*(SN(4)-SN(1))+C(3)*(CP(3)-CP(6))-S(3)*
     1(SN(6)-SN(3))+C(7)*(CP(7)-CP(4))-S(7)*(SN(4)-SN(7))+C(9)*(CP(9)
     1-CP(6))-S(9)*(SN(6)-SN(9))-CC*(C(2)*(CP(2)-CP(5))-S(2)*(SN(5)
     1  -SN(2))+C(8)*(CP(8)-CP(5))-S(8)*(SN(5)-SN(8)))
      AG=C(1)*(SP(4)-SP(1))-S(1)*(CN(4)-CN(1))+C(3)*(SP(6)-SP(3))-S(3)*
     1(CN(6)-CN(3))+C(7)*(SP(4)-SP(7))-S(7)*(CN(4)-CN(7))+C(9)*(SP(6)-
     1SP(9))-S(9)*(CN(6)-CN(9))-CC*(C(2)*(SP(5)-SP(2))-S(2)*(CN(5)-CN(
     12))+C(8)*(SP(5)-SP(8))-S(8)*(CN(5)-CN(8)))
      ZMNG=CMPLX(RL,AG)*15./(SIN(DZN)*SIN(DZM))
      RETURN
      END
```

```
      SUBROUTINE SICI(SI,CI,X)
      Z=ABS(X)
      IF(Z-4.)1,1,4
    1 Y=(4.-Z)*(4.+Z)
    3 SI=X*(((((1.753141E-9*Y+1.568988E-7)*Y+1.374168E-5)*Y+6.939889E4).
     1*Y+1.964882E-2)*Y+4.395509E-1)
      CI=((5.772156E-1+ALOG(Z))/Z-Z*(((((1.386985E-10*Y+1.584996E-8)*Y
     1+1.725752E-6)*Y+1.185999E-4)*Y+4.990920E-3)*Y+1.315308E-1))*Z
      RETURN
    4 SI=SIN(Z)
      Y=COS(Z)
      Z=4./Z
      U=(((((((((4.048069E-3*Z-2.279143E-2)*Z+5.515070E-2)*Z-7.261642E2).
     1*Z+4.987716E-2)*Z-3.332519E-3)*Z-2.314617E-2)*Z-1.134958E-5)*Z
     2+6.250011E-2)*Z+2.583989E-10
      V=((((((((((-5.108699E-3*Z+2.819179E-2)*Z-6.537283E-2)*Z
     1+7.902034E-2)*Z-4.400416E-2)*Z-7.945556E-3)*Z+2.601293E-2)*Z
     2-3.764000E-4)*Z-3.122418E-2)*Z-6.646441E-7)*Z+2.500000E-1
      CI=Z*(SI*V-Y*U)
      SI=-Z*(SI*U+Y*V)      +1.570796
      RETURN
      END


      SUBROUTINE LINVRT(Z,NW,NP,M2)
C     IMPEDANCE MATRIX INVERSION ROUTINE FOR PLANAR ARRAY
C     -INPUT SUBMATRIXES Z0,Z1,Z2,...ETC.
C     -RETURN COMPACT ADMITTANCE SUBMATIRXES
      COMPLEX Z(1)
      DIMENSION IA(2),IB(2)
      COMPLEX PS1(50),PS2(50),DEL(100),ST(50),CMPLX
      IT=07
      JT=08
      REWIND IT
      REWIND JT
C
C     STORAGE REQUIREMENT-
C                           PS1(NP**2)
C                           PS2(NP**2)
C                          DEL(2*NP**2)
C                          ST(NP**2)
C
C
C      CALC DEL(-1) AND PS((0),0).
      N2=NP*NP
      DO 5   I=1,N2
    5  DEL(I)=Z(I)
      N=NW-1
      CALL LINEC(DEL,NP)
      IF(N.LE.0) GO TO 100
      CALL MATMLT(DEL,Z(N2+1),PS1,NP)
```

```
      CALL WTAPE(1,N2,PS1,IT)
C      IA(1) - START ADDRESS OF PS((M-1),0)
C      IA(2) - START ADDRESS OF PS((M),0)
C      IB(1) - START ADDRESS OF DEL(M-2)
C      IB(2) - START ADDRESS OF DEL(M-1)
      IA(1)=1
      IA(2)=1
      IB(1)=1
      IB(2)=N2+1
      MZ=N2+N2+1
      MM=0
C
C      ITERATE ON M=1,2,... N.  FOR M=N, ONLY CALC DEL(M-1)
      DO 45   M=1,N
      I0=IA(1)+MM
      MM=MM+N2
      I1=IA(2)+MM
C      I0      - START ADDRESS OF PS((M-1),M-1)
C      I1 - START ADDRESS OF PS((M),M)
C
C      CALC DEL(M-1)
      CALL RTAPE(I0,N2,PS1,IT)
      CALL MATMLT(PS1,PS1,ST,NP)
      IJ=0
      DO 20       J=1,NP
      DO 20       I=1,NP
      IJ=IJ+1
      ST(IJ)=-ST(IJ)
  20      IF(I.EQ.J) ST(IJ)=1.+ST(IJ)
      CALL LINEQ(ST,NP)
      ID=IB(1)
      ID1=IB(2)
      CALL MATMLT(ST,DEL(ID),DEL(ID1),NP)
      IF(M.EQ.N) GO TO 50
C
C      CCLC PS((M),M)
      MZZ=MZ
      MS=IA(1)
      DO 25   I=1,N2
      ST(I)=Z(MZZ)
  25   MZZ=MZZ+1
      MZZ=MZ-N2
      DO 30       IS=1,M
   9   FORMAT(1X,I20/)
      CALL RTAPE(MS,N2,PS1,IT)
      CALL TRMMLT(PS1,Z(MZZ),ST,NP)
C       TRMMLT ACCUMULATES IN ST - TRANSP(PS(MS)*Z(MZZ))
      MS=MS+N2
  30      MZZ=MZZ-N2
      MZ=MZ+N2
      CALL MATMLT(DEL(ID1),ST,PS2,NP)
C       CALC PS((M,R) FOR R=0,1,... M-1.
```

```
      I0R=IA(1)
      I1R=IA(2)
      IMR=I0
      DO 40       IR=1,M
      CALL RTAPE(IMR,N2,PS1,IT)
      CALL MATMLT(PS1,PS2,ST,NP)
      IMR=IMR-N2
      CALL RTAPE(I0R,N2,PS1,IT)
      DO 42 I=1,N2
      PS1(I)=PS1(I)-ST(I)
 42    CONTINUE
      CALL WTAPE(I1R,N2,PS1,JT)
      I1R=I1R+N2
      I0R=I0R+N2
 40    CONTINUE
      CALL WTAPE(I1,N2,PS2,JT)
      I=JT
      JT=IT
      IT=I
      I=IA(1)
      IA(1)=IA(2)
      IA(2)=I
      I=IB(1)
      IB(1)=IB(2)
 45     IB(2)=I
      M2P=NP*M2
C
C      CALC Y(0,0) SUBMATRIX    ;Y(0,0)=DEL(N-1)
C
C
 50    CALL SHIFT(Z(1),DEL(IB(2)),NP,M2)
C
C
C      CALC Y(R,0) SUBMATRIX  ; Y(R,0)=-PS((N-1),(R-1))*DEL(N-1)
C      R=1,.....,N
C
C
      M2P=M2*NP
      I0R=IA(1)
      I1R=M2P+1
      DO 60 I=1,N
      CALL RTAPE(I0R,N2,PS1,IT)
      CALL MULT2(PS1,Z(1),Z(I1R),NP,M2)
      I0R=I0R+N2
 60   I1R=I1R+M2P
C
C
C      CALC Y(0,R) SUBMATRIX  ; Y(0,R)=TRANS(Y(R,0))
C      Y(0,R)=-DEL(N-1)*TRANS(PS(N-1),(R-1))
C      R=1,.....,N/2
C     DEL(N-1)=Y(0,0)=TRANS(DEL(N-1))
C
```

```
      MPW=NW*M2P
      NM=N/2
      I0R=IA(1)
      I1R=MPW+1
      DO 70 I=1,NM
      CALL RTAPE(I0R,N2,PS1,IT)
      CALL TRANS(PS1,DEL(IB(1)),NP)
      CALL SHIFT(ST,DEL(IB(1)),NP,M2)
      CALL MULT2(DEL(IB(2)),ST,Z(I1R),NP,M2)
      I0R=I0R+N2
 70   I1R=I1R+MPW
C
C
C       CALC Y(R,S)   ;   S=1,...,N/2 , R=1,...,N
C       Y(R,S)=Y(R-1,S-1)+PS(R-1)*DEL*TRANS(PS(S-1)-PS(N-R)*DEL*TRANS(
C       PS(N-S))
C
C
      IJ=MPW+1
      I1R=(N-1)*N2+IA(1)
      I4R=MPW+1
      DO 90 IS=1,NM
      IJ=IJ+M2P
      I2R=(N-1)*N2+IA(1)
      I3R=IA(1)
      DO 80 IR=1,N
      CALL RTAPE(I1R,N2,PS1,IT)
      CALL TRANS(PS1,DEL(IB(1)),NP)
      CALL SHIFT(ST,DEL(IB(1)),NP,M2)
      CALL MULT2(DEL(IB(2)),ST,DEL(IB(1)),NP,M2)
      CALL RTAPE(I2R,N2,PS1,IT)
      CALL MULT2(PS1,DEL(IB(1)),ST,NP,M2)
      CALL RTAPE(I3R,N2,PS1,IT)
      CALL MULT2(PS1,Z(I4R),DEL(IB(1)),NP,M2)
      KK=IB(1)
      JI=IJ-(NW+1)*M2P
      DO 88 K=1,M2P
      Z(IJ)=Z(JI)+DEL(KK)-ST(K)
      JI=JI+1
      KK=KK+1
 88    IJ=IJ+1
      IJT=IJ-M2P
      I3R=I3R+N2
 80   I2R=I2R-N2
      I1R=I1R-N2
 90   I4R=I4R+MPW
      RETURN
  100       IF(N.EQ.0) GO TO 110
      PRINT 1010
1010 FORMAT(// 10X 22HILLEGAL CALL TO LINVET //)
 110        DO 115   I=1,N2
115    Z(I)=DEL(I)
1000   RETURN
      END
```

```
      SUBROUTINE MATMLT(A,B,C,NP)
C       CALCULATES C=A*B,  A,B,C ARE NPXNP MATRICES OF
C       COMPLEX NUMBERS.
      COMPLEX A(1),B(1),C(1),D
      IJ=0
      L=1
      DO 220      J=1,NP
      DO 215   I=1,NP
      IJ=IJ+1
      D=0.
      KJ=L
      IK=I
      DO 210      K=1,NP
      D=D+A(IK)*B(KJ)
      IK=IK+NP
  210      KJ=KJ+1
  215   C(IJ)=D
  220      L=L+NP
      RETURN
      END
C
      SUBROUTINE TRMMLT(A,B,C,NP)
C       ACCUMULATES IN C    -TRANSP(A)*B
      COMPLEX A(1),B(1),C(1),D
      IJ=0
      L=1
      DO 130      J=1,NP
      M=1
      DO 125   I=1,NP
      IJ=IJ+1
      D=0.
      KI=M
      KJ=L
      DO 120      K=1,NP
      D=D+A(KI)*B(KJ)
      KI=KI+1
  120      KJ=KJ+1
      M=M+NP
  125   C(IJ)=C(IJ)-D
  130      L=L+NP
      RETURN
      END
C
C     GENERAL MATRIX INVERSION ROUTINE
      SUBROUTINE LINEQ(C,LL)
      COMPLEX C(1),STOR,STO,ST,S
      DIMENSION LR(58)
      COMPLEX X
      CABQ(X)=REAL(X)*REAL(X)+AIMAG(X)*AIMAG(X)
      DO 145   I=1,LL
      LR(I)=I
  145   CONTINUE
      M1=0
```

```
      DO 180       M=1,LL
      K=M
      DO 155    I=M,LL
      K1=M1+I
      K2=M1+K
      IF(CABQ(C(K1))-CABQ(C(K2))) 155,155,150
  150      K=I
  155   CONTINUE
      LS=LR(M)
      LR(M)=LR(K)
      LR(K)=LS
      K2=M1+K
      STOR=C(K2)
      J1=0
      DO 160       J=1,LL
      K1=J1+K
      K2=J1+M
      STO=C(K1)
      C(K1)=C(K2)
      C(K2)=STO/STOR
      J1=J1+LL
  160      CONTINUE
      K1=M1+M
      C(K1)=1./STOR
      DO 175    I=1,LL
      IF(I-M) 165,175,165
  165   K1=M1+I
      ST=C(K1)
      C(K1)=0.
      J1=0.
      DO 170       J=1,LL
      K1=J1+I
      K2=J1+M
      C(K1)=C(K1)-C(K2)*ST
      J1=J1+LL
  170      CONTINUE
  175   CONTINUE
      M1=M1+LL
  180      CONTINUE
      J1=0.
      DO 205    J=1,LL
      IF(J-LR(J)) 185,200,185
  185   LRJ=LR(J)
      J2=(LRJ-1)*LL
  190      DO 195    I=1,LL
      K2=J2+I
      K1=J1+I
      S=C(K2)
      C(K2)=C(K1)
      C(K1)=S
  195   CONTINUE
```

```
      LR(J)=LR(LRJ)
      LR(LRJ)=LRJ
      IF(J-LR(J)) 185,200,185
  200      J1=J1+LL
  205   CONTINUE
      RETURN
      END
      SUBROUTINE SHIFT(A,B,NP,M2)
      COMPLEX A(1),B(1)
C     MATRIX A(NP*M2) IS EXTRACTED FROM SQUARE MATRIX B(NP*NP)
      M1=NP/M2
      K=0
      L=(M1/2)*NP
      DO 1 J=1,M2
      DO 2 I=1,NP
      K=K+1
      L=L+1
  2   A(K)=B(L)
  1   L=L+(M1-1)*NP
      RETURN
      END
      SUBROUTINE MULT2(A,B,C,NP,M2)
      COMPLEX A(1),B(1),C(1),CMPLX,D
C     CALCULATE MATRIX MULTIPLICATION OF C=-A*B
C     WHERE A=NP*NP & B=NP*M2 & C=NP*M2
      IJ=0
      DO 1 J=1,M2
      DO 2 I=1,NP
      JK=(J-1)*NP+1
      D=CMPLX(0.0,0.0)
      IJ=IJ+1
      IK=I
      DO 3 K=1,NP
      D=D+A(IK)*B(JK)
      IK=IK+NP
  3   JK=JK+1
  2    C(IJ)=-D
  1   CONTINUE
      RETURN
      END
      SUBROUTINE TRANS(A,B,NP)
      COMPLEX A(1),B(1)
C      MATRIX  B=TRANSPOSE OF A
      K=0
      DO 1 J=1,NP
      L=J
      DO 1 I=1,NP
      K=K+1
      B(K)=A(L)
  1    L=L+NP
      RETURN
      END
```

```
      SUBROUTINE RTAPE(IO,N2,PS,IT)
C     READ IN A BLOCK OF DATA FROM TAPE
      COMPLEX PS(50)
      REWIND IT
      KK=IO-1
      LL=KK/N2
      IF(LL.EQ.0) GO TO 2
      DO 1 I=1,LL
 1    READ(IT)
 2     READ(IT) PS
      RETURN
      END
      SUBROUTINE WTAPE(IO,N2,PS,IT)
C     WRITE ARRAY PS(I) ONTO TAPE
      COMPLEX PS(50)
      REWIND IT
      KK=IO-1
      LL=KK/N2
      IF(LL.EQ.0) GO TO 2
      DO 1 I=1,LL
 1    READ(IT)
 2     WRITE(IT) PS
      RETURN
      END


      SUBROUTINE BLK2(M1,M2,M,A,B)
C     GENERATE SYMMETRIC TOEPLITZ MATRIX BY 1-ST ROW & COLUMN
      COMPLEX A(1),B(1)
      M12=M1*M2
      M123=M12*M1
      M1234=M123*M2
      DO 100 N=1,M2
      DO 100 I=1,M2
      DO 100 J=1,M1
      DO 100 L=1,M1
      K1=IABS(L-J)+1+M1*IABS(I-N)
      IF(I.EQ.N) GO TO 15
      IF(I.LT.N) GO TO 16
      IF(L.LT.J) K1=K1+M12-(IABS(I-N)+M1)
      GO TO 15
 16    IF(L.GT.J) K1=K1+M12-(IABS(I-N)+M1)
 15    K=L+M1*(I-1)+M12*(J-1)+M123*(N-1)+M1234*(M-1)
      B(K)=A(K1)
 100   CONTINUE
      RETURN
      END
      SUBROUTINE NOMUL(M1,DZ,AK,Z2)
C     CALCULATE IMPEDANCE & ADMITTANCE MATRIX OF A DIPOLE
      COMPLEX Z2(1),ZMNG
      ZN=0.0
```

```
      L=0
      DO 1 I=1,M1
      ZM=0.0
      DO 2 J=1,M1
      L=L+1
      Z2(L)=ZMNG(ZM,ZN,DZ,DZ,AK)
      Z2(L)=Z2(L)*0.01
2      ZM=ZM+DZ
1      ZN=ZN+DZ
      RETURN
      END


      SUBROUTINE FAR(SS,NR,NT,NY,NK,NS,NJ,HX,HY,HZ,M,DZ,PH,TE,
     1TOT1,TOT2,N,M1,V)
C     CALCULATE FAR FIELD E-FIELD AND GAIN OF GIVEN Z-DIRECTED
C     DIPOLES WITH KNOWN CURRENT DISTRIBUTION
      COMPLEX AZ,TERM,YJ0,JY1,E2,SS(1),PIN,V(1)
      DIMENSION PH(1),TE(1),TOT1(1),TOT2(1)
      DIMENSION HX(1),HY(1),HZ(1)
      COMMON AA(180),BB(180)
      PIN=CMPLX(0.,0.)
      K=(M1+1)/2
      DO 1 I=1,N
      PIN=PIN+V(I)*CONJG(SS(K))
1     K=K+M1
      NA=NR+1
      POWER=REAL(PIN)
      NB=NT+1
      NC=NK+1
      ND=NS+1
      LL=0
      BIG=0.0
      DO 11 LX=NC,ND,NJ
      LM=LX-1
      THE=0.0174533*FLOAT(LX-1)
      CTH=COS(THE)
      STH=SIN(THE)
      STST=STH*STH
      K2=0
      DO 11 LK=NA,NB,NY
      LO=LK-1
      PC=0.0174533*FLOAT(LK-1)
      PC=COS(PC)
      PS=SIN(PC)
      AZ=CMPLX(0.0,0.0)
      DO 44 J=1,N
      YZ=STH*(PC*HX(J)+HY(J)*PS)
      YJ0=CMPLX(0.0,YZ)
      TERM=CEXP(YJ0)
      TS=SIN(DZ)
      TC=COS(DZ)
```

```
      MC=(J-1)*M1+1
      MB=J*M1
      ZDZ=HZ(J)
      DO 47 I=MC,MB
      ZDZ=ZDZ+DZ
      YJ1=CMPLX(0.0,ZDZ*CTH)
      E2=CEXP(YJ1)
      IF(LX.EQ.1.OR.LX.EQ.181) GO TO 46
      AZ=AZ+2.*TERM*E2/(TS*STST)*(COS(DZ*CTH)-TC)*SS(I)
      GO TO 47
 46   AZ=AZ+TERM*E2*DZ*SS(I)
 47    CONTINUE
 44   CONTINUE
      LL=LL+1
      TT=CABS(AZ)*STH
      IF(TT.GT.BIG) BIG=TT
      PP=ATAN2(AIMAG(AZ),REAL(AZ))/0.0174533
      PP=(377./12.5663706)*TT**2/POWER
      AA(LL)=TT
      BB(LL)=PP
      TE(LL)=TE(LL)+TT**2
      TOT1(LL)=TOT1(LL)+TT
      PH(LL)=PH(LL)+PP**2
      TOT2(LL)=TOT2(LL)+PP
 11   CONTINUE
      M=LL
 92    RETURN
      END


      SUBROUTINE STDV(TOT1,TOT2,PH,TE,NR,NT,NY,NK,NS,NJ,ST1,ST2,IN)
C     DATA PROCESSING OF THE FAR FIELD POINTS
      DIMENSION ST1(1),ST2(1),TOT1(1),TOT2(1),TE(1),PH(1)
      PRINT 13
 13   FORMAT(///8X,'THE',7X,'PHI ',6X,'MEAN E-FIELD',
     $15X,'STD   ',10X,'MEAN GAIN',16X,'STD',///)
      NA=NR+1
      NB=NT+1
      NC=NK+1
      ND=NS+1
      LL=0
      IN1=IN-1
      IF(IN1.EQ.0) IN1=1
      DO 11 LX=NC,ND,NJ
      DO 11 LK=NA,NB,NY
      LL=LL+1
      ST1(LL)=SQRT(ABS(TE(LL)-TOT1(LL)**2/FLOAT(IN))/FLOAT(IN1))
      ST2(LL)=SQRT(ABS(PH(LL)-TOT2(LL)**2/FLOAT(IN))/FLOAT(IN1))
      TOT1(LL)=TOT1(LL)/FLOAT(IN)
      TOT2(LL)=TOT2(LL)/FLOAT(IN)
      ITH=LX-1
      IPC=LK-1
```

```
      PRINT 12,ITH,IPC,TOT1(LL),ST1(LL),TOT2(LL),ST2(LL)
   11  CONTINUE
      MAX=(LL+1)/2
      WRITE(2,15) TOT2(MAX),ST2(MAX)
      PRINT 15,TOT2(MAX),ST2(MAX)
   15 FORMAT(///1X,'   AVERAGE BROADSIDE GAIN =',F20.6/,
     &1X,'   STD                          =',F20.6/)
   12 FORMAT(1X,2I10,1P4E20.6)
      RETURN
      END


      SUBROUTINE TAPER(V,M1,M2,M3,HX,HY,HZ)
C     NON-UNIFORM EXCITATION MULTIPLIER
      COMPLEX V(1)
      READ 50,RX,RZ
   50 FORMAT(5F10.5)
      DIMENSION VV(100),PP(100),HX(1),HY(1),HZ(1)
      PRINT 77
   77 FORMAT(//1X,'MAGNITUDE TAPER & PHASE SHIFT IN EACH DIPOLE',//)
      M23=M2*M3
      CALL TAP(M2,M3,HX,HZ,VV)
      CALL STEER(M2,M3,RX,RZ,HX,HZ,PP)
      PRINT 40
   40 FORMAT(//1X,'    ELEMENT ',5X,'MAGNITUDE TAPER',5X,
     $'PHASE SHIFT',//)
      PRINT 10,(I,VV(I),PP(I),I=1,M23)
      DO 1 I=1,M23
   10 FORMAT(1X,I10,2F17.5)
      V(I)=V(I)*VV(I)*CMPLX(COS(PP(I)),SIN(PP(I)))
    1 CONTINUE
      RETURN
      END
      SUBROUTINE STEER(M2,M3,RX,RZ,HX,HZ,PP)
C     PROGRESSIVE PHASE SHIFT ON EACH DIPOLE -
C     STEERING THE MAIN BEAM IN BOTH DIRECTION
      DIMENSION PP(1),HX(1),HZ(1)
      PI2=6.2831853
      THX=(90.-RX)*PI2/360.
      THZ=(90.-RZ)*PI2/360.
      L=0
      XK=(HX(2)-HX(1))*COS(THX)
      ZK=(HZ(M2+1)-HZ(1))*COS(THZ)
      DO 100 I=1,M3
      DO 100 J=1,M2
      L=L+1
      PP(L)=FLOAT(J-1)*XK+FLOAT(I-1)*ZK
  100 CONTINUE
      RETURN
      END
```

```
      SUBROUTINE TAP(M2,M3,HX,HZ,VV)
C     MAGNITUDE TAPER OF EXCITATION IN BOTH DIRECTION
      DIMENSION HX(1),HZ(1),VV(1)
      PI2=6.2831853
      HFX=(HX(M2)-HX(1))*0.5
      HFZ=(HZ(M2*(M3-1)+1)-HZ(1))*0.5
      L=0
      DO 100 I=1,M3
      DO 100 J=1,M2
      L=L+1
      X=(HX(L)-HFX)/PI2
      Z=(HZ(L)-HFZ)/PI2
      VV(L)=FUNX(X)*FUNZ(Z)
  100 CONTINUE
      RETURN
      END
      FUNCTION FUNX(X)
      FUNX=EXP(-(ABS(X)))
      RETURN
      END
      FUNCTION FUNZ(Z)
      FUNZ=EXP(-(ABS(Z)))
      RETURN
      END


      SUBROUTINE MULT(Z,V,CUR,M1,M2,M3)
C     GIVEN HALF OF THE COMPACT Y-MATRIX & VOLTAGE,CALCULATE CURRENT
      COMPLEX Z(1),V(1),CUR(1),A
      M123=M1*M2*M3
      M23=M2*M3
      N2=(M23+1)/2
      IF(M3.LT.M2) CALL ORDER(V,1,M2,M3)
      DO 1 I=1,M123
      A=CMPLX(0.0,0.0)
      I2=M123-I+1
      DO 2 J=1,N2
      J2=M23-J+1
      L1=(J-1)*M123+I
      L2=(J-1)*M123+I2
      IF(J.NE.J2) A=A+Z(L2)*V(J2)
      A=A+Z(L1)*V(J)
    2  CONTINUE
      CUR(I)=A
    1  CONTINUE
      IF(M3.LT.M2) GO TO 3
      RETURN
    3 CALL ORDER(CUR,M1,M3,M2)
      CALL ORDER(V,1,M3,M2)
      RETURN
      END
```

```
      SUBROUTINE MULT3(Z2,V,CUR2,M1,M2,M3)
      COMPLEX V(1),CUR2(1),Z2(1)
C     CALCULATE THE CURRENT ON EACH ELEMENT OF AN ARRAY
C     WITHOUT TAKING ACCOUNT THE MUTUAL EFFECT
      M23=M2*M3
      MM=((M1+1)/2-1)*M1
      L=0
      DO 1 I=1,M23
      DO 2 J=1,M1
      L=L+1
      CUR2(L)=Z2(MM+J)*V(I)
 2     CONTINUE
 1     CONTINUE
      RETURN
      END


      SUBROUTINE ORDER(V,M1,M2,M3)
C     REORDER THE SEQUENCE OF EACH DIPOLE IN ARRAY
      COMPLEX V(1),VV(300)
      L=0
      DO 1 I=1,M2
      K=I
      DO 2 J=1,M3
      N=(K-1)*M1
      DO 4 M=1,M1
      N=N+1
      L=L+1
      VV(L)=V(N)
 4    CONTINUE
 2    K=K+M2
 1    CONTINUE
      M123=M1*M2*M3
      DO 3 I=1,M123
 3    V(I)=VV(I)
      RETURN
      END
```

```
      SUBROUTINE VOLT(V,VP,M2,M3,IX,AM1,AM2,SD1,SD2)
C     GENERATE RANDOM ERROR EXCITATIONS FOR ARRAY-
C     NORMAL DISTRIBUTION  OF BOTH MAGNITUDE & PHASE
C     ERRORS ARE ASSUMED
      COMPLEX V(1),VP(1)
      M23=M2*M3
      DO 200 I=1,M23
    2 CALL RND(G1,AM1,SD1,IX)
      IF(G 1) 2,3,3
    3 CALL RND(G2,AM2,SD2,IX)
      IF(G 2-3.14159265)4,5,3
    4 IF(G 2+3.14159265)3,5,5
    5 V(I)= VP(I)*G1*CMPLX(COS(G2),SIN(G2))
  200 CONTINUE
      RETURN
      END



      SUBROUTINE RND(G,AMEAN,STD,IX)
      A=0.0
      KD=12
      IF(STD.GT.3.141593) KD=1
      DO 7 I=1,KD
      IY=IX*65539
      IF(IY) 10,12,12
   10 IY=-IY
   12 YFL=IY
      IX=IY
      YFL=YFL*.291038305E-10
    7 A=A+YFL
      G=(A-6.0)*STD+AMEAN
      IF(STD.GT.3.141593) G=(A-0.5)*3.14159265*2.
   20 RETURN
      END
```